The Astronomical Journal, 124:1670–1694, 2002 September

POST–T TAURI STARS IN THE NEAREST OB ASSOCIATION

Eric E. Mamajek, Michael R. Meyer, and James Liebert
Steward Observatory, Department of Astronomy, University of Arizona, 933 North Cherry Avenue, Tucson, AZ 85721;
eem@as.arizona.edu
Received 2002 February 28; accepted 2002 May 20

ABSTRACT

We present results of a spectroscopic survey of X-ray– and proper-motion–selected samples of late-type stars in the Lower Centaurus–Crux (LCC) and Upper Centaurus–Lupus (UCL) subgroups of the nearest OB association: Scorpius-Centaurus. The primary goals of the survey are to determine the star formation history of the OB subgroups and to assess the frequency of accreting stars in a sample dominated by "post–T Tauri" pre–main-sequence (PMS) stars. We investigate two samples: (1) proper-motion candidates from the ACT Catalog and Tycho Reference Catalog (TRC) with X-ray counterparts in the *ROSAT* All-Sky Survey (RASS) Bright Source Catalog and (2) G- and K-type stars in the *Hipparcos* catalog found to be candidate members by de Zeeuw et al. We obtained optical spectra of 130 candidates with the Siding Spring 2.3 m dual-beam spectrograph. PMS stars were identified by (1) strong Li λ6707 absorption, (2) subgiant surface gravities, (3) proper motions consistent with Sco-Cen membership, and (4) H-R diagram positions consistent with being PMS. We find 93% of the RASS-ACT/TRC stars to be probable PMS members, compared with 73% of the *Hipparcos* candidates. We demonstrate that measuring the gravity-sensitive band ratio of Sr II λ4077 to Fe I λ4071 is a valuable means of discriminating PMS and zero-age main-sequence (ZAMS) stars. Using secular parallaxes and *Hipparcos*, Tycho-2, and Two Micron All Sky Survey photometry, we construct an H-R diagram. Depending on the choice of published evolutionary tracks, we find the mean ages of the PMS populations to range between 17 and 23 Myr for LCC and 15 and 22 Myr for UCL. Taking into account observational errors, it appears that 95% of the low-mass star formation in each subgroup must have occurred in less than 8 Myr (LCC) and 12 Myr (UCL). Using the Bertelli et al. tracks, we find main-sequence turnoff ages for *Hipparcos* B-type members to be 16 $\pm$ 1 Myr for LCC and 17 $\pm$ 1 Myr for UCL. Contrary to previous findings, it appears that LCC is coeval with, or slightly older than, UCL. The secular parallaxes of the Sco-Cen PMS stars yield distances of 85–215 pc, with 12 of the LCC members lying within 100 pc of the Sun. Only one out of 110 ($0.9^{+2.1}_{-0.8}$%; 1 σ) PMS solar-type stars in the sample with ages of 13 $\pm$ 1 (s.e.) $\pm$ 6 (1 σ) Myr and masses of 1.3 $\pm$ 0.2 (1 σ) $M_\odot$ shows both enhanced Hα emission and a *K*-band excess indicative of accretion from a truncated circumstellar disk: the nearby ($d \simeq 86$ pc) classical T Tauri star PDS 66.

Key words: open clusters and associations: individual (Scorpius OB2, Lower Centaurus–Crux, Upper Centaurus–Lupus) — stars: activity — stars: formation — stars: kinematics — stars: pre–main-sequence — X-rays

1. INTRODUCTION

Post–T Tauri stars (PTTSs) are low-mass, pre–main-sequence (PMS) stars with properties intermediate between T Tauri stars found in molecular clouds (both "classical," with evidence for accretion from a circumstellar disk and "weak lined," lacking such evidence, hereafter CTTSs and WTTSs; ages less than a few megayears) and zero-age main-sequence stars (ZAMS; ages greater than 30–100 Myr). Although strict observational criteria do not exist for classifying PTTSs as such, a working definition is a low-mass star (less than 2 $M_\odot$) that is Li-rich compared with stars in ZAMS open clusters such as the $\sim$120 Myr old Pleiades, and whose theoretical H-R position [log $T_{\rm eff}$ and log $(L/L_\odot)$] is above the main sequence (Herbig 1978; Jensen 2001). Since these criteria also apply to CTTSs and WTTSs, one could argue that, in addition, PTTSs should be located in regions devoid of nearby molecular gas or nebulosity. Classifying PTTSs by these criteria has complications: (1) few young field stars not associated with well-studied molecular clouds currently have accurately measured distances (hence known luminosities), (2) unresolved binarity can make stars with known distances appear more luminous, and thus younger, and (3) there is a dispersion in observed Li abundances among stars with the same masses and ages in coeval open clusters. Pre–main-sequence stars exhibit considerable chromospheric (Hα and Ca H and K) and coronal X-ray emission. Only a few PTTS candidates were known before the *Einstein* and *ROSAT* X-ray missions, and X-ray surveys have become the primary means of identifying these PMS stars.

Investigations of pre–main-sequence evolution have been hampered by a lack of large samples of well-characterized PTTSs. This deficit has impacted studies of PMS angular momentum evolution (e.g., Rebull et al. 2002; Bouvier et al. 1997), stellar multiplicity (e.g., Köhler et al. 2000), and circumstellar disk evolution (e.g., Spangler et al. 2001; Haisch, Lada, & Lada 2001). The nearest PTTSs also provide optimal targets for young exoplanet and brown dwarf searches (e.g., Lowrance et al. 2000). These objects are much more luminous early in their evolution, and the closest targets enable characterization of the smallest orbital radii. With a post–T Tauri population in a nearby OB association, we can address basic questions such as how long the star formation persists in a giant molecular cloud and what is the duration of the accretion phase for young solar-type stars.

Identifying a bona fide PTTS sample can be accomplished by searching for low-mass members of nearby fossil OB associations. The Sco-Cen OB complex (Sco OB2) is the nearest OB association to the Sun (mean subgroup distances range from 118 to 145 pc; de Zeeuw et al. 1999, hereafter dZ99) and covers roughly 2000 deg^2 ($\sim$5%) of the sky. The complex is made up of three kinematic subgroups (Blaauw 1946) with nuclear ages ranging from 5 to 15 Myr, a molecular cloud currently undergoing star formation (the ρ Oph complex, Wilking, Lada, & Young 1989; Blaauw 1991; de Geus 1992), and perhaps several smaller cloud complexes in the vicinity (e.g., the Lupus, Corona Australis, Chamaeleon, Musca, and Coalsack clouds). The three subgroups are Upper Scorpius (US; age 5–6 Myr), Upper Centaurus–Lupus (UCL; age 14–15 Myr), and Lower Centaurus–Crux (LCC; age 11–12 Myr, de Geus, de Zeeuw, & Lub 1989). US has been studied extensively in recent years (e.g., Preibisch & Zinnecker 1999, and references therein), but UCL and LCC have received relatively little attention.

In this work, we investigate the low-mass (less than 2 $M_\odot$) membership of the two oldest Sco-Cen OB subgroups (LCC and UCL) using recently available astrometric catalogs (*Hipparcos*, ACT, the Tycho Reference Catalog [TRC], and Tycho-2), the Two Micron All Sky Survey (2MASS), and the *ROSAT* All-Sky Survey (RASS). We conduct a spectroscopic survey of two samples: (1) an X-ray–selected sample of late-type stars from the kinematic candidate membership lists of Hoogerwerf (2000), and (2) the G–K type *Hipparcos* members of the OB subgroups from dZ99. In § 2, we discuss the procedure for selecting candidate PMS stars from both samples, and § 3 discusses the observations and assembled database. Section 4 describes the data analysis and characterization of our stellar sample, and § 5 discusses the selection of PMS stars, sample contamination, and completeness. Section 6 describes how we construct an H-R diagram for the subgroups, and § 7 presents results regarding the ages of the subgroups, their age spreads, and the frequency of accretion disks around PMS stars. Section 8 discusses the star formation history of LCC and UCL, and § 9 summarizes the findings of our survey.

2. SELECTION OF CANDIDATE PMS STARS

2.1. *The Hipparcos Sample*

DZ99 lists *Hipparcos* Sco-Cen members that were selected using *both* de Bruijne's (1999a) refurbished convergent point method and Hoogerwerf & Aguilar's (1999) spaghetti method. Their membership lists contained 31 G–K stars in UCL and 21 G–K stars in LCC (their Table C1). Most of these bright stars have been classified in the Michigan Spectral Survey (e.g., Houk & Cowley 1975); however, SIMBAD[1] reveals that most have been studied no further. We limit the survey to the 30 G–K candidates with Michigan luminosity classes IV or V (see Table 1). Stars with borderline F/G Michigan types were not observed. HIP 63962 and 73777 met the criteria but were not observed. DZ99 estimated the contamination by G–K type interlopers of all luminosity classes to be 32% for LCC and 24% for UCL. Of these 31 stars, 17 also have RASS BSC X-ray counterparts within 40″.

[1] See http://simbad.u-strasbg.fr/Simbad.

2.2. *The RASS-ACT/TRC Sample*

To identify lower mass members of an OB association, one can search for stars whose proper motions are similar to those of high-mass members. The high-mass membership and moving group solution for each OB subgroup were determined by dZ99 and de Bruijne (1999b). Thousands of faint stars in the ACT and TRC astrometric catalogs[2] were identified by Hoogerwerf (2000) as candidate low-mass LCC and UCL members. A high degree of contamination from interlopers is expected because of the similarity of the space motions of the subgroups to that of the local standard of rest, compounded by the low galactic latitude of the subgroups. The selection of ACT/TRC candidate members is described in detail in § 4 of Hoogerwerf (2000).

The Hoogerwerf ACT/TRC membership lists for LCC and UCL were slightly modified and filtered to produce the final target list. First, we requested from R. Hoogerwerf (1999, private communication) candidate membership lists with different color-magnitude constraints from that described in Hoogerwerf (2000). The new color-magnitude selection box is essentially a polygon defined by the Schmidt-Kaler (1982) empirical zero-age main sequence ($B-V$ vs. M_V) at the mean distance for each subgroup (dZ99), where we take all stars $\Delta M_V = 3$ mag above and $\Delta M_V = 1$ mag below the ZAMS line. Hoogerwerf originally selected only those stars within $\Delta M_V = 1.5$ mag above the ZAMS, but this could inadvertently omit younger members or binaries. The selection box contained 1353 ACT and TRC stars in LCC and 1874 stars in UCL. In order to target low-mass, solar-type stars with G–K spectral types, we retained only those stars with Johnson $(B-V) \geq 0.58$ mag (the unreddened color of G0 dwarfs; Drilling & Landolt 2000). No red $B-V$ limit was imposed. After the color-magnitude selection, we retained only those stars that were identified as kinematic members in *both* the ACT and TRC astrometric catalogs. This final color selection of the ACT/TRC lists resulted in 785 UCL candidates and 679 LCC candidates.

In order to further filter the target list, we selected only those ACT/TRC candidates that had *ROSAT* All-Sky Survey Bright Source Catalog (RASS BSC) X-ray counterparts. Voges et al. (1999) cross-referenced the RASS BSC with the Tycho catalog and found that 68% of the optical–X-ray correlations were within 13″, and 90% of the correlations were within 25″. In plotting a histogram of the separation distance between RASS BSC X-ray sources and ACT/TRC stars, we independently find 40″ to be an optimal search radius. No constraints on X-ray hardness ratio were imposed in the target selection. In order to calculate X-ray luminosities, we assume the X-ray energy conversion factor for the *ROSAT* PSPC detector from Fleming et al. (1995). The linearity of this X-ray efficiency relation spans the temperature range of stellar coronae from inactive subdwarf stars to extremely active RS Canum Venaticorum and T Tauri stars. Not surprisingly, the kinematic selection of

[2] The ACT (Urban, Corbin, & Wycoff 1998) and TRC catalogs (Høg et al. 1998) were used for target selection for this project in 1999, but we use the photometry and astrometry from the Tycho-2 catalog (available in 2000; Høg et al. 2000a, 2000b) in the data analysis. The Tycho-2 catalog was a joint USNO/Copenhagen project, and its data supersede the contents of the ACT and TRC catalogs.

TABLE 1

Properties of de Zeeuw et al. (1999) Sco-Cen G–K Candidate Members

HIP (1)	OB Group (2)	α (J2000.0) (3)	δ (J2000.0) (4)	$\mu_{\alpha*}$ (mas yr^{-1}) (5)	μ_δ (mas yr^{-1}) (6)	V (mag) (7)	$B-V$ (mag) (8)	Sp. MSS (9)	J (mag) (10)	H (mag) (11)	K_s (mag) (12)	Notes (13)
57524	LCC	11 47 24.55	−49 53 03.0	−33.7 ± 0.8	−10.2 ± 1.0	9.07	0.63 ± 0.02	G3/5 VP q2	7.91 ± 0.02	7.59 ± 0.06	7.51 ± 0.02	1RXS J114724.3−495250, TWA 19A
58996	LCC	12 05 47.48	−51 00 12.1	−37.5 ± 0.8	−11.5 ± 0.8	8.89	0.63 ± 0.02	G1 V q1	7.67 ± 0.01	7.37 ± 0.03	7.27 ± 0.01	var(0.06), 1RXS J120547.8−510007
59854	LCC	12 16 27.84	−50 08 35.8	−29.1 ± 1.3	−8.6 ± 1.0	9.34	0.67 ± 0.02	G3 V q1	8.04 ± 0.01	7.69 ± 0.02	7.61 ± 0.03	1RXS J121627.9−500829
60885	LCC	12 28 40.05	−55 27 19.3	−34.9 ± 0.8	−16.0 ± 0.7	8.89	0.64 ± 0.02	G1 q4	7.68 ± 0.02	7.40 ± 0.05	7.28 ± 0.03	var(0.02), 1RXS J122840.3−552707
60913	LCC	12 29 02.25	−64 55 00.6	−37.5 ± 1.2	−11.4 ± 0.9	9.04	0.73 ± 0.02	G5 V q1	7.60 ± 0.01	7.26 ± 0.01	7.14 ± 0.01	
62445	LCC	12 47 51.87	−51 26 38.2	−30.4 ± 1.0	−8.7 ± 1.0	9.52	0.80 ± 0.03	G8/K0 V q3	7.79 ± 0.01	7.38 ± 0.03	7.25 ± 0.01	var(0.10), 1RXS J124751.7−512638
63797	LCC	13 04 30.96	−65 55 18.5	−42.4 ± 1.0	−14.2 ± 0.8	8.48	0.74 ± 0.01	G3 V q1	7.02 ± 0.04	6.79 ± 0.02	6.71 ± 0.01	
63847	LCC	13 05 05.29	−64 13 55.3	−36.5 ± 1.1	−19.5 ± 1.3	9.18	0.73 ± 0.02	G5 V q4	7.78 ± 0.01	7.44 ± 0.03	7.36 ± 0.03	var(0.03)
65423	LCC	13 24 35.12	−55 57 24.2	−29.0 ± 1.0	−13.0 ± 1.0	9.59	0.66 ± 0.03	(G3w)F7 q2	8.45 ± 0.01	8.16 ± 0.03	8.10 ± 0.01	1RXS J132435.3−555719
65517	LCC	13 25 47.83	−48 14 57.9	−39.0 ± 1.2	−20.3 ± 1.0	9.76	0.60 ± 0.04	K0/2 V+(G) q3	8.50 ± 0.02	8.18 ± 0.03	8.08 ± 0.03	var(0.05, $P = 1.09$ days), V966 Cen, 1RXS J132548.2−481451
66001	LCC	13 31 53.61	−51 13 33.1	−29.0 ± 1.5	−20.1 ± 1.1	9.84	0.72 ± 0.04	G5/6 V q3	8.43 ± 0.01	8.00 ± 0.03	7.83 ± 0.01	1RXS J133152.6−511335
66941	LCC	13 43 08.69	−69 07 39.5	−32.7 ± 0.7	−19.8 ± 0.9	7.57	0.74 ± 0.01	G2 IV/V q2	6.21 ± 0.01	5.85 ± 0.03	5.77 ± 0.01	var(0.08), CCDM 1343−6908, 1RXS J134306.8−690754
67522	UCL	13 50 06.28	−40 50 08.8	−29.3 ± 1.5	−22.9 ± 1.0	9.79	0.67 ± 0.04	G1 V q2	8.58 ± 0.01	8.30 ± 0.04	8.16 ± 0.02	1RXS J135005.7−405001
68726	UCL	14 04 07.12	−37 15 50.5	−16.9 ± 0.8	−16.7 ± 0.7	7.11	0.72 ± 0.02	G3 IV/V q3	5.29 ± 0.00	5.40 ± 0.04	4.92 ± 0.05	CCDM 14041−3716
71178	UCL	14 33 25.78	−34 32 37.7	−28.1 ± 1.6	−28.0 ± 1.4	10.18	0.81 ± 0.06	G8/K0 V q3	8.52 ± 0.01	8.06 ± 0.02	7.94 ± 0.02	var(0.15), V1009 Cen
72070	UCL	14 44 30.96	−39 59 20.6	−20.9 ± 1.5	−24.0 ± 1.4	9.32	0.64 ± 0.03	G3 V q3	8.19 ± 0.01	7.93 ± 0.02	7.81 ± 0.01	
74501	UCL	15 13 29.22	−55 43 54.6	−16.1 ± 0.8	−24.0 ± 0.8	7.47	0.78 ± 0.01	G2 IV q1	5.86 ± 0.01	5.48 ± 0.02	5.20 ± 0.01	
75924	UCL	15 30 26.29	−32 18 11.6	−31.7 ± 2.4	−31.9 ± 2.3	8.80	0.65 ± 0.03	G6 V q2	7.37 ± 0.01	7.05 ± 0.03	6.92 ± 0.02	1RXS J153026.1−321815
76472	UCL	15 37 04.66	−40 09 22.1	−20.2 ± 1.7	−27.6 ± 1.4	9.39	0.73 ± 0.03	G5 V q2	7.98 ± 0.01	7.63 ± 0.05	7.52 ± 0.01	1RXS J153706.0−400929
77015	UCL	15 43 29.86	−38 57 38.6	−20.5 ± 1.6	−31.7 ± 1.2	9.66	0.61 ± 0.03	G3 V q1	8.61 ± 0.01	8.34 ± 0.03	8.32 ± 0.02	
77081	UCL	15 44 21.05	−33 18 55.0	−19.1 ± 1.8	−29.5 ± 1.4	9.69	0.75 ± 0.04	G8 V q2	8.27 ± 0.02	7.86 ± 0.03	7.79 ± 0.02	
77135	UCL	15 44 57.69	−34 11 53.7	−20.6 ± 3.3	−25.9 ± 2.5	9.88	0.78 ± 0.02	G6/G8 IV/V q3	8.43 ± 0.02	8.04 ± 0.02	8.23 ± 0.04	CCDM 15450−3412, 1RXS J154458.0−341143
77144	UCL	15 45 01.83	−40 50 31.0	−19.4 ± 1.3	−31.1 ± 1.4	9.46	0.57 ± 0.03	G1 V q1	8.30 ± 0.01	7.97 ± 0.03	7.88 ± 0.02	var(0.11), 1RXS J154502.0−405043
77524	UCL	15 49 44.98	−39 25 09.1	−24.5 ± 2.0	−25.2 ± 1.8	10.64	1.09 ± 0.12	K0 (V) q3	8.81 ± 0.01	8.27 ± 0.02	8.13 ± 0.02	1RXS J154944.7−392509
77656	UCL	15 51 13.73	−42 18 51.3	−18.0 ± 1.2	−30.0 ± 1.0	9.58	0.74 ± 0.04	G8 V q3	8.15 ± 0.03	7.78 ± 0.06	7.67 ± 0.02	1RXS J155113.5−421858
79610	UCL	16 14 43.02	−38 38 43.5	−14.1 ± 3.4	−29.4 ± 3.2	9.24	0.52 ± 0.03	G1/G2 V q1	8.07 ± 0.01	7.85 ± 0.03	7.98 ± 0.03	CCDM 16147−3839
80636	UCL	16 27 52.34	−35 47 00.4	−13.1 ± 2.1	−25.5 ± 1.2	9.37	0.68 ± 0.03	G6 V q2	8.04 ± 0.01	7.71 ± 0.01	7.62 ± 0.01	1RXS J162752.8−354702
81380	UCL	16 37 12.87	−39 00 38.1	−14.4 ± 2.1	−21.5 ± 1.6	9.82	0.66 ± 0.05	G2/5 V q3	8.45 ± 0.02	8.09 ± 0.04	7.99 ± 0.03	
81447	UCL	16 38 05.53	−34 01 10.6	−11.3 ± 1.5	−23.9 ± 1.0	9.08	0.54 ± 0.05	G1 IV/V q1	7.91 ± 0.02	7.66 ± 0.03	7.55 ± 0.03	
81775	UCL	16 42 10.36	−31 30 15.0	−14.1 ± 1.5	−18.3 ± 1.3	9.44	0.64 ± 0.04	G5 V q2	8.36 ± 0.02	8.37 ± 0.05	8.08 ± 0.04	

Notes.—Units of right ascension are hours, minutes, and seconds, and units of declination are degrees, arcminutes, and arcseconds. Col. (1): *Hipparcos* ID; col. (2): OB subgroup region; cols. (3) and (4): J2000.0 position; cols. (5) and (6): proper-motion components (mas yr^{-1}, where $\mu_{\alpha*} = \mu_\alpha \cos\delta$); col. (7): V magnitude (Johnson); col. (8): $B-V$ color (Johnson); col. (9): spectral types from the Michigan Spectral Survey (MSS, Vols. 1–3); "q1" indicates the flag "quality = 1" in the MSS catalog, where $q = 1$, 2 stars are judged to have reliable spectral types; cols. (10)–(12): 2MASS JHK_s magnitudes; col. (13): notes on variability, X-ray counterparts, and multiple star system name (CCDM) from *Hipparcos*. "*Var.(N.NN)*" indicates that the H6 field in the *Hipparcos* catalog is identified as being variable in the broad H_p passband. The magnitude scatter *N.NN* in H_p is listed, and period P if found. Near-IR photometry is from the preliminary 2MASS database. The name is given of RASS BSC X-ray sources within 40″ of *Hipparcos* stars; many of the variable stars are also *ROSAT* sources. Astrometric data and optical photometry are from from the *Hipparcos* catalog (ESA 1997).

ACT/TRC stars also selected many of the same stars as in the *Hipparcos* sample (HIP 57524, 59854, 62445, 65423, 66001, 66941, 67522, 75924, 76472, 77135, 77524, 77656, and 80636). These stars are retained in the *Hipparcos* sample (Table 1) and are omitted from the RASS-ACT/TRC list (Table 2). The final target list of 96 RASS-ACT/TRC stars (40 LCC and 56 UCL) is given in Table 2.

3. OBSERVATIONS

Blue and red optical spectra of the PMS candidates were taken simultaneously with the dual-beam spectrograph (DBS) on the Siding Spring 2.3 m telescope on the nights of 2000 April 20–24. The DBS instrument is detailed in Rodgers, Conroy, & Bloxham (1988). Using a 2″ wide slit, we used the B600 line mm^{-1} grating in first order on the blue channel, yielding 2.8 Å FWHM resolution from 3838–5423 Å. The red channel observations were done with the R1200 line mm^{-1} grating in first order, yielding 1.3 Å FWHM resolution over 6205–7157 Å. The five nights of bright time were predominantly clear to partly cloudy. Signal-to-noise ratios of ∼50–200 per resolution element were typically reached with integration times of 120–720 s. Flat fields and bias frames were observed at the beginning and end of each night. NeAr λ-calibration arcs and spectrophotometric standards were observed every few hours. The spectra were reduced using standard IRAF routines. In order to remove low-order chromatic effects from the band-ratio measurements, we spectrophotometrically calibrated all of the target spectra using two standard stars from Hamuy et al. (1994). A total of 118 program stars (§§ 2.1 and 2.2) and 20 MK spectral standards (§ 4.1.1) were observed. The major stellar absorption features of one of the single standard G stars were shifted to a zero-velocity wavelength scale. The spectra of all of the stars were then cross-correlated against this standard star using the IRAF task FXCOR and then shifted to the common, rest-frame wavelength scale. This was done to ensure proper identification of weak lines, as well as to make sure that the band-ratio measurements were sampling the same spectral range in each stellar spectrum.

4. ANALYSIS OF SPECTRA

4.1. *Spectral Types and Luminosity Classification*

4.1.1. *Standard Stars*

We observed 20 spectral standards including dwarfs and subgiants (luminosity classes IV and V) and a few giants (III). A summary of their properties is listed in Table 3. To permit quantitative examination of trends in the strengths of spectral features, as well as interpolation between spectral types, we adopt the numerical subtype scaling of Keenan (1984; i.e., here listed as "Sp.," where G0 = 30, G2 = 31, K0 = 34, etc.). All of the standard stars are classified on the MK system by Keenan & McNeil (1989), except for HR 7061 (Garcia 1989). Table 3 also lists their spectral types as given in the Michigan Spectral Survey atlases of N. Houk (e.g., Houk 1978). The sample standard deviation of a linear fit between the Keenan and Houk spectral types for dwarfs and subgiants, on Keenan's subtype scale, is σ(Sp.) = 0.6 subtypes. The ∼0.6 subtype uncertainty probably represents the best that can be done using spectral types determined by different authors.

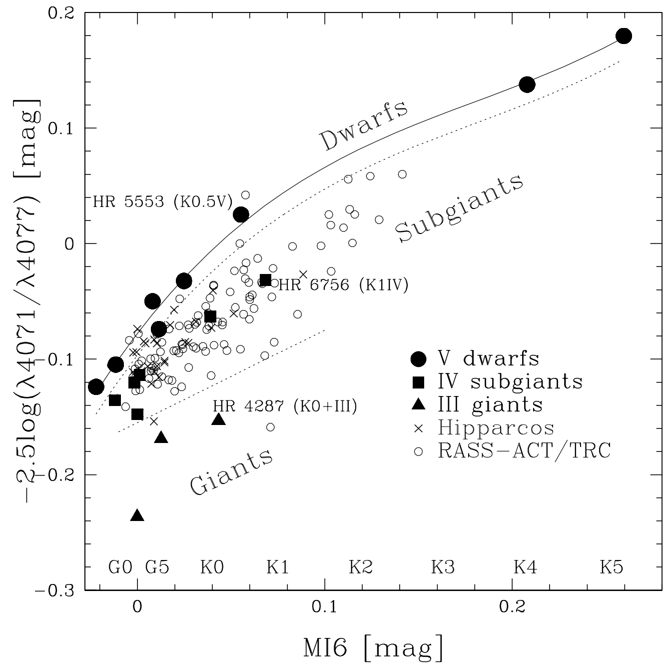

FIG. 1.—MI6 band ratio ($T_{\rm eff}$ indicator) vs. Fe I λ4071/Sr II λ4077 band ratio (surface gravity indicator). The solid line is a polynomial fit to only the dwarf standards. The dashed lines separate dwarfs, subgiants, and giants. The dwarf-subgiant dashed line is −2 times the σ-residual below the dwarf regression, whereas the subgiant-giant boundary is placed somewhat arbitrarily to resolve the observed subgiant and giant loci. Empirically, this diagram suggests that most of the target stars are consistent with being G- and K-type subgiants, with few giant and dwarf interlopers. A few early K standards are noted for reference.

The adopted spectral types are those of Keenan & McNeil's; however, the luminosity classification was verified (and some changed) by virtue of (1) the position of the stars on a color-magnitude diagram based on *Hipparcos* data, (2) the position in a temperature versus Sr II λ4077/Fe I λ4071 diagram (see § 4.1.3, Fig. 1), and (3) the published log g estimates. Although changing the classification of some standards may appear imprudent, the H-R diagram positions, Sr/Fe line ratio, and derived log g values (Cayrel de Strobel, Soubiran, & Ralite 2001) *are all consistent with our new adopted luminosity classes.*[3] In every case, the difference was only half of a luminosity class, and only five out of 20 of the stars were changed. Notes on the revised luminosity classifications are given in Appendix B.

4.1.2. *Visual Classification*

The blue spectrum of each star was assigned a spectral type visually by E. M. through comparison with the standards in Table 3. In order to distinguish subtypes, we focused on several features such as the G band (λ4310), Ca I λ4227, Cr I λ4254 and nearby Fe lines, and the Mg b lines λ5167, λ5173, and λ5184. Balmer lines were ignored because of chromospheric emission. After making an initial guess through comparison with a wide range of spectral

[3] *Hipparcos* data also led Keenan & Barnbaum (1999) to revise the luminosity classes of a few giant star standards at the half luminosity class level.

TABLE 2

PROPERTIES OF RASS-ACT/TRC CANDIDATES

Name TYC (1)	OB Group (2)	α (J2000.0) (3)	δ (J2000.0) (4)	$\mu_{\alpha*}$ (mas yr^{-1}) (5)	μ_δ (mas yr^{-1}) (6)	V_T (mag) (7)	B_T-V_T (mag) (8)	J (mag) (9)	H (mag) (10)	K_s (mag) (11)	1RXS Name (12)	Sep. (arcsec) (13)	X-ray (counts s^{-1}) (14)	HR1 (15)	Table 4 No.
9212-2011-1	LCC	10 57 49.38	−69 13 59.9	−36.1 ± 2.4	5.7 ± 2.3	10.49 ± 0.04	1.09 ± 0.08	8.49 ± 0.03	8.02 ± 0.05	7.79 ± 0.01	J105751.2−691402	10	1.61E−01	0.31	1
8625-388-1	LCC	11 32 08.34	−58 03 20.0	−41.6 ± 3.1	−1.4 ± 3.0	10.02 ± 0.03	1.02 ± 0.06	8.09 ± 0.02	7.64 ± 0.04	7.48 ± 0.02	J113209.3−580319	7	8.25E−02	0.03	2
8222-105-1	LCC	11 35 03.76	−48 50 22.0	−24.7 ± 2.0	−7.0 ± 1.9	10.35 ± 0.03	0.75 ± 0.05	9.22 ± 0.02	8.93 ± 0.03	8.86 ± 0.03	J113501.5−485011	24	1.01E−01	0.49	...
8982-3046-1	LCC	12 04 14.42	−64 18 51.7	−28.9 ± 3.9	−4.7 ± 3.7	10.09 ± 0.03	0.75 ± 0.05	8.82 ± 0.01	8.50 ± 0.02	8.40 ± 0.02	J120413.3−641837	16	2.77E−01	0.32	...
8982-3213-1	LCC	12 04 48.87	−64 09 55.4	−32.9 ± 3.5	+0.8 ± 3.1	9.49 ± 0.02	0.79 ± 0.03	8.05 ± 0.01	7.71 ± 0.01	7.61 ± 0.01	J120448.2−640942	13	3.47E−01	0.46	3
8640-2515-1	LCC	12 06 13.54	−57 02 16.8	−24.6 ± 2.8	−7.7 ± 2.6	10.77 ± 0.05	0.81 ± 0.08	9.25 ± 0.03	8.84 ± 0.03	8.77 ± 0.03	J120613.9−570215	3	1.44E−01	0.27	4
8644-802-1	LCC	12 09 41.86	−58 54 45.0	−33.8 ± 3.1	−11.8 ± 2.8	10.21 ± 0.03	1.26 ± 0.07	8.31 ± 0.01	7.81 ± 0.01	7.66 ± 0.01	J120941.5−585440	5	2.33E−01	0.16	5
8644-340-1	LCC	12 11 31.43	−58 16 53.2	−36.0 ± 2.6	−8.7 ± 1.8	10.29 ± 0.04	1.00 ± 0.07	8.58 ± 0.01	8.09 ± 0.03	7.96 ± 0.02	J121131.9−581651	4	2.41E−01	0.09	6
9231-1566-1	LCC	12 11 38.14	−71 10 36.0	−38.9 ± 1.4	−8.3 ± 1.4	9.23 ± 0.02	0.79 ± 0.03	7.68 ± 0.01	7.31 ± 0.04	7.19 ± 0.02	J121137.3−711032	5	2.68E−01	0.34	7
8636-2515-1	LCC	12 12 35.75	−55 20 27.3	−34.5 ± 2.1	−13.4 ± 2.3	10.58 ± 0.04	1.11 ± 0.08	8.73 ± 0.02	8.25 ± 0.03	8.13 ± 0.02	J121236.4−552037	11	1.83E−01	−0.02	8
8242-1324-1	LCC	12 14 34.09	−51 10 12.5	−35.7 ± 2.1	−12.9 ± 1.9	10.38 ± 0.03	1.05 ± 0.06	8.69 ± 0.01	8.26 ± 0.04	8.13 ± 0.02	J121434.2−511004	8	1.77E−01	0.32	9
8637-2610-1	LCC	12 14 52.31	−55 47 03.6	−38.3 ± 3.6	−7.2 ± 3.4	9.73 ± 0.02	0.92 ± 0.04	8.04 ± 0.02	7.66 ± 0.02	7.52 ± 0.01	J121452.4−554704	0	5.65E−01	0.37	10
8645-1339-1	LCC	12 18 27.64	−59 43 12.9	−41.6 ± 3.7	−1.9 ± 3.3	10.82 ± 0.05	0.95 ± 0.09	8.45 ± 0.01	7.84 ± 0.01	7.73 ± 0.01	J121828.6−594307	8	1.78E−01	0.39	11
8641-2187-1	LCC	12 18 58.02	−57 37 19.2	−36.5 ± 1.8	−10.2 ± 1.5	9.96 ± 0.03	1.02 ± 0.05	7.96 ± 0.01	7.47 ± 0.04	7.31 ± 0.01	J121858.2−573713	5	2.93E−01	0.23	12
8983-98-1	LCC	12 19 21.64	−64 54 10.4	−37.0 ± 3.0	−11.2 ± 2.8	10.21 ± 0.04	1.01 ± 0.07	8.03 ± 0.01	7.55 ± 0.01	7.38 ± 0.01	J121919.4−645406	14	2.55E−01	0.26	13
8633-508-1	LCC	12 21 16.48	−53 17 44.9	−36.8 ± 1.9	−7.7 ± 1.8	9.41 ± 0.02	0.76 ± 0.03	8.08 ± 0.01	7.74 ± 0.02	7.65 ± 0.02	J122116.7−531747	3	4.34E−01	−0.03	14
8238-1462-1	LCC	12 21 55.65	−49 46 12.5	−37.4 ± 1.5	−14.2 ± 1.3	10.10 ± 0.03	0.90 ± 0.05	8.49 ± 0.02	8.05 ± 0.02	8.02 ± 0.03	J122155.9−494609	3	1.13E−01	0.59	15
8234-2856-1	LCC	12 22 04.30	−48 41 24.9	−30.0 ± 2.0	−12.1 ± 1.9	10.59 ± 0.04	0.95 ± 0.06	8.78 ± 0.02	8.27 ± 0.03	8.17 ± 0.01	J122204.0−484118	7	1.10E−01	0.88	16
8633-28-1	LCC	12 22 33.23	−53 33 49.0	−31.7 ± 1.5	−7.7 ± 1.5	9.49 ± 0.02	0.72 ± 0.03	8.18 ± 0.01	7.91 ± 0.04	7.78 ± 0.02	J122233.4−533347	2	1.43E−01	0.00	17
8641-1281-1	LCC	12 23 40.13	−56 16 32.5	−33.1 ± 3.3	−14.0 ± 3.0	10.94 ± 0.06	0.94 ± 0.09	9.02 ± 0.02	8.53 ± 0.05	8.37 ± 0.03	J122339.9−561628	4	8.03E−02	0.15	18
8992-605-1	LCC	12 36 38.97	−63 44 43.5	−37.8 ± 2.0	−9.7 ± 1.9	9.98 ± 0.03	1.10 ± 0.05	8.02 ± 0.01	7.51 ± 0.01	7.35 ± 0.01	J123637.5−634446	10	2.17E−01	0.09	19
8646-166-1	LCC	12 36 58.97	−54 12 18.0	−32.3 ± 3.3	−13.9 ± 3.0	10.50 ± 0.04	1.07 ± 0.07	8.75 ± 0.04	8.28 ± 0.03	8.16 ± 0.02	J123657.4−541217	13	1.06E−01	0.44	20
8654-1115-1	LCC	12 39 37.96	−57 31 40.7	−35.2 ± 2.5	−21.9 ± 2.4	10.21 ± 0.03	0.88 ± 0.05	8.67 ± 0.01	8.23 ± 0.04	8.13 ± 0.03	J123938.4−573141	3	2.34E−01	0.33	21
8659-2604-1	LCC	12 41 18.17	−58 25 56.0	−37.7 ± 2.5	−17.6 ± 2.3	10.01 ± 0.03	0.81 ± 0.05	8.40 ± 0.01	8.02 ± 0.02	7.89 ± 0.01	J124118.5−582556	2	1.19E−01	0.81	22
8992-420-1	LCC	12 44 34.82	−63 31 46.2	−31.2 ± 3.3	−7.7 ± 3.0	10.91 ± 0.05	1.40 ± 0.14	8.54 ± 0.01	8.01 ± 0.01	7.87 ± 0.01	J124432.6−633139	16	2.11E−01	0.39	23
8249-52-1	LCC	12 45 06.76	−47 42 58.2	−31.2 ± 1.3	−14.4 ± 1.3	10.48 ± 0.04	0.86 ± 0.06	8.70 ± 0.02	8.23 ± 0.02	8.10 ± 0.01	J124506.9−474254	4	2.22E−01	0.30	24
7783-1908-1	LCC	12 48 07.79	−44 39 16.8	−39.7 ± 1.3	−18.0 ± 1.3	9.82 ± 0.03	0.93 ± 0.05	8.12 ± 0.01	7.69 ± 0.05	7.51 ± 0.02	J124807.6−443913	4	4.33E−01	0.05	25
8655-149-1	LCC	12 48 48.18	−56 35 37.8	−29.4 ± 1.7	−9.4 ± 1.7	10.31 ± 0.03	0.92 ± 0.05	8.88 ± 0.01	8.48 ± 0.02	8.39 ± 0.02	J124847.4−563525	13	9.77E−02	0.77	26
9245-617-1	LCC	12 58 25.58	−70 28 49.2	−43.1 ± 1.5	−18.7 ± 1.5	10.01 ± 0.03	0.98 ± 0.06	8.20 ± 0.02	7.70 ± 0.06	7.56 ± 0.02	J125824.6−702848	4	2.30E−01	0.11	27
8648-446-1	LCC	13 01 50.70	−53 04 58.3	−32.6 ± 4.4	−19.5 ± 4.0	11.18 ± 0.06	1.02 ± 0.13	9.44 ± 0.02	8.91 ± 0.02	8.78 ± 0.02	J130153.7−530446	29	8.19E−02	0.12	28
8652-1791-1	LCC	13 02 37.54	−54 59 36.8	−25.5 ± 2.0	−6.6 ± 2.0	10.35 ± 0.03	0.72 ± 0.05	8.86 ± 0.01	8.57 ± 0.03	8.48 ± 0.02	J130237.2−545933	4	1.59E−01	0.92	29
8258-1878-1	LCC	13 06 40.12	−51 59 38.6	−33.3 ± 2.4	−15.7 ± 2.2	10.62 ± 0.04	0.91 ± 0.07	8.90 ± 0.01	8.44 ± 0.04	8.27 ± 0.01	J130638.5−515948	17	8.46E−02	0.58	30
8990-701-1	LCC	13 13 28.11	−60 00 44.6	−26.6 ± 3.0	−5.3 ± 2.8	10.08 ± 0.02	0.70 ± 0.04	8.76 ± 0.01	8.45 ± 0.02	8.42 ± 0.02	J131327.3−600032	13	1.23E−01	0.36	...
8259-689-1	LCC	13 14 23.84	−50 54 01.9	−27.4 ± 2.1	−16.4 ± 1.9	10.48 ± 0.04	0.96 ± 0.08	8.68 ± 0.03	8.27 ± 0.03	8.10 ± 0.04	J131424.3−505402	4	2.72E−01	0.41	31
8649-251-1	LCC	13 17 56.94	−53 17 56.2	−23.4 ± 3.4	−8.3 ± 3.2	10.48 ± 0.05	0.72 ± 0.08	8.86 ± 0.03	8.49 ± 0.05	8.39 ± 0.03	J131754.9−531758	18	1.60E−01	0.36	32
8248-539-1	LCC	13 22 04.46	−45 03 23.1	−26.7 ± 1.6	−13.3 ± 1.4	10.10 ± 0.03	0.77 ± 0.06	8.97 ± 0.03	8.63 ± 0.05	8.55 ± 0.03	J132204.7−450312	10	7.06E−02	0.53	33
9246-971-1	LCC	13 22 07.54	−69 38 12.3	−40.8 ± 2.5	−23.0 ± 2.3	10.54 ± 0.04	1.08 ± 0.08	8.28 ± 0.03	7.65 ± 0.02	7.31 ± 0.01	J132207.2−693812	1	1.58E−01	0.59	34
8663-1375-1	LCC	13 34 20.26	−52 40 36.1	−33.4 ± 1.6	−21.1 ± 1.3	9.37 ± 0.02	0.71 ± 0.03	8.04 ± 0.01	7.69 ± 0.04	7.56 ± 0.03	J133420.0−524032	4	2.51E−01	0.44	35
7796-1788-1	UCL	13 37 57.29	−41 34 41.9	−36.7 ± 1.2	−24.2 ± 1.2	10.17 ± 0.04	0.97 ± 0.06	8.47 ± 0.01	8.03 ± 0.04	7.89 ± 0.02	J133758.0−413448	10	2.22E−01	0.27	36
8667-283-1	LCC	13 43 28.53	−54 36 43.5	−44.0 ± 1.8	−20.8 ± 1.8	9.39 ± 0.02	0.77 ± 0.03	8.03 ± 0.01	7.68 ± 0.01	7.63 ± 0.02	J134332.7−543638	36	4.81E−01	0.22	37
8270-2015-1	UCL	13 47 50.55	−49 02 05.5	−24.3 ± 2.2	−14.7 ± 2.0	10.91 ± 0.07	0.90 ± 0.11	9.30 ± 0.01	8.81 ± 0.05	8.70 ± 0.03	J134748.0−490158	26	1.50E−01	−0.10	38
8263-2453-1	UCL	13 52 47.80	−46 44 09.2	−22.7 ± 1.3	−18.9 ± 1.4	9.69 ± 0.03	0.72 ± 0.04	8.41 ± 0.02	8.07 ± 0.04	7.94 ± 0.01	J135247.0−464412	8	1.96E−01	0.67	39
7811-2909-1	UCL	14 02 20.73	−41 44 50.8	−27.6 ± 2.0	−19.4 ± 1.9	10.80 ± 0.06	0.90 ± 0.10	8.99 ± 0.02	8.55 ± 0.04	8.42 ± 0.03	J140220.9−414435	15	9.68E−02	0.37	40
7815-2029-1	UCL	14 09 03.58	−44 38 44.4	−20.9 ± 1.1	−22.6 ± 1.1	9.46 ± 0.02	0.71 ± 0.04	8.25 ± 0.01	7.98 ± 0.05	7.86 ± 0.02	J140902.6−443838	12	1.73E−01	0.67	41
9244-814-1	LCC	14 16 05.67	−69 17 36.0	−29.4 ± 2.4	−16.0 ± 2.3	10.21 ± 0.03	0.72 ± 0.06	8.74 ± 0.01	8.39 ± 0.02	8.36 ± 0.02	J141605.3−691756	20	6.10E−02	0.47	42
8285-847-1	UCL	14 16 57.91	−49 56 42.3	−23.2 ± 1.1	−22.1 ± 1.1	8.77 ± 0.01	0.71 ± 0.02	7.43 ± 0.02	7.12 ± 0.02	7.03 ± 0.01	J141658.4−495648	7	1.59E−01	0.15	...
8282-516-1	UCL	14 27 05.56	−47 14 21.8	−25.5 ± 1.7	−21.2 ± 1.6	10.68 ± 0.05	0.95 ± 0.08	9.06 ± 0.03	8.65 ± 0.03	8.52 ± 0.03	J142705.3−471420	3	1.53E−01	−0.12	43
7817-622-1	UCL	14 28 09.30	−44 14 17.4	−18.4 ± 2.0	−20.6 ± 1.9	9.87 ± 0.03	0.90 ± 0.05	8.31 ± 0.01	7.93 ± 0.03	7.78 ± 0.03	J142809.6−441438	20	1.45E−01	0.13	44
7813-224-1	UCL	14 28 19.38	−42 19 34.1	−19.7 ± 1.5	−19.8 ± 1.7	10.55 ± 0.05	0.79 ± 0.09	8.92 ± 0.01	8.51 ± 0.03	8.40 ± 0.03	J142817.6−421958	31	2.23E−01	0.34	45
7814-1450-1	UCL	14 37 04.22	−41 45 03.0	−21.5 ± 2.0	−19.1 ± 1.9	9.77 ± 0.02	0.72 ± 0.04	8.26 ± 0.01	7.90 ± 0.02	7.80 ± 0.03	J143704.6−414504	4	1.68E−01	0.58	46
8683-242-1	UCL	14 37 50.23	−54 57 41.1	−18.3 ± 2.5	−25.8 ± 2.4	10.80 ± 0.06	0.77 ± 0.09	8.94 ± 0.01	8.46 ± 0.02	8.32 ± 0.02	J143750.9−545708	33	2.20E−01	0.07	47

TABLE 2—*Continued*

Name TYC (1)	OB Group (2)	α (J2000.0) (3)	δ (J2000.0) (4)	$\mu_{\alpha *}$ (mas yr^{-1}) (5)	μ_δ (mas yr^{-1}) (6)	V_T (mag) (7)	B_T-V_T (mag) (8)	J (mag) (9)	H (mag) (10)	K_s (mag) (11)	1RXS Name (12)	Sep. (arcsec) (13)	X-ray (counts s^{-1}) (14)	HR1 (15)	Table 4 No.
8283-264-1	UCL	14 41 35.00	−47 00 28.8	−29.6 ± 1.3	−27.4 ± 1.2	10.09 ± 0.03	0.88 ± 0.04	8.43 ± 0.01	7.98 ± 0.03	7.88 ± 0.03	J144135.3−470039	11	6.12E−01	0.15	48
8283-2795-1	UCL	14 47 31.77	−48 00 05.7	−29.6 ± 2.3	−16.7 ± 2.3	10.79 ± 0.06	0.75 ± 0.09	9.37 ± 0.01	9.04 ± 0.01	8.96 ± 0.03	J144732.2−480019	14	7.37E−02	0.50	49
7305-380-1	UCL	14 50 25.81	−35 06 48.6	−18.2 ± 2.6	−15.8 ± 2.6	10.83 ± 0.07	0.97 ± 0.13	8.75 ± 0.03	8.24 ± 0.02	8.11 ± 0.03	J145025.4−350645	6	9.03E−02	0.35	50
7828-2913-1	UCL	14 52 41.98	−41 41 55.2	−22.6 ± 2.2	−21.4 ± 2.1	11.02 ± 0.09	1.35 ± 0.22	9.05 ± 0.02	8.40 ± 0.02	8.29 ± 0.03	J145240.7−414206	17	1.30E−01	0.21	51
7310-2431-1	UCL	14 57 19.63	−36 12 27.4	−26.6 ± 1.6	−22.3 ± 1.7	10.36 ± 0.05	0.97 ± 0.09	8.78 ± 0.03	8.44 ± 0.04	8.30 ± 0.03	J145720.4−361242	17	8.67E−02	0.69	52
7310-503-1	UCL	14 58 37.70	−35 40 30.4	−21.4 ± 2.2	−26.0 ± 2.3	10.88 ± 0.07	1.37 ± 0.20	8.65 ± 0.01	8.08 ± 0.03	7.90 ± 0.01	J145837.6−354036	5	8.30E−02	0.60	53
7824-1291-1	UCL	14 59 22.76	−40 13 12.1	−26.0 ± 1.4	−26.5 ± 1.6	9.80 ± 0.04	0.86 ± 0.07	8.34 ± 0.01	7.97 ± 0.04	7.82 ± 0.02	J145923.0−401319	7	1.87E−01	0.35	54
7833-2037-1	UCL	15 00 51.88	−43 31 21.0	−20.1 ± 2.1	−19.1 ± 2.0	11.23 ± 0.08	0.81 ± 0.13	9.31 ± 0.03	8.88 ± 0.02	8.75 ± 0.03	J150052.5−433107	15	7.57E−02	0.39	55
7829-504-1	UCL	15 01 11.56	−41 20 40.6	−14.9 ± 1.7	−15.1 ± 1.7	10.09 ± 0.03	0.77 ± 0.06	8.78 ± 0.03	8.47 ± 0.05	8.33 ± 0.03	J150112.0−412040	4	1.78E−01	0.41	56
8297-1613-1	UCL	15 01 58.82	−47 55 46.4	−22.2 ± 1.7	−18.2 ± 1.6	10.22 ± 0.04	0.71 ± 0.07	8.91 ± 0.01	8.59 ± 0.02	8.51 ± 0.02	J150158.5−475559	13	5.07E−02	0.42	57
7319-749-1	UCL	15 07 14.81	−35 04 59.6	−34.1 ± 2.4	−30.1 ± 2.5	10.59 ± 0.06	1.00 ± 0.11	8.87 ± 0.01	8.42 ± 0.05	8.35 ± 0.03	J150714.5−350500	3	7.39E−02	0.71	58
7833-1106-1	UCL	15 08 00.55	−43 36 24.9	−21.8 ± 1.4	−16.5 ± 1.4	9.93 ± 0.03	0.87 ± 0.06	8.20 ± 0.01	7.86 ± 0.04	7.71 ± 0.02	J150759.9−433642	18	8.84E−02	0.88	...
7833-2400-1	UCL	15 08 37.75	−44 23 16.9	−17.9 ± 2.1	−17.6 ± 2.0	10.91 ± 0.07	0.80 ± 0.11	9.33 ± 0.03	8.95 ± 0.02	8.81 ± 0.03	J150836.0−442325	20	1.73E−01	0.45	59
7833-2559-1	UCL	15 08 38.50	−44 00 52.1	−23.5 ± 2.1	−24.2 ± 1.9	10.61 ± 0.05	0.70 ± 0.09	8.95 ± 0.02	8.54 ± 0.03	8.54 ± 0.03	J150838.5−440048	4	1.21E−01	0.19	60
8293-92-1	UCL	15 09 27.93	−46 50 57.2	−19.9 ± 2.1	−16.1 ± 2.0	10.60 ± 0.05	1.09 ± 0.09	8.39 ± 0.04	7.83 ± 0.04	7.72 ± 0.02	J150928.2−465109	12	7.77E−02	1.00	...
8294-2230-1	UCL	15 12 50.18	−45 08 04.5	−19.8 ± 2.1	−22.4 ± 2.0	10.79 ± 0.07	0.85 ± 0.11	9.13 ± 0.01	8.74 ± 0.03	8.67 ± 0.02	J151250.0−450822	17	1.45E−01	0.19	61
8694-1685-1	UCL	15 18 01.74	−53 17 28.8	−28.7 ± 2.5	−28.3 ± 2.3	10.21 ± 0.04	0.86 ± 0.07	8.51 ± 0.02	8.12 ± 0.04	8.01 ± 0.02	J151802.0−531719	10	2.23E−01	−0.04	62
7822-158-1	UCL	15 18 26.91	−37 38 02.1	−22.5 ± 2.6	−28.3 ± 2.6	11.11 ± 0.09	0.87 ± 0.15	9.07 ± 0.03	8.63 ± 0.04	8.53 ± 0.03	J151827.3−373808	7	1.30E−01	0.37	63
8295-1530-1	UCL	15 25 59.65	−45 01 15.8	−21.9 ± 2.2	−21.3 ± 2.0	10.98 ± 0.07	0.88 ± 0.12	9.45 ± 0.02	8.98 ± 0.02	8.88 ± 0.02	J152600.9−450113	13	6.10E−02	−0.15	64
7326-928-1	UCL	15 29 38.58	−35 46 51.3	−21.7 ± 2.0	−26.1 ± 2.1	10.54 ± 0.06	1.07 ± 0.11	8.77 ± 0.01	8.27 ± 0.03	8.19 ± 0.03	J152937.7−354656	11	1.05E−01	0.21	65
7318-593-1	UCL	15 31 21.93	−33 29 39.5	−25.8 ± 2.5	−31.5 ± 2.5	10.99 ± 0.08	0.72 ± 0.12	9.39 ± 0.03	8.95 ± 0.06	8.81 ± 0.03	J153121.8−333002	23	9.34E−02	0.06	...
7327-1934-1	UCL	15 37 02.14	−31 36 39.8	−17.8 ± 1.6	−29.0 ± 1.6	10.06 ± 0.04	0.70 ± 0.06	8.28 ± 0.03	7.76 ± 0.04	7.72 ± 0.02	J153701.9−313647	7	3.92E−01	0.32	66
7840-1280-1	UCL	15 37 11.30	−40 15 56.8	−16.7 ± 1.9	−22.5 ± 1.9	10.55 ± 0.05	1.24 ± 0.10	8.98 ± 0.01	8.46 ± 0.05	8.31 ± 0.03	J153711.6−401608	11	2.27E−01	−0.14	67
7848-1659-1	UCL	15 38 43.06	−44 11 47.4	−23.2 ± 1.6	−28.4 ± 1.5	10.36 ± 0.05	0.85 ± 0.08	8.81 ± 0.05	8.36 ± 0.04	8.22 ± 0.03	J153843.1−441149	1	1.41E−01	−0.01	68
6785-510-1	UCL	15 39 24.41	−27 10 21.9	−20.2 ± 1.7	−29.8 ± 1.6	9.65 ± 0.03	0.81 ± 0.05	8.04 ± 0.03	7.64 ± 0.03	7.53 ± 0.01	J153924.0−271035	14	2.33E−01	0.59	69
7331-782-1	UCL	15 44 03.77	−33 11 11.2	−22.2 ± 2.6	−29.7 ± 2.6	10.97 ± 0.07	0.95 ± 0.12	9.05 ± 0.02	8.55 ± 0.01	8.41 ± 0.03	J154404.1−331120	10	7.72E−02	0.42	70
7845-1174-1	UCL	15 45 52.25	−42 22 16.5	−18.0 ± 1.5	−30.4 ± 1.6	10.61 ± 0.05	1.15 ± 0.09	8.69 ± 0.02	8.09 ± 0.04	7.94 ± 0.02	J154552.7−422227	11	4.13E−01	0.07	71
8317-551-1	UCL	15 46 51.79	−49 19 04.7	−19.7 ± 1.6	−27.9 ± 1.5	10.29 ± 0.04	1.04 ± 0.08	8.69 ± 0.01	8.36 ± 0.03	8.31 ± 0.02	J154651.5−491922	17	1.78E−01	0.07	72
7842-250-1	UCL	15 56 59.05	−39 33 43.1	−15.1 ± 2.0	−21.6 ± 2.0	10.90 ± 0.07	0.94 ± 0.12	9.20 ± 0.02	8.83 ± 0.03	8.70 ± 0.03	J155659.0−393400	16	9.87E−02	−0.02	73
7333-1260-1	UCL	16 01 07.93	−32 54 52.5	−18.3 ± 1.4	−29.6 ± 1.5	9.58 ± 0.02	0.73 ± 0.04	8.46 ± 0.01	8.16 ± 0.04	8.08 ± 0.02	J160108.0−325455	3	1.93E−01	0.34	74
7333-719-1	UCL	16 01 08.97	−33 20 14.2	−12.3 ± 2.1	−23.0 ± 2.2	10.99 ± 0.07	1.15 ± 0.16	9.01 ± 0.02	8.55 ± 0.03	8.46 ± 0.03	J160108.9−332021	7	9.66E−02	0.75	75
7863-1629-1	UCL	16 03 45.37	−43 55 49.2	−12.5 ± 1.1	−22.6 ± 1.4	9.74 ± 0.03	1.06 ± 0.05	7.93 ± 0.02	7.42 ± 0.03	7.30 ± 0.01	J160345.8−435544	6	4.09E−01	0.21	76
7855-1106-1	UCL	16 03 52.50	−39 39 01.3	−16.4 ± 2.4	−28.4 ± 2.3	11.12 ± 0.08	1.15 ± 0.18	8.98 ± 0.03	8.35 ± 0.03	8.21 ± 0.03	J160352.0−393901	5	1.29E−01	−0.02	77
7851-1-1	UCL	16 05 45.00	−39 06 06.5	−16.8 ± 2.2	−31.1 ± 2.2	10.63 ± 0.06	1.00 ± 0.10	8.93 ± 0.02	8.52 ± 0.04	8.36 ± 0.03	J160545.8−390559	11	1.57E−01	0.46	78
7355-317-1	UCL	16 13 58.02	−36 18 13.4	−18.4 ± 2.0	−32.3 ± 2.1	11.26 ± 0.09	1.17 ± 0.21	9.41 ± 0.02	8.98 ± 0.03	8.84 ± 0.03	J161357.9−361813	1	1.74E−01	0.03	79
8319-1687-1	UCL	16 14 52.01	−50 26 18.5	−19.9 ± 2.1	−29.2 ± 2.0	10.50 ± 0.05	0.96 ± 0.09	8.38 ± 0.01	7.91 ± 0.01	7.76 ± 0.01	J161451.3−502621	7	2.37E−01	0.15	80
7852-51-1	UCL	16 18 38.56	−38 39 11.8	−25.9 ± 1.3	−34.0 ± 1.5	9.09 ± 0.02	0.69 ± 0.03	8.02 ± 0.01	7.79 ± 0.05	7.69 ± 0.02	J161839.0−383927	16	1.62E−01	−0.06	81
7857-648-1	UCL	16 21 12.19	−40 30 20.6	−9.1 ± 1.4	−28.1 ± 1.4	10.67 ± 0.05	1.01 ± 0.09	8.97 ± 0.02	8.55 ± 0.02	8.43 ± 0.02	J162112.0−403032	11	1.29E−01	0.13	82
7857-514-1	UCL	16 23 29.55	−39 58 00.8	−12.5 ± 2.1	−24.1 ± 2.1	10.73 ± 0.06	0.88 ± 0.09	9.47 ± 0.02	9.10 ± 0.03	8.99 ± 0.03	J162330.1−395806	8	7.93E−02	0.18	83
7853-227-1	UCL	16 27 30.55	−37 49 21.6	−10.0 ± 2.5	−23.4 ± 2.6	11.05 ± 0.07	0.84 ± 0.12	9.29 ± 0.02	8.81 ± 0.04	8.66 ± 0.03	J162730.0−374929	9	6.24E−02	1.00	84
7353-2640-1	UCL	16 31 42.03	−35 05 17.2	−16.2 ± 1.9	−27.6 ± 2.0	10.72 ± 0.05	0.81 ± 0.08	9.19 ± 0.02	8.75 ± 0.02	8.63 ± 0.02	J163143.7−350521	20	8.92E−02	0.52	85
7349-2191-1	UCL	16 35 35.99	−33 26 34.7	−6.0 ± 1.8	−23.0 ± 2.1	11.09 ± 0.07	0.93 ± 0.13	8.99 ± 0.02	8.44 ± 0.03	8.28 ± 0.02	J163533.9−332631	25	1.65E−01	0.37	86
7858-526-1	UCL	16 38 38.47	−39 33 03.5	−10.4 ± 1.3	−19.2 ± 1.3	9.05 ± 0.02	0.73 ± 0.04	7.52 ± 0.01	7.25 ± 0.02	7.15 ± 0.01	J163839.2−393307	9	8.45E−02	0.61	...
7858-830-1	UCL	16 39 59.30	−39 24 59.2	−9.7 ± 2.2	−18.9 ± 2.2	10.68 ± 0.08	0.84 ± 0.12	8.67 ± 0.02	8.26 ± 0.04	8.12 ± 0.02	J163958.7−392457	7	7.39E−02	0.96	87
7871-1282-1	UCL	16 42 24.00	−40 03 29.7	−11.1 ± 1.5	−20.2 ± 1.3	9.70 ± 0.03	0.88 ± 0.06	8.03 ± 0.03	7.63 ± 0.05	7.46 ± 0.02	J164224.5−400329	5	9.83E−02	0.44	88

Notes.—Col. (1): Tycho-2 name; col. (2): OB subgroup region; cols. (3) and (4): J2000.0 position from Tycho-2 catalog; cols. (5) and (6): proper motion (α^*, δ components) in mas yr^{-1} (where $\mu_{\alpha *} = \mu_\alpha \cos \delta$); col. (7): V_T magnitude; col. (8): $B-V_T$ color; cols. (9)–(11): 2MASS JHK_s magnitudes; col. (12): X-ray counterpart name in RASS BSC; col. (13): optical–X-ray separation; col. (14): X-ray count rate (ct s^{-1}); col. (15): Hardness ratio HR1; col. (16): number in Table 4 if star is found to be PMS or PMS? in nature. X-ray data is from RASS BSC (Voges et al. 1999), astrometry and optical photometry are from Tycho-2 catalog (Høg et al. 2000b), and near-IR photometry is from the 2MASS working database.

TABLE 3
Spectral Standard Stars

HD	HR	MK Sp.Type	V (mag)	$\pi \pm \sigma_\pi$ (mas)	$B-V$ (mag)	[Fe/H] Adopted	MSS Sp.Type	Adopted Sp.Type	Notes
182640	7377	F0 IV	3.36	65.1 ± 0.8	0.32	. . .	F2 V	F0 IV	a,b
173677	7061	F6 V	4.19	52.4 ± 0.7	0.48	−0.1	. . .	F6 IV–V	c
84117	3862	F9 V	4.93	67.2 ± 0.7	0.53	. . .	G0 V	F9 V	
121370	5235	G0 IV	2.68	88.2 ± 0.8	0.58	0.2	. . .	G0 IV	b
89010	4030	G1.5 IV–V	5.95	32.9 ± 0.9	0.66	0.0	. . .	G1.5 IV–V	
126868	5409	G2 IV	4.84	24.2 ± 1.0	0.69	0.0	G3 V	G2 III–IV	a,d
161239	6608	G2 IIIb	5.73	26.1 ± 0.6	0.68	. . .	. . .	G2 IV	
146233	6060	G2 Va	5.49	71.3 ± 0.9	0.65	0.0	G5 V	G2 V	a
94481	4255	G4 III	5.65	8.0 ± 0.8	0.83	. . .	K0 III+(G)	G4 III	
117176	5072	G4 V	4.97	55.2 ± 0.7	0.71	−0.1	. . .	G4 IV–V	e
188376	7597	G5 IV	4.70	42.0 ± 0.9	0.75	−0.1	G3/5 III	G5 IV	f
115617	5019	G6.5 V	4.74	117.3 ± 0.7	0.71	0.0	G5 V	G6.5 V	
114946	4995	G7 IV–V	5.31	25.9 ± 0.7	0.86	−0.1:	G8 III/IV	G7 IV	
188512	7602	G8 IV	3.71	73.0 ± 0.8	0.86	0.0:	. . .	G8 IV	a
165760	6770	G8 III	4.64	13.7 ± 0.8	0.95	−0.1	. . .	G8 III	
95272	4287	K0+ III	4.08	18.7 ± 1.0	1.08	−0.1:	K1 III	K0+III	
131511	5553	K0.5 V	6.00	86.7 ± 0.8	0.84	. . .	. . .	K0.5 V	a
165438	6756	K1 IV	5.74	28.6 ± 0.8	0.97	0.0	K0 IV	K1 IV	
131977	5568	K4 V	5.72	169.3 ± 1.7	1.02	0.0	K4 V	K4 V	
120467	. . .	K6 Va	8.16	70.5 ± 1.0	1.26	. . .	. . .	K6 V	

Notes.—(MSS) Michigan Spectral Survey, Vols. 1–5 (Houk & Cowley 1975; Houk 1978, 1982; Houk & Smith-Moore 1988; Houk & Swift 1999). The [Fe/H] estimate is adopted from the compilation of published values in Cayrel de Strobel et al. 2001. A semicolon after the [Fe/H] value indicates considerable scatter (greater than 0.2 dex) in the published estimates.

[a] SIMBAD lists as variable or suspected variable, but *Hipparcos* finds scatter in $H_p \leq 0.015$ mag. The typical scatter for the other standard stars was 0.005 mag in H_p (*Hipparcos* magnitude), with none greater than 0.01 mag.

[b] Spectroscopic binary.

[c] From standard list of Garcia 1989 and originally in Johnson & Morgan 1953, but not listed in either Keenan & Yorka 1988 or Keenan & McNeil 1989.

[d] HR 5409 is a resolved binary (separation of 5″) listed by SIMBAD as a variable star, but *Hipparcos* found the scatter in the H_p band to be only 0.015 mag.

[e] HR 5072 is the planet host 70 Vir. Keenan & McNeil 1989 call it G4 V, however it is G5 V in virtually every other reference (e.g., Gray, Graham, & Hoyt 2001). We retain Keenan's classification.

[f] *Hipparcos* " G " binary.

types, a final visual spectral type was assigned through comparison to standards within ±2 subtypes of the initial guess.

To test the accuracy of our visual classification, we compared our spectral types to those of quality 1 or 2 in the Michigan Spectral Survey. The average difference is not significant: -0.4 ± 0.6 (1 σ sample standard deviation) subtypes (on Keenan's scale). The 12 *Hipparcos* stars were later visually typed a second time. Between the two estimates for each star, we estimate that the 1 σ uncertainty in our visual spectral types is 0.6 subtypes. This is comparable to the dispersion between the Keenan and Houk spectral types for the standards themselves.

4.1.3. *Quantitative Spectral Type Estimation*

A two-dimensional quantitative spectral type (subtype plus luminosity class) can be estimated using integrated fluxes over narrow bands sensitive to temperature and surface gravity. We tested various ratios defined by Malyuto & Schmidt-Kaler (1997) and Rose (1984) for this purpose, as well as from Gray's (2000)[4] spectral atlas. In testing band ratios as temperature indicators for our standards, we noticed that some had slight surface gravity dependencies. A surface gravity dependence in our temperature indicators could systematically affect our $T_{\rm eff}$ estimates. We first discuss our surface gravity indicator and then define our temperature estimators using only subgiant and dwarf standards, thus mitigating the effects of surface gravity.

The most widely used surface gravity diagnostic for G and K stars is the ratio between Sr II λ4077 and nearby Fe lines (e.g., Keenan & McNeil 1976; Gray 2000). In thin and thick disk dwarfs, the abundance ratio [Sr/Fe] is within ∼0.1 dex of solar for most stars (Mashonkina & Gehren 2001). A quantitative surface gravity (luminosity class) indicator was established by Rose (1984) from low-resolution spectra using the maximum absorption line depth for Sr II λ4077 and the average for the atomic Fe λ4045 and λ4063 lines. We measure the fluxes in 3 Å bands centered on the Sr II λ4077 line and the Fe I λ4071 line. Ratios between the λ4077 line and the other nearby Fe lines (λ4045 and λ4063) did not distinguish subgiants and giants.

For a temperature estimator, we adopted index 6 of Malyuto & Schmidt-Kaler (1997) (λλ5125–5245/λλ5245–5290), hereafter referred to as " MI6." The temperature sensitivity of this indicator largely reflects differing amounts of line blanketing in these two wavelength regimes—mainly by the Mg *b* lines (λ5167, λ5173, and λ5184) and many Fe lines (e.g., Fe I λ5270). Although the Mg *b* lines are somewhat surface gravity sensitive, within the log g and $T_{\rm eff}$ regime of our standards and program stars, the temperature sensitivity is dominant. The difference in central wavelength between the two bandpasses is only 82 Å, and the effects of reddening are negligible (Mathis 1990). For a temperature indicator, we fitted a low-order polynomial to MI6 versus

[4] See http://nedwww.ipac.caltech.edu/level5/Gray/.

Sp. for the dwarf and subgiant standard stars (see Appendix C) that has a 1 σ sample standard deviation of 0.6 subtypes.

Figure 1 plots the temperature-sensitive MI6 index versus our surface gravity discriminant (Sr II λ4077/Fe I λ4071). The dwarf standards form a very narrow sequence in Figure 1, *confirming the lack of cosmic scatter in* [Sr/Fe] *values among field stars and the insensitivity of* log *g to spectral type for G–K dwarfs*. The polynomial fit to the dwarf data is given in Appendix C. There is a gap between the dwarf and subgiant loci between ~1 and 2.5 σ (sample standard deviation) of the dwarf locus polynomial, and we set the subgiant/dwarf separation at 2 σ. We classify stars within 2 σ of the solid dwarf line in Figure 1 as dwarfs (four of 96 RASS-ACT/TRC stars and four of 20 HIP stars) and three stars near the giant locus (TYC 8992-605-1, HIP 68726, and HIP 74501) as giants. We classify the rest as subgiants.

Gray (2000) suggests Y II λ4376/Fe I λ4383 as a surface gravity indicator for late G stars using low-resolution spectra. From the solar spectral atlas of Wallace, Hinkle, & Livingston (1998), it appears that Gray's low-resolution Y II λ4376 feature is actually a blend of several lines of nearly equal strength. In order to test the properties of this band ratio, we measure the flux in 3 Å windows centered on wavelengths 4383.6 and 4374.5 Å. Plotting this ratio against spectral type for the standard stars showed a very tight locus for the dwarfs; however; luminosity classes IV–V, IV, and III were indistinguishable from the dwarfs and each other. We found this ratio unsuitable for the purposes of luminosity classification of our targets, but we find it to be an excellent temperature estimator for FGK dwarfs, subgiants, and giants. Among the 20 standards, the measurement of the λ4374/λ4383 band ratio versus spectral type gives a tight correlation (sample standard deviation 1 $\sigma = 0.6$ subtypes). We adopt the λ4374/λ4383 band ratio as our third independent estimator of spectral type (polynomial fit is given in Appendix C).

4.1.4. *Final Spectral Types*

The three temperature-type estimates agree well for the majority of the program stars. The mean difference between the MI6 and visual spectral types is 0.7 subtypes. The mean difference between the λ4374/λ4383 band-ratio types and the visual types is 0.6 subtypes. We calculate a mean spectral type and standard error of the mean using the three classifications. The mean is unweighted since all three relations appeared to have 1 σ sample standard deviations of $\approx$0.6 subtypes in their accuracy. The average standard error of the mean is 0.5 subtypes. We believe that using multiple techniques mitigates the effects that rapid rotation, binarity, etc., can introduce into visual classification alone. The spectral types are listed in Tables 4, 5, and 6.

4.2. *Additional Spectroscopic Diagnostics*

4.2.1. *Chromospheric* Hα *Emission*

Medium-to-low resolution spectra of chromospherically active stars show the Hα line to be partially filled in or even fully in emission. We measure the equivalent width (EW) of the entire Hα feature; our resolution is insufficient to separate the "core" chromospheric emission from the photospheric Hα absorption line. A significant number of our stars show Hα emission (19% of the RASS-ACT/TRC G–K type stars). We characterize our targets stars as chromospherically active or inactive through comparing the Hα EW to that of standards of identical spectral type. Figure 2 shows the EW(Hα) data for our targets and standard stars. Stars more than 2σ above the dwarf/subgiant EW(Hα) relation (a quadratic regression; see Appendix C) are considered to be active. The stars with Hα in emission (negative EWs) have an "e" appended to their spectral types in Tables 4, 5, and 6. The Hα EWs for each star are also listed in these tables.

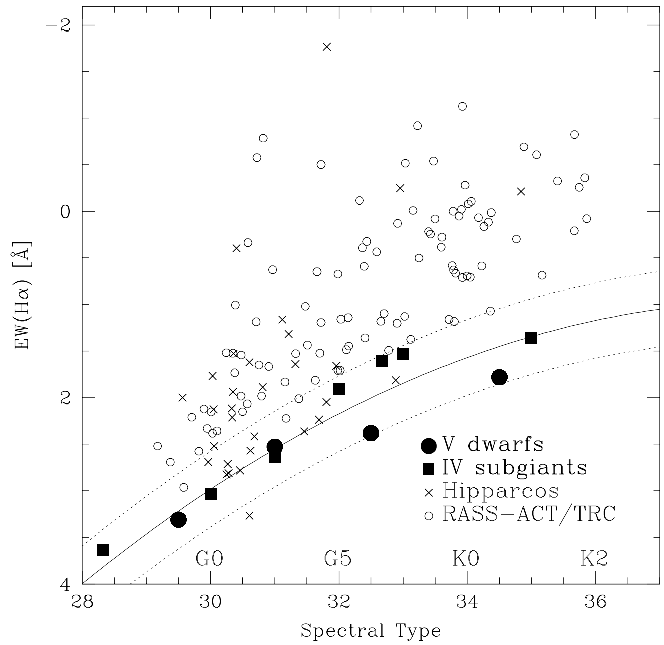

FIG. 2.—Hα EWs for the PMS candidates compared with inactive field dwarfs and subgiants. Symbols are the same as for Fig. 1. The solid line is the average EW(Hα) for dwarf and subgiant standard stars. The dashed line represents the $\pm 2\ \sigma$ residual scatter in the relation (encompassing all of the standards). Stars above this line are clearly chromospherically active; however, those within the 2 σ scatter have Hα emission similar to older field stars.

4.2.2. Li I λ6707 *Equivalent Width*

The presence of strong Li absorption in the spectra of late-type stars is a well-known diagnostic of stellar youth. Because of the extended timescale for significant Li depletion in stars of ~1 $M_\odot$, *strong Li absorption is necessary but not a sufficient indicator of PMS nature for G stars*. However, it is a powerful age discriminant when combined with our surface gravity indicator.

Many studies have shown that the EW of Li I λ6707 can be overestimated at low spectral resolution (e.g., Covino et al. 1997), especially for G–K stars. With a resolution of 1.3 Å, we consider our EWs to be approximate. The EWs were measured with Voigt profiles in the IRAF routine SPLOT. The continuum level was estimated from nearby pseudocontinuum peaks. We subtract the contribution from the neighboring Fe I λ6707.4 Å feature using the prescription of Soderblom et al. (1993). In order to test the validity of our Li EWs, we divided several of our Li-rich targets by standard stars of the same spectral type. The ratioed spectra exhibit only a major absorption feature at λ6707. The division also removes the effects of blending by Fe lines (assuming the same stars have similar EWs). The EWs of this feature in the divided spectra corresponded well with our previous measurements; however, the uncertainties in the

TABLE 4

LCC and UCL Pre–Main-Sequence Members from de Zeeuw et al. (1999) List

HIP (1)	OB Group (2)	α (J2000.0) (3)	δ (J2000.0) (4)	π_{HIP} (mas) (5)	π_{sec} (mas) (6)	P_1 (%) (7)	P_3 (%) (8)	Spec. Type (9)	log (T_{eff}) (K) (10)	log ($L/L_\odot$) (dex) (11)	A_V (mag) (12)	EW(Hα) (Å) (13)	EW(Li) (Å) (14)	log (L_X) (ergs s^{-1}) (15)	log (L_X/L_{bol}) (16)	DM97 Age, Mass (17)	PS01 Age, Mass (18)	SDF00 Age, Mass (19)	Class (20)	Notes (21)
57524	LCC	11 47 24.55	−49 53 03.0	9.62 ± 1.39	8.83 ± 0.60	81	97	F9 IV	3.783 ± 0.004	0.44 ± 0.06	0.30 ± 0.10	2.0	0.18	30.8	−3.3	15, 1.3	15, 1.2	19, 1.3	PMS	HD 102458, TWA 19
58996	LCC	12 05 47.48	−51 00 12.1	9.78 ± 1.16	9.79 ± 0.52	91	99	G1 IV	3.772 ± 0.005	0.43 ± 0.05	0.14 ± 0.04	3.3	0.21	30.5	−3.6	13, 1.3	13, 1.3	18, 1.3	PMS?	HD 105070
59854	LCC	12 16 27.84	−50 08 35.8	8.24 ± 1.78	7.67 ± 0.61	99	100	G1 IV	3.772 ± 0.006	0.49 ± 0.07	0.37 ± 0.11	1.6	0.20	30.9	−3.2	12, 1.4	11, 1.3	16, 1.3	PMS	HD 106725[a]
60885	LCC	12 28 40.05	−55 27 19.3	7.06 ± 1.13	9.49 ± 0.52	14	78	G0 IV	3.778 ± 0.005	0.46 ± 0.05	0.16 ± 0.05	2.7	0.13	30.3	−3.8	14, 1.3	13, 1.3	18, 1.3	PMS?	HD 108568
60913	LCC	12 29 02.25	−64 55 00.6	10.48 ± 1.12	9.82 ± 0.58	100	100	G4.5 IV	3.758 ± 0.008	0.43 ± 0.05	0.21 ± 0.04	2.0	0.19	<29.7	< −4.3	10, 1.4	11, 1.3	16, 1.3	PMS?	HD 108611
62445	LCC	12 47 51.87	−51 26 38.1	6.61 ± 1.54	7.70 ± 0.55	13	75	G4.5 IVe	3.758 ± 0.013	0.62 ± 0.06	0.66 ± 0.06	−1.8	0.24	30.7	−3.4	7, 1.6	5, 1.6	11, 1.5	PMS	SB3?, V940 Cen
63847	LCC	13 05 05.29	−64 13 55.3	9.56 ± 1.35	10.18 ± 0.61	48	89	G3 IV	3.764 ± 0.007	0.36 ± 0.06	0.33 ± 0.06	1.6	0.22	<29.7	< −4.3	14, 1.3	15, 1.2	19, 1.3	PMS	HD 113466
65517	LCC	13 25 47.83	−48 14 57.9	9.59 ± 1.44	10.56 ± 0.57	50	91	G1.5 IV	3.770 ± 0.006	0.02 ± 0.05	0.14 ± 0.08	1.9	0.17	30.4	−3.3	NA, 1.0	39, 1.0	NA, 1.2	PMS	V966 Cen[b]
66001	LCC	13 31 53.61	−51 13 33.1	5.99 ± 1.71	7.88 ± 0.62	82	97	G2.5 IV	3.766 ± 0.011	0.33 ± 0.07	0.11 ± 0.10	1.2	0.28	30.6	−3.2	15, 1.2	17, 1.2	20, 1.2	PMS	HD 117524
66941	LCC	13 43 08.69	−69 07 39.5	8.05 ± 0.95	9.37 ± 0.52	97	100	G0.5 IV	3.775 ± 0.008	1.09 ± 0.05	0.38 ± 0.04	2.1	0.16	31.1	−3.5	2, 2.4	4, 2.0	4, 2.1	PMS	SB, HD 119022[c]
67522	UCL	13 50 06.28	−40 50 08.8	7.94 ± 1.64	7.91 ± 0.60	93	99	G0.5 IV	3.775 ± 0.006	0.25 ± 0.07	0.02 ± 0.10	2.2	0.15	30.4	−3.5	20, 1.2	24, 1.1	28, 1.2	PMS	HD 120411
71178	UCL	14 33 25.78	−34 32 37.6	9.76 ± 1.90	8.71 ± 0.56	99	100	G8 IVe	3.741 ± 0.012	0.16 ± 0.06	0.35 ± 0.08	−0.2	0.26	<29.8	< −3.9	13, 1.2	18, 1.1	22, 1.1	PMS	V1009 Cen
75924	UCL	15 30 26.29	−32 18 11.6	10.91 ± 3.21	9.79 ± 0.79	16	57	G2.5 IV	3.765 ± 0.006	0.69 ± 0.07	0.37 ± 0.07	1.3	0.24	30.9	−2.9	7, 1.6	4, 1.7	10, 1.5	PMS	HD 138009[d]
76472	UCL	15 37 04.66	−40 09 22.1	5.70 ± 1.63	7.24 ± 0.49	95	99	G1 IV	3.774 ± 0.008	0.60 ± 0.06	0.29 ± 0.10	0.4	0.24	30.8	−3.3	10, 1.4	10, 1.4	14, 1.4	PMS	HD 138995
77081	UCL	15 44 21.05	−33 18 55.0	6.63 ± 1.61	7.66 ± 0.59	69	92	G7.5 IV	3.742 ± 0.008	0.35 ± 0.07	0.15 ± 0.06	1.8	0.25	<29.9	< −4.1	8, 1.4	11, 1.3	15, 1.3	PMS?	HD 140374
77135	UCL	15 44 57.69	−34 11 53.7	6.98 ± 2.92	7.20 ± 0.96	91	96	G4 IV	3.760 ± 0.006	0.42 ± 0.12	0.08 ± 0.05	2.2	0.23	30.5	−3.4	11, 1.4	11, 1.3	16, 1.3	PMS?	HD 140463[e]
77144	UCL	15 45 01.83	−40 50 31.0	6.45 ± 1.42	8.00 ± 0.53	43	86	G0 IV	3.778 ± 0.007	0.36 ± 0.06	0.08 ± 0.05	1.8	0.17	30.6	−3.4	17, 1.2	19, 1.2	22, 1.3	PMS	HD 140421
77524	UCL	15 49 44.98	−39 25 09.1	6.63 ± 1.93	6.63 ± 0.76	96	99	K1− IVe	3.705 ± 0.013	0.23 ± 0.10	−0.03 ± 0.10	−0.2	0.32	30.5	−3.3	4, 1.4	8, 1.3	9, 1.4	PMS	HD 141277[f]
77656	UCL	15 51 13.73	−42 18 51.3	6.52 ± 1.37	7.70 ± 0.52	100	100	G5 IV	3.756 ± 0.009	0.41 ± 0.06	0.52 ± 0.09	1.7	0.30	30.3	−3.8	10, 1.4	11, 1.3	16, 1.3	PMS	SB2, HD 141521
80636	UCL	16 27 52.34	−35 47 00.4	8.54 ± 1.64	6.56 ± 0.52	33	82	G0.5 IV	3.774 ± 0.007	0.65 ± 0.07	0.39 ± 0.08	1.5	0.21	30.9	−3.3	9, 1.5	10, 1.4	13, 1.5	PMS	HD 148187, V1056 Sco
81380	UCL	16 37 12.87	−39 00 38.1	7.27 ± 1.91	4.99 ± 0.53	92	99	G0 IV	3.777 ± 0.009	0.74 ± 0.10	0.33 ± 0.09	2.5	0.14	<30.3	< −4.0	8, 1.6	4, 1.7	11, 1.5	PMS	HD 149551
81447	UCL	16 38 05.53	−34 01 10.6	5.90 ± 1.41	5.80 ± 0.52	87	97	G0.5 IV	3.775 ± 0.005	0.78 ± 0.08	0.03 ± 0.07	2.8	0.13	<30.2	< −4.3	7, 1.6	4, 1.7	10, 1.6	PMS?	HD 149735

Notes.—Col. (1): *Hipparcos* catalog ID; col. (2): OB subgroup; cols. (3) and (4): J2000.0 position; col. (5): *Hipparcos* astrometric parallax; col. (6): kinematic parallax estimate (see § 6.3); col. (7): membership probability (with $v_{disp} = 1$ km s^{-1}); col. (8): membership probability (with $v_{disp} = 3$ km s^{-1}); col. (9): spectral type (see § 4.1); col. (10): effective temperature (see § 6.2); col. (11): luminosity (see § 6.4); col. (12): extinction A_V (see § 6.4); col. (13): equivalent width of Hα λ6562.8; col. (14): corrected EW of Li i λ6707.8; col. (15): X-ray luminosity (see § 2.2; approximate upper limits assume RASS PSPC detection limit of 0.05 ct s^{-1} and HR1 = 0); col. (16): logarithm of ratio between X-ray and bolometric luminosities; col. (17): age (in Myr) and mass (in $M/M_\odot$) using DM97 tracks; col. (18): age (in Myr) and mass (in $M/M_\odot$) using PS01 tracks; col. (19): age (in Myr) and mass (in $M/M_\odot$) using SDF00 tracks; col. (20): class; (PMS) pre–main sequence, (PMS?) probably pre–main sequence (see § 5.1); col. (21): notes; (SB) spectroscopic binary.

[a] CCDM J12165-5009AB. Unresolved binary ($\rho = 0''.2$).

[b] The Michigan Spectral Survey (Houk 1978) classifies this star as K0/2(V)+(G) (quality = 3). We found it to be much earlier (G1.5) and note that the published $b-y$ and $B-V$ colors support an early G classification.

[c] Star " E " of Soderblom, King, & Henry 1998 high-resolution survey of active southern stars. It is the most Li-rich of the very active stars in the Soderblom sample. We did not resolve this tight, equal-brightness binary ($\rho = 0''.2$; CCDM J13431-6908AB).

[d] CCDM J15304-3218AB. Both stars were on the slit ($\rho = 1''.5$).

[e] [KWS97] Lupus 1 26 = CCDM J15450-3412AB. Binary is resolved ($\rho = 3''.4$) but both were on-slit.

[f] [KWS97] TTS 79 = CCDM J15450-3412AB. Unresolved binary ($\rho = 0''.2$).

TABLE 5

Pre–Main-Sequence LCC and UCL RASS-ACT/TRC Members

ID No. (1)	TYC (2)	OB Group (3)	α (J2000.0) (4)	δ (J2000.0) (5)	π_{sec} (mas) (6)	P_1 (%) (7)	P_3 (%) (8)	Spec. Type (9)	log (T_{eff}) (K) (10)	log ($L/L_\odot$) (dex) (11)	A_V (mag) (12)	EW(Hα) (Å) (13)	EW(Li) (Å) (14)	log L_X (ergs s^{-1}) (15)	log (L_X/L_{bol}) (16)	DM97 Age, Mass (17)	PS01 Age, Mass (18)	SDF00 Age, Mass (19)	Class (20)	Names and Notes (21)
1	9212-2011-1	LCC	10 57 49.38	−69 13 59.9	9.76 ± 1.01	79	94	K1+IV	3.699 ± 0.010	0.02 ± 0.09	0.35 ± 0.06	0.7	0.34	30.3	−3.3	6, 1.2	12, 1.1	15, 1.2	PMS	
2	8625-388-1	LCC	11 32 08.34	−58 03 20.0	10.78 ± 1.21	59	84	G7 IV	3.747 ± 0.013	0.19 ± 0.10	0.68 ± 0.13	0.4	0.45	29.9	−3.7	14, 1.2	18, 1.1	23, 1.2	PMS	HD 304428; SB2
3	8982-3213-1	LCC	12 04 48.87	−64 09 55.4	8.36 ± 1.27	12	49	G1 IV	3.773 ± 0.005	0.44 ± 0.13	0.60 ± 0.11	1.5	0.21	30.8	−3.2	13, 1.3	12, 1.3	18, 1.3	PMS	HD 104919
4	8640-2515-1	LCC	12 06 13.54	−57 02 16.8	6.48 ± 1.06	90	97	G4 IV	3.760 ± 0.007	0.15 ± 0.14	1.45 ± 0.06	0.6	0.23	30.6	−3.1	20, 1.1	25, 1.1	28, 1.2	PMS	
5	8644-802-1	LCC	12 09 41.86	−58 54 45.0	9.00 ± 1.14	65	88	K0 IVe	3.720 ± 0.013	0.20 ± 0.11	0.28 ± 0.10	−0.1	0.33	30.5	−3.2	6, 1.4	11, 1.2	14, 1.3	PMS	
6	8644-340-1	LCC	12 11 31.43	−58 16 53.2	9.29 ± 0.91	95	99	G9 IV	3.729 ± 0.008	0.05 ± 0.09	0.28 ± 0.10	0.3	0.31	30.5	−3.2	13, 1.2	20, 1.1	24, 1.1	PMS	PPM 770135
7	9231-1566-1	LCC	12 11 38.14	−71 10 36.0	10.15 ± 0.68	91	98	G3.5 IV	3.762 ± 0.005	0.39 ± 0.06	0.48 ± 0.08	1.4	0.27	30.5	−3.5	12, 1.3	12, 1.3	18, 1.3	PMS	HD 105923
8	8636-2515-1	LCC	12 12 35.75	−55 20 27.3	9.24 ± 0.90	50	84	K0+IV	3.717 ± 0.007	0.00 ± 0.09	0.48 ± 0.12	0.2	0.34	30.3	−3.2	11, 1.2	19, 1.1	23, 1.1	PMS	PPM 770145
9	8242-1324-1	LCC	12 14 34.09	−51 10 12.5	9.41 ± 0.83	82	96	G9 IV	3.733 ± 0.008	0.01 ± 0.08	−0.02 ± 0.05	0.2	0.33	30.4	−3.2	16, 1.1	24, 1.0	27, 1.1	PMS	
10	8637-2610-1	LCC	12 14 52.31	−55 47 03.6	9.72 ± 1.31	62	84	G6 IV	3.750 ± 0.007	0.28 ± 0.12	0.87 ± 0.12	0.6	0.27	30.9	−2.9	12, 1.3	14, 1.2	20, 1.2	PMS	HIP 59721[a]
11	8645-1339-1	LCC	12 18 27.64	−59 43 12.9	10.42 ± 1.32	4	32	K1.5 IVe	3.695 ± 0.010	0.03 ± 0.11	0.12 ± 0.08	−0.3	0.30	30.3	−3.1	5, 1.2	11, 1.2	13, 1.2	PMS	
12	8641-2187-1	LCC	12 18 58.02	−57 37 19.2	9.46 ± 0.74	97	99	G9.5 IV	3.724 ± 0.013	0.32 ± 0.07	0.49 ± 0.14	0.1	0.35	30.6	−3.2	5, 1.5	9, 1.3	11, 1.4	PMS	PPM 770205, SB?
13	8983-98-1	LCC	12 19 21.64	−64 54 10.4	9.74 ± 1.13	89	97	K1− IV	3.707 ± 0.010	0.26 ± 0.10	0.25 ± 0.05	0.3	0.32	30.5	−3.2	3, 1.5	8, 1.3	9, 1.4	PMS	
14	8633-508-1	LCC	12 21 16.48	−53 17 44.9	9.31 ± 0.78	27	77	G1.5 IV	3.770 ± 0.007	0.31 ± 0.07	0.44 ± 0.07	1.6	0.21	30.7	−3.3	16, 1.2	19, 1.2	22, 1.2	PMS	HD 107441
15	8238-1462-1	LCC	12 21 55.65	−49 46 12.5	9.85 ± 0.66	86	98	G5.5 IV	3.754 ± 0.007	0.08 ± 0.06	0.14 ± 0.06	1.5	0.28	30.2	−3.4	21, 1.1	27, 1.0	30, 1.1	PMS	PPM 758910
16	8234-2856-1	LCC	12 22 04.30	−48 41 24.9	7.96 ± 0.81	85	97	K0 IVe	3.721 ± 0.012	0.10 ± 0.09	0.21 ± 0.07	−0.1	0.34	30.4	−3.2	9, 1.3	14, 1.1	19, 1.2	PMS	
17	8633-28-1	LCC	12 22 33.23	−53 33 49.0	8.07 ± 0.69	53	89	G0 IV	3.778 ± 0.005	0.41 ± 0.08	0.41 ± 0.11	2.2	0.20	30.3	−3.7	15, 1.3	16, 1.2	19, 1.3	PMS	SAO 239893
18	8641-1281-1	LCC	12 23 40.13	−56 16 32.5	8.92 ± 1.19	66	87	K0+ IV	3.715 ± 0.017	−0.09 ± 0.12	0.44 ± 0.09	1.1	0.36	30.0	−3.4	14, 1.1	24, 1.0	27, 1.0	PMS	SB2
19	8992-605-1	LCC	12 36 38.97	−63 44 43.5	9.73 ± 0.82	56	88	K0+ III	3.717 ± 0.017	0.25 ± 0.08	0.39 ± 0.06	0.6	0.37	30.4	−3.4	5, 1.5	9, 1.3	12, 1.4	PMS?	PPM 779078, SB2[b]
20	8646-166-1	LCC	12 36 58.97	−54 12 18.0	8.64 ± 1.18	92	97	K0 IV	3.721 ± 0.006	0.04 ± 0.12	0.11 ± 0.05	0.7	0.32	30.3	−3.4	11, 1.2	18, 1.1	22, 1.1	PMS	
21	8654-1115-1	LCC	12 39 37.96	−57 31 40.7	10.22 ± 0.96	3	39	G7.5 IV	3.742 ± 0.012	−0.06 ± 0.08	0.30 ± 0.07	0.1	0.26	30.4	−3.1	24, 1.0	34, 0.9	46, 1.1	PMS	
22	8659-2604-1	LCC	12 41 18.17	−58 25 56.0	10.26 ± 0.95	58	87	G1.5 IVe	3.771 ± 0.011	0.14 ± 0.08	0.67 ± 0.14	−0.6	0.29	30.2	−3.4	24, 1.1	30, 1.1	17, 1.2	PMS	HD 110244, SB2
23	8992-420-1	LCC	12 44 34.82	−63 31 46.2	7.97 ± 1.19	59	84	K1 IVe	3.704 ± 0.012	0.25 ± 0.13	0.27 ± 0.08	−0.7	0.38	30.6	−3.0	3, 1.4	8, 1.3	9, 1.4	PMS	HD 311894, EB[c]
24	8249-52-1	LCC	12 45 06.76	−47 42 58.2	8.34 ± 0.62	94	99	G8.5 IV	3.738 ± 0.011	0.13 ± 0.07	0.38 ± 0.14	0.0	0.30	30.6	−3.1	13, 1.2	19, 1.1	23, 1.1	PMS	HD 110817
25	7783-1908-1	LCC	12 48 07.79	−44 39 16.8	10.97 ± 0.59	21	75	G6 IVe	3.751 ± 0.013	0.14 ± 0.05	0.18 ± 0.08	−0.1	0.28	30.6	−3.1	18, 1.1	22, 1.1	26, 1.1	PMS	HD 111227
26	8655-149-1	LCC	12 48 48.18	−56 35 37.8	7.56 ± 0.73	56	89	G5 IV	3.755 ± 0.008	0.14 ± 0.09	0.53 ± 0.13	1.2	0.22	30.4	−3.4	19, 1.1	24, 1.1	27, 1.1	PMS	PPM 770473
27	9245-617-1	LCC	12 58 25.58	−70 28 49.2	11.73 ± 0.69	80	96	K0+ IV	3.714 ± 0.010	−0.01 ± 0.06	0.46 ± 0.12	0.0	0.37	30.3	−3.3	10, 1.2	18, 1.1	22, 1.1	PMS	PPM 785798[d]
28	8648-446-1	LCC	13 01 50.70	−53 04 58.3	9.22 ± 1.51	75	88	K2− IV	3.690 ± 0.008	−0.37 ± 0.14	0.55 ± 0.10	0.2	0.33	30.0	−3.3	19, 0.9	38, 0.8	40, 0.9	PMS	
29	8652-1791-1	LCC	13 02 37.54	−54 59 36.8	6.40 ± 0.81	16	67	G1 IV	3.772 ± 0.006	0.35 ± 0.11	0.38 ± 0.05	2.1	0.17	30.8	−3.1	16, 1.2	18, 1.2	21, 1.3	PMS	HD 113180
30	8258-1878-1	LCC	13 06 40.12	−51 59 38.6	8.91 ± 0.90	94	95	K0 IVe	3.722 ± 0.019	−0.05 ± 0.09	0.17 ± 0.09	−0.3	0.34	30.2	−3.4	15, 1.1	24, 1.0	27, 1.0	PMS	
31	8259-689-1	LCC	13 14 23.84	−50 54 01.9	7.70 ± 0.81	87	97	G5.5 IV	3.754 ± 0.010	0.25 ± 0.10	0.27 ± 0.09	1.1	0.32	30.8	−2.9	14, 1.2	17, 1.1	21, 1.2	PMS	
32	8649-251-1	LCC	13 17 56.94	−53 17 56.2	5.99 ± 1.21	56	81	G1 IV	3.774 ± 0.008	0.43 ± 0.18	0.22 ± 0.11	1.0	0.30	30.7	−3.2	14, 1.3	14, 1.3	18, 1.3	PMS	SB2
33	8248-539-1	LCC	13 22 04.46	−45 03 23.1	7.16 ± 0.67	71	94	G0 IV	3.779 ± 0.006	0.18 ± 0.08	0.22 ± 0.08	2.1	0.15	30.3	−3.6	26, 1.2	30, 1.1	NA, 1.2	PMS	HD 116099
34	9246-971-1	LCC	13 22 07.54	−69 38 12.3	11.57 ± 0.95	82	95	K1 IVe	3.702 ± 0.017	0.00 ± 0.08	0.17 ± 0.07	−39.9	0.37	30.2	−3.2	7, 1.2	14, 1.1	17, 1.2	PMS	PDS 66, CTT[e]
35	8663-1375-1	LCC	13 34 20.26	−52 40 36.1	9.50 ± 0.66	100	100	G1 IV	3.774 ± 0.007	0.32 ± 0.06	0.45 ± 0.10	1.7	0.22	30.5	−3.4	17, 1.2	20, 1.2	23, 1.3	PMS	HD 117884, SB?
36	7796-1788-1	UCL	13 37 57.29	−41 34 41.9	10.23 ± 0.52	49	88	K0 IV	3.723 ± 0.007	0.00 ± 0.05	−0.07 ± 0.05	0.7	0.30	30.4	−3.2	13, 1.2	21, 1.0	25, 1.1	PMS	SAO 224291
37	8667-283-1	LCC	13 43 28.53	−54 36 43.5	11.70 ± 0.75	2	45	G2 IV	3.769 ± 0.007	0.13 ± 0.06	0.28 ± 0.12	1.7	0.20	30.6	−3.2	23, 1.1	29, 1.1	27, 1.2	PMS	HIP 66963
38	8270-2015-1	UCL	13 47 50.55	−49 02 05.5	6.75 ± 0.79	73	92	G8 IVe	3.740 ± 0.011	0.05 ± 0.10	0.45 ± 0.13	−0.5	0.29	30.5	−3.2	17, 1.1	24, 1.0	27, 1.1	PMS	
39	8263-2453-1	UCL	13 52 47.80	−46 44 09.2	6.92 ± 0.57	74	95	G0 IV	3.778 ± 0.008	0.44 ± 0.07	0.34 ± 0.08	2.4	0.18	30.8	−3.3	14, 1.3	14, 1.3	18, 1.3	PMS	HD 120812
40	7811-2909-1	UCL	14 02 20.73	−41 44 50.8	7.69 ± 0.71	58	87	G9 IV	3.733 ± 0.013	0.07 ± 0.08	0.90 ± 0.12	0.2	0.23	30.3	−3.3	14, 1.2	20, 1.1	24, 1.1	PMS	2E 1359.2−4130?
41	7815-2029-1	UCL	14 09 03.58	−44 38 44.4	7.05 ± 0.49	9	67	F9 IV	3.783 ± 0.005	0.50 ± 0.06	0.38 ± 0.06	3.0	0.11	30.7	−3.5	14, 1.3	12, 1.3	18, 1.3	PMS?	HD 123484
42	9244-814-1	LCC	14 16 05.67	−69 17 36.0	8.15 ± 0.92	11	57	G1 IV	3.773 ± 0.007	0.19 ± 0.10	0.62 ± 0.08	2.2	0.13	30.1	−3.7	22, 1.1	27, 1.1	300, 1.2	PMS	HD 124329
43	8282-516-1	UCL	14 27 05.56	−47 14 21.8	7.57 ± 0.63	89	98	G7 IV	3.745 ± 0.010	0.06 ± 0.08	0.17 ± 0.04	1.1	0.26	30.4	−3.3	19, 1.1	25, 1.0	28, 1.1	PMS	
44	7817-622-1	UCL	14 28 09.30	−44 14 17.4	6.23 ± 0.71	52	85	G5.5 IV	3.754 ± 0.008	0.54 ± 0.10	0.33 ± 0.07	1.4	0.22	30.6	−3.5	7, 1.5	9, 1.4	12, 1.4	PMS	HD 126670
45	7813-224-1	UCL	14 28 19.38	−42 19 34.1	6.27 ± 0.61	87	97	G3.5 IV	3.762 ± 0.008	0.33 ± 0.09	0.37 ± 0.07	1.0	0.21	30.8	−3.0	14, 1.3	16, 1.2	20, 1.2	PMS	PPM 760384
46	7814-1450-1	UCL	14 37 04.22	−41 45 03.0	6.41 ± 0.70	88	97	G0.5 IV	3.775 ± 0.008	0.59 ± 0.10	0.18 ± 0.06	1.5	0.17	30.7	−3.4	10, 1.4	10, 1.4	14, 1.4	PMS	HD 128242[f]
47	8683-242-1	UCL	14 37 50.23	−54 57 41.1	7.59 ± 0.94	20	65	K0+ IV	3.715 ± 0.015	0.08 ± 0.11	0.30 ± 0.06	0.1	0.32	30.6	−3.0	8, 1.3	14, 1.1	18, 1.2	PMS	
48	8283-264-1	UCL	14 41 35.00	−47 00 28.8	9.11 ± 0.52	94	99	G4 IV	3.759 ± 0.013	0.20 ± 0.06	0.02 ± 0.07	1.2	0.23	30.9	−2.8	18, 1.2	22, 1.1	25, 1.2	PMS	PPM 760547
49	8283-2795-1	UCL	14 47 31.77	−48 00 05.7	7.68 ± 0.81	1	21	G2.5 IV	3.766 ± 0.008	−0.05 ± 0.09	0.43 ± 0.07	1.8	0.17	30.2	−3.4	NA, NA	44, 1.0	NA, 1.2	PMS	
50	7305-380-1	UCL	14 50 25.81	−35 06 48.6	5.27 ± 0.87	73	90	K0 IV	3.723 ± 0.015	0.52 ± 0.15	0.21 ± 0.08	0.0	0.28	30.6	−3.3	3, 1.8	4, 1.6	7, 1.7	PMS	RX J1450.4−3507[g]
51	7828-2913-1	UCL	14 52 41.98	−41 41 55.2	6.89 ± 0.75	84	95	K1 IVe	3.701 ± 0.010	0.10 ± 0.10	0.61 ± 0.10	−0.6	0.35	30.5	−3.2	5, 1.3	10, 1.2	12, 1.3	PMS	
52	7310-2431-1	UCL	14 57 19.63	−36 12 27.4	7.59 ± 0.61	13	64	G6 IV	3.750 ± 0.011	0.18 ± 0.07	0.15 ± 0.06	1.4	0.25	30.3	−3.4	16, 1.2	20, 1.1	24, 1.2	PMS	RX J1457.3−3613[g]
53	7310-503-1	UCL	14 58 37.70	−35 40 30.4	7.36 ± 0.77	82	94	K2− IVe	3.689 ± 0.008	0.21 ± 0.09	0.23 ± 0.11	−0.3	0.37	30.3	−3.4	2, 1.3	6, 1.4	7, 1.5	PMS	RX J1458.6−3541[g]
54	7824-1291-1	UCL	14 59 22.76	−40 13 12.1	8.17 ± 0.57	85	97	G3 IV	3.764 ± 0.008	0.32 ± 0.06	0.40 ± 0.06	1.5	0.23	30.5	−3.4	15, 1.2	17, 1.2	20, 1.2	PMS	RX J1459.3−4013[g]
55	7833-2037-1	UCL	15 00 51.88	−43 31 21.0	6.14 ± 0.72	78	94	G9 IV	3.731 ± 0.012	0.16 ± 0.11	0.30 ± 0.09	0.1	0.33	30.4	−3.2	10, 1.3	15, 1.1	19, 1.2	PMS	RX J1500.8−4331[g]
56	7829-504-1	UCL	15 01 11.56	−41 20 40.6	4.67 ± 0.62	94	99	G0.5 IV	3.774 ± 0.008	0.64 ± 0.12	0.48 ± 0.08	1.5	0.24	31.0	−3.3	9, 1.5	10, 1.4	13, 1.4	PMS	RX J1501.2−4121, SB?[g]
57	8297-1613-1	UCL	15 01 58.82	−47 55 46.4	6.43 ± 0.62	25	74	G1.5 IV	3.770 ± 0.006	0.29 ± 0.09	0.22 ± 0.10	2.0	0.20	30.2	−3.8	17, 1.2	20, 1.2	23, 1.2	PMS	

TABLE 5—*Continued*

ID No. (1)	TYC (2)	OB Group (3)	α (J2000.0) (4)	δ (J2000.0) (5)	π_{sec} (mas) (6)	P_1 (%) (7)	P_3 (%) (8)	Spec. Type (9)	log (T_{eff}) (K) (10)	log ($L/L_\odot$) (dex) (11)	A_V (mag) (12)	EW(Hα) (Å) (13)	EW(Li) (Å) (14)	log L_X (ergs s^{-1}) (15)	log (L_X/L_{bol}) (16)	DM97 Age, Mass (17)	PS01 Age, Mass (18)	SDF00 Age, Mass (19)	Class (20)	Names and Notes (21)
58	7319-749-1	UCL	15 07 14.81	−35 04 59.6	9.92 ± 0.82	12	52	G9.5 IV	3.727 ± 0.011	−0.12 ± 0.08	0.44 ± 0.10	1.2	0.25	30.0	−3.4	20, 1.0	32, 0.9	38, 1.0	PMS	RX J1507.2−3505[h]
59	7833-2400-1	UCL	15 08 37.75	−44 23 16.9	5.55 ± 0.72	81	95	G1.5 IVe	3.770 ± 0.011	0.29 ± 0.12	0.13 ± 0.11	−0.8	0.27	30.9	−2.9	17, 1.2	20, 1.2	23, 1.2	PMS	RX J1508.6−4423, SB2[h]
60	7833-2559-1	UCL	15 08 38.50	−44 00 52.1	7.46 ± 0.71	85	96	G1.5 IV	3.771 ± 0.009	0.20 ± 0.09	0.11 ± 0.07	1.2	0.24	30.4	−3.3	21, 1.1	26, 1.1	29, 1.2	PMS	RX J1508.7−4400[h]
61	8294-2230-1	UCL	15 12 50.18	−45 08 04.5	6.61 ± 0.72	100	100	G5 IV	3.756 ± 0.008	0.19 ± 0.10	0.27 ± 0.07	1.7	0.24	30.6	−3.1	17, 1.2	21, 1.1	25, 1.2	PMS	RX J1512.8−4508A[h]
62	8694-1685-1	UCL	15 18 01.74	−53 17 28.8	9.74 ± 0.93	14	60	G7 IV	3.746 ± 0.009	0.08 ± 0.09	0.77 ± 0.07	1.2	0.27	30.4	−3.3	18, 1.1	24, 1.0	27, 1.1	PMS	
63	7822-158-1	UCL	15 18 26.91	−37 38 02.1	7.89 ± 0.86	97	99	G9 IV	3.729 ± 0.016	0.05 ± 0.10	0.72 ± 0.08	0.4	0.26	30.4	−3.0	13, 1.2	20, 1.1	24, 1.1	PMS	RX J1518.5−3738[h]
64	8295-1530-1	UCL	15 25 59.65	−45 01 15.8	6.73 ± 0.73	40	77	G8 IV	3.740 ± 0.012	−0.02 ± 0.10	0.19 ± 0.05	1.1	0.26	30.1	−3.5	21, 1.0	29, 1.0	34, 1.1	PMS	RX J1526.0−4501[h]
65	7326-928-1	UCL	15 29 38.58	−35 46 51.3	7.39 ± 0.71	93	98	K0+ IV	3.718 ± 0.010	0.17 ± 0.09	0.16 ± 0.05	0.1	0.25	30.3	−3.4	7, 1.4	11, 1.2	15, 1.2	PMS	RX J1529.6−3546[h]
66	7327-1934-1	UCL	15 37 02.14	−31 36 39.8	7.41 ± 0.59	32	79	G6 IV	3.750 ± 0.009	0.42 ± 0.07	0.43 ± 0.05	0.4	0.23	30.9	−3.0	9, 1.4	11, 1.3	14, 1.3	PMS	SAO 206807[i]
67	7840-1280-1	UCL	15 37 11.30	−40 15 56.8	6.11 ± 0.67	99	100	G8.5 IVe	3.736 ± 0.014	0.25 ± 0.10	0.40 ± 0.10	−0.9	0.30	30.7	−3.2	9, 1.3	12, 1.2	17, 1.2	PMS	HIP 76477[h]
68	7848-1659-1	UCL	15 38 43.06	−44 11 47.4	8.04 ± 0.58	82	96	G8.5 IV	3.736 ± 0.008	0.08 ± 0.07	0.62 ± 0.05	0.5	0.27	30.3	−3.4	15, 1.2	21, 1.1	24, 1.1	PMS	RX J1538.7−4411[h]
69	6785-510-1	UCL	15 39 24.41	−27 10 21.9	7.89 ± 0.61	72	93	G5 IV	3.755 ± 0.007	0.46 ± 0.07	0.28 ± 0.06	1.7	0.21	30.7	−3.3	9, 1.4	10, 1.3	14, 1.4	PMS	HIP 76673[j]
70	7331-782-1	UCL	15 44 03.77	−33 11 11.2	8.08 ± 0.86	99	100	K0 IVe	3.723 ± 0.013	0.01 ± 0.10	0.47 ± 0.06	−1.1	0.30	30.2	−3.3	13, 1.2	20, 1.1	24, 1.1	PMS	
71	7845-1174-1	UCL	15 45 52.25	−42 22 16.5	7.71 ± 0.58	32	79	K2− IVe	3.690 ± 0.007	0.12 ± 0.07	0.80 ± 0.08	−0.8	0.39	30.9	−2.9	3, 1.3	8, 1.3	9, 1.3	PMS	RX J1545.9−4222[h]
72	8317-551-1	UCL	15 46 51.79	−49 19 04.7	7.55 ± 0.59	96	99	G7.5 IV	3.744 ± 0.007	0.21 ± 0.07	0.29 ± 0.08	1.5	0.26	30.5	−3.3	13, 1.2	16, 1.1	21, 1.2	PMS	HD 329929
73	7842-250-1	UCL	15 56 59.05	−39 33 43.1	5.74 ± 0.70	99	100	G9.5 IV	3.726 ± 0.007	0.21 ± 0.11	0.35 ± 0.06	1.2	0.21	30.5	−3.4	8, 1.4	12, 1.2	16, 1.2	PMS	
74	7333-1260-1	UCL	16 01 07.93	−32 54 52.5	7.60 ± 0.55	87	97	G0 IV	3.779 ± 0.006	0.33 ± 0.06	0.15 ± 0.07	2.3	0.11	30.6	−3.4	18, 1.2	21, 1.2	25, 1.3	PMS	HD 143358
75	7333-719-1	UCL	16 01 08.97	−33 20 14.2	5.69 ± 0.74	64	89	G5 IV	3.756 ± 0.012	0.41 ± 0.12	0.16 ± 0.06	0.7	0.26	30.6	−3.1	10, 1.4	11, 1.3	16, 1.3	PMS	RX J1601.1−3320[h]
76	7863-1629-1	UCL	16 03 45.37	−43 55 49.2	5.63 ± 0.51	62	92	G9.5 IV	3.725 ± 0.014	0.75 ± 0.08	0.51 ± 0.06	0.7	0.35	31.2	−3.1	1, 2.1	3, 1.8	4, 2.0	PMS	HIP 78684[h,k]
77	7855-1106-1	UCL	16 03 52.50	−39 39 01.3	7.14 ± 0.79	83	95	K2− IVe	3.687 ± 0.010	0.09 ± 0.10	0.18 ± 0.06	−0.4	0.38	30.4	−3.2	3, 1.2	8, 1.3	9, 1.3	PMS	RX J1603.8−3938, SB2[h]
78	7851-1-1	UCL	16 05 45.00	−39 06 06.5	7.69 ± 0.75	61	87	G6.5 IV	3.749 ± 0.010	0.13 ± 0.09	0.19 ± 0.05	0.3	0.32	30.5	−3.1	17, 1.1	22, 1.1	26, 1.1	PMS	RX J1605.8−3905[h]
79	7355-317-1	UCL	16 13 58.02	−36 18 13.4	8.10 ± 0.71	90	97	G9 IVe	3.732 ± 0.014	−0.13 ± 0.08	0.31 ± 0.09	−0.5	0.27	30.4	−2.9	23, 1.0	36, 0.9	45, 1.0	PMS	[l]
80	8319-1687-1	UCL	16 14 52.01	−50 26 18.5	7.77 ± 0.72	81	95	G9.5 IV	3.726 ± 0.010	0.34 ± 0.08	0.39 ± 0.07	0.6	0.32	30.6	−3.1	5, 1.5	9, 1.3	11, 1.4	PMS	CD −50°10271
81	7852-51-1	UCL	16 18 38.56	−38 39 11.8	9.30 ± 0.54	5	57	F9 IV	3.780 ± 0.006	0.33 ± 0.05	0.32 ± 0.04	2.6	0.13	30.3	−3.8	18, 1.2	21, 1.2	25, 1.3	PMS	HIP 79908
82	7857-648-1	UCL	16 21 12.19	−40 30 20.6	6.43 ± 0.54	1	41	G8 IV	3.738 ± 0.007	0.23 ± 0.08	0.69 ± 0.06	1.4	0.25	30.5	−3.3	10, 1.3	13, 1.2	18, 1.2	PMS	RX J1621.2−4030[i]
83	7857-514-1	UCL	16 23 29.55	−39 58 00.8	5.91 ± 0.72	91	97	G3 IV	3.764 ± 0.007	0.11 ± 0.11	0.95 ± 0.08	2.0	0.20	30.4	−3.4	23, 1.1	29, 1.1	200, 1.1	PMS?	RX J1623.5−3938[i]
84	7853-227-1	UCL	16 27 30.55	−37 49 21.6	5.55 ± 0.85	66	87	G9.5 IV	3.726 ± 0.010	0.21 ± 0.14	0.50 ± 0.06	0.6	0.35	30.5	−3.3	8, 1.4	12, 1.2	16, 1.2	PMS	
85	7353-2640-1	UCL	16 31 42.03	−35 05 17.2	7.01 ± 0.69	92	98	G7.5 IV	3.742 ± 0.009	0.05 ± 0.09	0.33 ± 0.05	1.2	0.24	30.4	−3.3	18, 1.1	25, 1.0	28, 1.1	PMS	
86	7349-2191-1	UCL	16 35 35.99	−33 26 34.7	5.22 ± 0.69	7	52	K2− IV	3.687 ± 0.007	0.35 ± 0.12	0.34 ± 0.06	0.1	0.35	30.9	−3.0	1, 1.3	4, 1.5	4, 1.6	PMS	PPM 747873
87	7858-830-1	UCL	16 39 59.30	−39 24 59.2	4.63 ± 0.75	100	100	G4 IV	3.760 ± 0.010	0.74 ± 0.14	0.27 ± 0.07	1.5	0.24	30.7	−3.3	5, 1.8	4, 1.7	9, 1.6	PMS	HD 321857
88	7871-1282-1	UCL	16 42 24.00	−40 03 29.7	5.02 ± 0.54	92	98	G1 IV	3.772 ± 0.011	0.92 ± 0.10	0.74 ± 0.08	0.3	0.18	30.7	−3.7	5, 1.9	4, 1.9	7, 1.8	PMS	HD 150372

Notes.—Col. (1): short ID; col. (2): Tycho-2 name; col. (3): OB subgroup; cols. (4) and (5): J2000.0 position; col. (6): kinematic parallax estimate (see § 6.3); col. (7): membership probability (with $v_{disp} = 1$ km s^{-1}); col. (8): membership probability (with $v_{disp} = 3$ km s^{-1}); col. (9): spectral type (see § 4.1); col. (10): effective temperature (see § 6.2); col. (11): luminosity (see § 6.4); col. (12): extinction A_V (see § 6.4); col. (13): equivalent width of Hα λ6562.8 (see § 4.2.1); col. (14): corrected EW of Li I λ6707.8 (see § 4.2.2); col. (15): X-ray luminosity (see § 2.2); col. (16): logarithm of ratio between X-ray and bolometric luminosities; col. (17): age (in Myr) and mass (in $M/M_\odot$) using DM97 tracks; col. (18): age (in Myr) and mass (in $M/M_\odot$) using PS01 tracks; col. (19): age (in Myr) and mass (in $M/M_\odot$) using SDF00 tracks; col. (20): class; (PMS) pre–main sequence, (PMS?) probably pre–main sequence (see § 5.1); col. (21): notes; (SB) spectroscopic binary.

[a] HIP 59721 is a common proper motion pair ($\rho = 24''$) with HD 106444 (=HIP 59716, F5 V, $\pi = 9.92 \pm 2.53$).

[b] *Einstein* Slew Survey source 1ES 1233-63.4.

[c] 2E 1241.6−6315. Eclipsing binary discovered in the All Sky Automated Survey (Pojmanski 1998): ASAS J124435−6331.8 (period = 2.6 days).

[d] 2E 1255.1−7012 = EUVE J1258−70.4.

[e] Hen 3-892 = IRAS 13185−6922. This is the lone CTTS identified in this survey. [O I] λ6300 is seen in emission (EW = 0.2 Å).

[f] CCDM J1437−4145AB. Unresolved binary ($\rho = 0''.4$).

[g] Young *ROSAT* star identified by Wichmann et al. 1997b.

[h] Young *ROSAT* star identified by Krautter et al. 1997.

[i] CCDM J15370−3127A = RX J1537.0−3136 = 2E 1533.9−3126? Our spectrum is of the bright ($V = 10$) primary; the BC components (both $V = 13$) are $4''$ away and off-slit.

[j] CCDM J15394−2710AB. Unresolved binary ($\rho = 0''.4$).

[k] CCDM J16038−4356AB. Unresolved binary ($\rho = 0''.3$).

[l] Faint companion off-slit ($\rho \simeq 4''$).

TABLE 6

RASS-ACT/TRC and *Hipparcos* Stars Rejected as Sco-Cen Members

Name (1)	α (J2000.0) (2)	δ (J2000.0) (3)	P_1 (%) (4)	P_3 (%) (5)	Sp. (6)	EW(Hα) (Å) (7)	EW(Li) (Å) (8)	$\log(L_X/L_{bol})$ (9)	Type (10)
TYC 8222-105-1.......	11 35 03.76	−48 50 22.0	71	93	F8.5 V	2.7	0.19	−3.4	ZAMS
TYC 8982-3046-1.....	12 04 14.42	−64 18 51.7	97	99	G1 V	2.0	0.20	−3.1	ZAMS
TYC 8990-701-1.......	13 13 28.11	−60 00 44.6	9	48	F9 V	2.2	0.11	−3.4	ZAMS
TYC 8285-847-1.......	14 16 57.91	−49 56 42.3	43	87	G2.5 IV	2.2	0.00	−3.9	Subgiant (CAB)
TYC 7833-1106-1.....	15 08 00.55	−43 36 24.9	4	53	G2 IV	0.6	0.00	−3.5	Active subgiant
TYC 8293-92-1	15 09 27.93	−46 50 57.2	28	71	K0 IV	0.7	0.05	−3.4	Active subgiant
TYC 7318-593-1.......	15 31 21.93	−33 29 39.5	94	98	G9.5 V	0.0	0.15	−3.3	Active dwarf
TYC 7858-526-1.......	16 38 38.47	−39 33 03.5	98	100	F8.5 IV	2.5	0.02	−4.0	Active subgiant (CAB)
HIP 63797...............	13 04 30.96	−65 55 18.5	9	73	G3.5 IV	2.4	0.00	< −4.5	Subgiant
HIP 65423[a]..............	13 24 35.12	−55 57 24.2	99	100	G0 V	2.1	0.18	−3.6	ZAMS
HIP 68726...............	14 04 07.12	−37 15 50.5	60	93	G0.5 III	1.9	0.00	< −5.1	Giant
HIP 72070...............	14 44 30.96	−39 59 20.6	62	91	G1 V	2.6	0.16	< −4.2	ZAMS
HIP 74501...............	15 13 29.22	−55 43 54.6	3	61	G1.5 III	2.4	0.03	< −4.9	Giant
HIP 77015...............	15 43 29.86	−38 57 38.6	61	91	G0.5 V	2.8	0.06	< −4.1	Dwarf
HIP 79610...............	16 14 43.02	−38 38 43.5	37	74	G0.5 V	2.7	0.03	< −4.2	Dwarf
HIP 81775...............	16 42 10.36	−31 30 15.0	14	67	G1 IV	2.8	0.04	< −4.1	Subgiant

Notes.—Col. (1): name from Tycho-2 or *Hipparcos* catalogs; cols. (2) and (3): J2000.0 position; col. (4): membership probability (with $v_{\rm disp} = 1$ km s^{-1}); col. (5): membership probability (with $v_{\rm disp} = 3$ km s^{-1}); col. (6): spectral type (see § 4.1); col. (7): equivalent width of Hα λ6562.8; col. (8): corrected EW of Li i λ6707.8; col. (9): logarithm of ratio between X-ray and bolometric luminosities (approximate upper limits assume RASS PSPC detection limit of 0.05 ct s^{-1} and HR1 = 0); col. (10): class of object.

[a] HD 116402. Cutispoto et al. 2002 measure EW(Li) = 220 mÅ, and $v \sin i = 35$ km s^{-1}.

EW appear to be ~20–50 mÅ (with the maximum value being for spectroscopic binaries).

Figure 3 shows the Li i λ6707 EWs for our RASS-ACT/TRC and *Hipparcos* targets, separated according to their luminosity class (§ 4.1.3). Effective temperatures ($T_{\rm eff}$) come from the final spectral type (see § 6.2). Most points lie above the Li i λ6707 EWs that characterize young open clusters, plotted as low-order polynomial fits for the IC 2602 (30 Myr; Randich et al. 1997), Pleiades (70–125 Myr; Soderblom et al. 1993; Basri, Marcy, & Graham 1996), and M34 clusters (250 Myr; Jones et al. 1997). The comparison is not completely fair, however, since the cluster ZAMS stars will be roughly 10% less massive than the corresponding PMS stars. Even if most of our program stars were older ZAMS stars, they still would be Li-rich compared with stars in the well-studied open clusters. We select as "Li-rich" those stars above the solid line in Figure 3. Considering the uncertainties in our EW(Li) measurements and the lack of any other ~10–20 Myr old PMS G–K type stellar samples with which to compare, we are not compelled to subdivide our sample further. We will reserve a more detailed investigation of the Li abundances for a future high-resolution spectral study. For the present, we are content to have demonstrated that we have identified a population that appears to be more Li-rich than ZAMS stars.

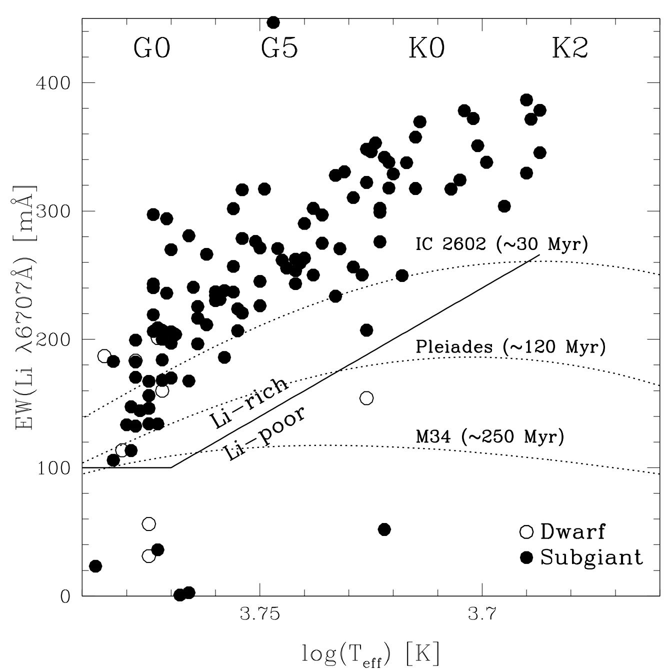

Fig. 3.—EWs for Li i λ6707 for the program stars compared with regression fits for stars in young open clusters (see § 4.2.2). We discuss assignment of dwarf and subgiant luminosity classes in § 4.1.3. The PMS candidates form an obvious locus, and we select all stars above the solid line as "Li-rich."

5. DEFINING THE PTTS SAMPLE

5.1. *Membership Status*

Our survey was designed to identify the PMS G- and K-type stars in the Sco-Cen OB association. We classified the late-type stars according to their positions in Figures 1, 2, and 3 (Table 7). We consider the 110 stars (85/96 RASS-ACT/TRC and 16/30 *Hipparcos*) classified as "Li-rich," "subgiant," and "active" as bona fide PTTSs ("PMS"). Li-rich stars with subgiant surface gravities and Hα EWs similar to the standard field stars (i.e., "inactive") are called "PMS?" Only three of the RASS-ACT/TRC stars, and six of the HIP stars are classified as PMS?. The lone object with giant-like surface gravity in the RASS-ACT/TRC X-ray–selected sample (TYC 8992-605-1) is Li-rich, and we also classify it as a PMS PTTS. The nine PMS? stars were included in our statistics concerning the star formation his-

TABLE 7
Stellar Classification Scheme

Adopted Classification	Li-rich	Hα Excess	Luminosity Class	N(R-T)	N(HIP)
PMS	Yes	Yes	IV	94	7
PMS?	Yes	No	IV	3	6
PMS CTTS[a]	Yes	Strong	IV	1	0
Young dwarf (ZAMS)	Yes	Yes/No	V	4	1
Active dwarf	No	Yes	V	1	0
Active subgiant	No	Yes	IV	4	0
Subgiant	No	No	IV	1	2
Giant	No	No	III	0	2
Dwarf (MS)	No	No	V	0	2
CAB[b]	No	No (wide)	IV	2	0
Total				107	20

Notes.—N(R-T) is number in RASS-ACT/TRC sample. N(HIP) is number in *Hipparcos* sample. " Li-rich " implies significant Li absorption and above the line in Fig. 3. " Active " means that the Hα equivalent widths are greater than 2 times the σ residual above the regression of values for field standard stars (Fig. 2; Appendix C), implying that chromospheric emission is filling in the absorption line. Luminosity classes are assigned according to a star's placement in Fig. 1.

[a] Included in PMS sample count.

[b] Included in subgiant sample count.

tory and disk frequency of the sample (§ 7) for a total of 110 candidate lower mass members of the LCC and UCL subgroups. All 13 stars selected in the RASS-ACT/TRC sample that overlapped with dZ99's membership lists were found to be PMS candidates. Our RASS-ACT/TRC sample (including the 13 dZ99 stars also selected) yielded a PMS hit rate of $(88 + 13)/(96 + 13) = 93\%$. Of the 30 dZ99 candidates we observed, 22/30 (73%) are classified as PMS or PMS?. The numbers of stars by membership class are listed in Table 7. PMS stars in the *Hipparcos* sample are listed in Table 4, and those in the RASS-ACT/TRC sample are given in Table 5. Li-rich stars with dwarflike surface gravity ($N = 5$) were considered young main-sequence field stars (ZAMS) and are listed along with other interlopers in Table 6.

5.2. *Sample Contamination*

The primary contaminants one would expect from an X-ray– and proper-motion–selected sample are X-ray–luminous ZAMS stars (ages $\approx$ 0.1–1 Gyr). Field ZAMS stars could occupy the same region of *UVW* velocity space and be selected in our study by virtue of their proper motions and X-ray emission. However, our selection of candidate Sco-Cen members uses a surface gravity criterion that should minimize contamination. Even if our surface gravity indicator was in error, we claim ZAMS stars do not dominate our sample. Field ZAMS stars exhibit a large spread in Li EWs (especially for the late G and early K stars); however, this is not observed in Figure 3. The star just below the " Li-rich " line in Figure 3 (TYC 7318-593-1; G9, EW(Li) $\simeq$ 150 mÅ) happens to be the sole RASS-ACT/TRC star with inferred log g *higher* than that of the dwarf standards in Figure 1. We consider TYC 7318-593-1 to be a field ZAMS star candidate because of its intermediate Li strength and high surface gravity.

We can rule out most of the PMS candidates being Li-rich *post-MS* stars. Based on the surveys of Li abundances in field subgiants by Randich et al. (1999) and Pallavicini, Cerruti-Sola, & Duncan (1987), we do not expect to find any post-MS subgiants with EW(λ6707) > 100 mÅ. Even if our measured EWs for the Li I λ6707 line are overestimated because of low spectral resolution, the overestimate would have to be greater than a factor of 2 to reconcile our sources with even the most Li-rich subgiants found in the Randich et al. survey. Our spectral analysis suggests that the majority of our sample stars are both Li-rich and above the main sequence (i.e., PMS).

Could some of our stars be *post*-MS chromospherically active binaries (CABs) or RS CVn systems? The light from an RS CVn system would be dominated by a rapidly rotating, evolved (subgiant) primary. Only six of our targets are Li-poor subgiants (HIP 63797, HIP 81775, TYC 8293-92-1, TYC 7833-1106-1, TYC 7858-526-1, and TYC 8285-847-1). The first three appear to be normal subgiants. TYC 7833-1106-1 is possibly a spectroscopic binary. TYC 7858-526-1 has a wide, broad Hα absorption line. It appears to be a multiple late F star (we classify it as F8.5; Houk 1982 classifies it as F5), so the star could hide a cosmic Li abundance because of the increased ionization of Li I in F stars (and correspondingly lower EW(Li)). The system could be a legitimate member, but we exclude it from the PMS sample. The subgiant TYC 8285-847-1 (HIP 69781 = V636 Cen) is probably a CAB. It is a previously known, grazing, eclipsing binary (e.g., Popper 1966), and its saturated X-ray emission argues for being a true CAB. Finally, the Li-rich star TYC 8992-605-1 (star 19; K0 +III) is the only RASS-ACT/TRC star that appears in the giant regime of Figure 1. The star is an obvious spectroscopic binary of nearly equal mass. We believe this star is probably a PMS binary, and include it in our PMS? sample. It appears that CABs are a negligible contaminant when using X-ray and kinematic selection in tandem with medium-dispersion spectroscopy to identify PMS populations.

5.3. *Sample Completeness*

We can make a rough estimate of how many stars our selection procedure should have detected by counting the number of massive Sco-Cen members in a certain mass range and assuming an initial mass function. We assume a complete membership census within a limited mass range (the revised B-star *Hipparcos* membership from dZ99) and then extrapolate how many stars we should have seen in our survey. We produce a theoretical H-R diagram for the subgroups' B stars (discussed at length in § 7.2) and calculate masses from the evolutionary tracks of Bertelli et al. (1994; $Z = 0.02$). We choose 2.5 $M_{\odot}$ as our lower mass boundary (roughly the lower limit for B stars) and adopt 13 $M_{\odot}$ as the upper mass boundary (slightly higher than the highest inferred mass from the main-sequence members). In this mass range, we count 32 LCC members and 56 UCL members. We use a Kroupa (2001) initial mass function (IMF) to predict how many low-mass stars might belong to the OB subgroups. Down to the hydrogen-burning limit (0.08 $M_{\odot}$), a total population of 1200^{+200}_{-300} stars in LCC and 2200 $\pm$ 300 stars in UCL is predicted (Poisson errors).[5] Between 1.1 and 1.4 $M_{\odot}$, the mass range of a 15 Myr old population that our survey can probe (see § 7.1 and Fig. 6), the Kroupa IMF predicts a population of 29^{+6}_{-5} stars in LCC and 51^{+8}_{-7} stars in UCL. In this mass range, our survey detects 36 PMS stars in LCC and 40 PMS stars in UCL. The number of observed PMS stars with 1.1–1.4 $M_{\odot}$ corresponds to $+1.1\ \sigma$ and $-1.6\ \sigma$ of the predicted number for LCC and UCL, respectively. This suggests that our survey is fairly complete for LCC, but we might be missing $\sim$10 members with masses of 1.1–1.4 $M_{\odot}$ in the more distant UCL subgroup, if the subgroup mass function is consistent with the field star IMF. The missing members of the UCL OB subgroup could be X-ray faint ($L_X \leq 10^{30.2}$ ergs s^{-1}) stars that we were capable of detecting in the closer LCC subgroup. The IMF extrapolation does suggest that we have likely found at least the majority of stars in this mass range in both OB subgroups (if not a complete census for LCC) and that our samples are representative of the total population.

6. H-R DIAGRAM

In order to investigate the star formation history of the LCC and UCL OB subgroups, we convert our observational data (spectral types, photometry, distances) into estimates of temperature and luminosity. We then use theoretical evolutionary tracks to infer ages and masses for our stars.

6.1. *Photometry*

The primary sources of photometry for our sample of association member candidates are the Tycho-2 catalog (Høg et al. 2000a, 2000b) and 2MASS working database. However, the Tycho and 2MASS bandpasses are nonstandard and must be converted to standard photometric systems to enable comparison with intrinsic colors of normal stars and the interstellar reddening vector. To convert the Tycho photometry to the Johnson system, we fitted low-order polynomials to the data in Table 2 of Bessell (2000; relations given in Appendix C). A caveat is that Bessell's calibrations are for B–G dwarfs and K–M giants. The majority of our stars appear to be PMS G–K stars, whose intrinsic colors should more closely match those of dwarfs rather than giants. To convert the 2MASS JHK_s data to the system of Bessell & Brett (1988), we use the conversions of Carpenter (2001). The original optical and near-IR photometry for our target stars is given in Tables 1 and 2.

6.2. *Temperature Scale*

To fix stellar properties as a function of spectral type, we adopt relations (i.e., intrinsic colors, bolometric corrections [BCs]) from Table A5 of Kenyon & Hartmann (1995). Previous studies have shown that colors and BCs as a function of $T_{\rm eff}$ are largely independent of surface gravity over the range of interest for this study (e.g., Bessell, Castelli, & Plez 1998). However, $T_{\rm eff}$ decreases with lower log g for FGK stars. After some investigation (see Appendix A), we decided to adopt the dwarf $T_{\rm eff}$ scale of Schmidt-Kaler (1982; which Kenyon & Hartmann 1995 also use) with a -35 K offset to account for the effects of lower log g in our sample stars. The scatter in published dwarf $T_{\rm eff}$ scales is 60 K (1 σ) among G stars, so while the shift is systematic, its magnitude is of the order of the uncertainties. The uncertainties in $T_{\rm eff}$ given in column (9) of Tables 4 and 5 include the uncertainty in spectral type and the scatter in published $T_{\rm eff}$ scales. The typical 1 σ uncertainties in $T_{\rm eff}$ for the PMS stars is $\approx$100 K.

6.3. *Secular Parallaxes*

All of the stars in our sample have published proper motions, but only a few dozen have trigonometric parallaxes measured by *Hipparcos*. The stars are distributed over hundreds of square degrees of sky and inhabit stellar associations that are tens of parsecs in depth. Adopting a standard distance for all of the stars in the association introduces unwanted scatter in the H-R diagram. With accurate proper motions available, we calculate individual distances to the PMS candidates using moving cluster or "secular" parallaxes (e.g., Smart 1968). We adopt the equations and formalism of de Bruijne (1999b), as well as his space motions and convergent points for the LCC and UCL OB subgroups. The uncertainties in the secular parallaxes are dominated by the uncertainties in the proper motion ($\sigma_{\pi} \propto \sigma_{\mu}$), but contain a term added in quadrature accounting for a projected 1 km s^{-1} internal velocity dispersion (see § 4 of de Bruijne 1999b). The secular parallax is only meaningful if the star is indeed a member of the group. Our spectroscopic survey has confirmed that most of the candidate stars are legitimately PMS, and that they are most likely members of the OB subgroups. Secular parallaxes for older, interloper stars are meaningless and ignored. In Tables 4 and 5, we list the secular parallaxes and membership probabilities for the PMS stars in our survey. We calculate membership probabilities P_1 and P_3 (using eqs. [4] and [6] from dZ99), which have assumed internal velocity dispersions of 1 km s^{-1} (de Bruijne 1999b) and 3 km s^{-1} (dZ99), respectively.

The robustness of our method can be illustrated (Fig. 4) by comparing the secular parallaxes ($\pi_{\rm sec}$) to the *Hipparcos* trigonometric parallaxes ($\pi_{\rm HIP}$). The uncertainties are typically 1–2 mas for the *Hipparcos* parallaxes and 0.5–1 mas for our secular parallax estimates. The secular and trigonometric parallaxes agree quite well for the few PMS stars in our sample for which *Hipparcos* measured the parallax. The secular parallaxes yield distance uncertainties of $\sim$5%–15% for most of the PMS stars.

[5] For low-number statistical uncertainties, we use the 1 σ values from Gehrels (1986) throughout.

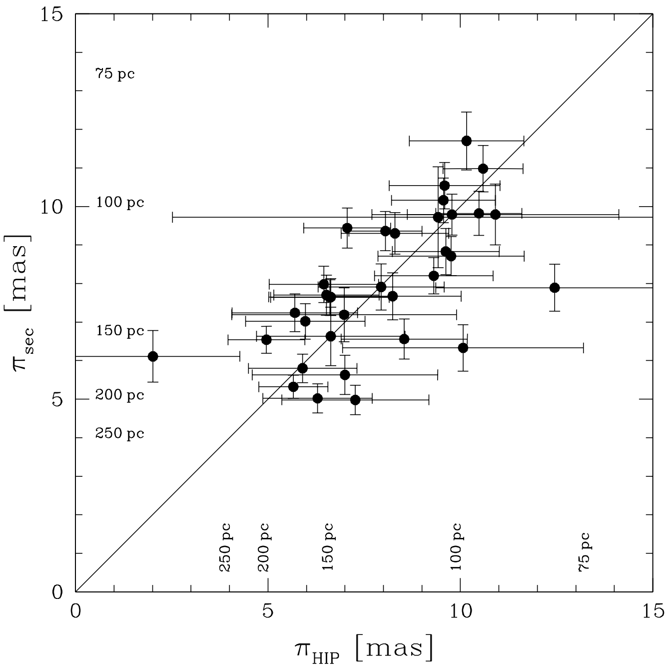

FIG. 4.—Comparison between *Hipparcos* astrometric parallaxes and our secular parallaxes calculated using the moving group method. Data points are PMS (and PMS?) association members from Tables 4 and 5.

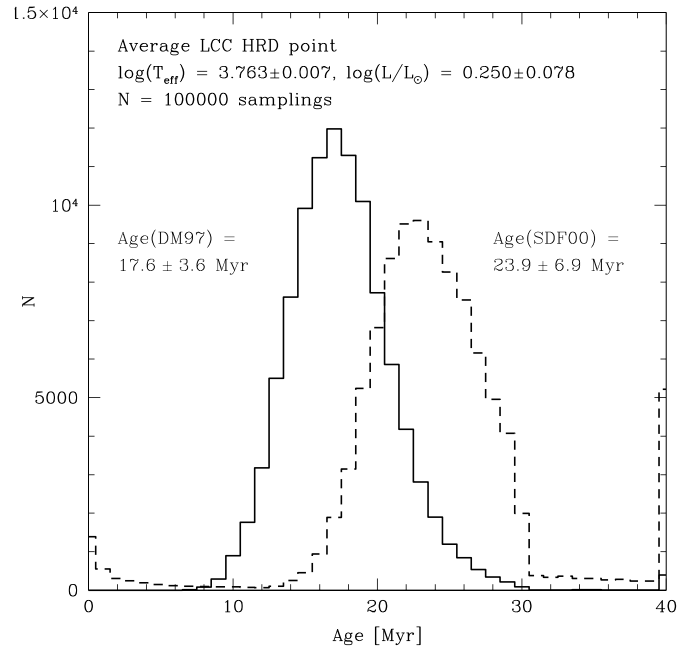

FIG. 5.—Histogram of the inferred ages from the DM97 and SDF00 tracks for a hypothetical LCC PMS star with average H-R diagram point [$T_{\rm eff}$, log $(L/L_\odot)$] and Gaussian uncertainties. The extreme right bin retains all points older than 40 Myr. The standard deviations are calculated using only stars with ages between 1 and 100 Myr.

6.4. *Luminosities*

With five-band photometry, a temperature and/or spectral type estimate, and a secular parallax, we calculate stellar luminosities for the PMS candidates. We adopt the absolute bolometric magnitude of the Sun ($M_{{\rm bol},\odot} = 4.64$) from Schmidt-Kaler (1982). In order to compromise between the uncertainties in luminosity due to reddening, photometric uncertainties, and possible K-band excess, we calculate the $M_{\rm bol}$ using the dereddened 2MASS J magnitude. We estimate the visual extinction from a weighted mean of A_V estimates from the color excess in $B-V$ and $V-J$. We took the $E(B-V)$ formula from Drilling & Landolt (2000), and the value of A_J/A_V (=0.294) was taken from the near-IR extinction law of Mathis (1990) for a central wavelength 1.22 μm. The reddening A_J typically ranged from 0 to 0.35 mag with formal uncertainties of $\sim$0.1 mag. The typical uncertainty in log $(L/L_\odot)$ for the PMS candidates is $\approx$0.08 dex. With the luminosities and X-ray fluxes from the RASS BSC catalog (Voges et al. 1999), we calculate the ratio of X-ray to bolometric radiation for the stars with X-ray counterparts. The derived values of log $(L_{\rm X}/L_{\rm bol})$ are in the range of $10^{-2.8}$ to $10^{-3.8}$, indicating coronal X-ray emission elevated above most ZAMS G-type stars (e.g., Pleiads; Stauffer et al. 1994).

6.5. *Evolutionary Tracks*

In order to infer theoretical masses and ages from our PMS candidates, we use the evolutionary tracks from D'Antona & Mazzitelli (1997, hereafter DM97; $Z = 0.02$, $x_{\rm D} = 2 \times 10^{-5}$), Siess, Dufour, & Forestini (2000, hereafter SDF00; $Z = 0.02$), and Palla & Stahler (2001, hereafter PS01). Ages and masses for a given log $T_{\rm eff}$ and log $(L/L_\odot)$ were calculated using an interpolation algorithm. Given the mean observational errors (σ[log $T_{\rm eff}$, log $(L/L_\odot)] = 0.007$, 0.078 dex for LCC PMS stars, and σ[log $T_{\rm eff}$, log $(L/L_\odot)] = 0.009$, 0.084 dex among UCL PMS stars), we estimate the isochronal age uncertainties for an individual star to be approximately 4, 5, and 7 Myr (DM97; PS01; SDF00) in LCC and 4, 5, and 5 Myr (DM97; PS01; SDF00) in UCL, as illustrated in Figure 5. The uncertainties in the interpolated masses are 0.1 $M_\odot$ for all three sets of tracks. Figure 6 shows the H-R diagram for the PMS candidates overlaid with the evolutionary tracks of DM97.

7. RESULTS

The ages of the low-mass population of LCC and UCL have not been estimated before, although de Geus et al. (1989) and de Zeeuw & Brand (1985) give main-sequence turnoff ages. In § 7.1, we estimate the PMS ages for the two subgroups and put an upper limit on the intrinsic age spread. In § 7.2, we calculate new turnoff ages for the subgroups using early B stars from the revised *Hipparcos* membership lists of dZ99.

7.1. *PMS Ages and Age Spread*

The H-R diagram for our PMS and PMS? stars is shown in Figure 6, overlaid with the evolutionary tracks of D'Antona & Mazzitelli (1997). The temperatures and luminosities of the PMS stars are given in columns (9) and (10) of Tables 4 and 5, along with their inferred masses and ages (cols. [15]–[17]). One notices immediately that the bulk of isochronal ages are in the range of $\sim$10–20 Myr. The age range is nearly identical for both groups. To assess the effects of our magnitude limit in biasing our mean age estimates, in Figure 7 we plot the mean PMS age (with standard errors of the mean) for the PMS subgroup samples as a function of minimum log $T_{\rm eff}$ cutoff. The magnitude bias of our survey is clearly apparent: the mean age systematically decreases when stars with log $T_{\rm eff} < 3.73$ are included in the

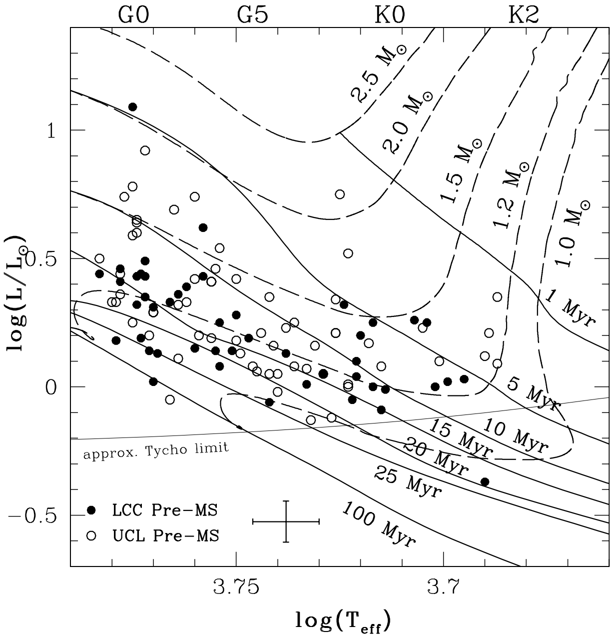

FIG. 6.—Theoretical H-R diagram for stars identified as PMS or PMS? in Tables 4 and 5 in the UCL (*open circles*) and LCC samples (*filled circles*). The PMS evolutionary tracks of DM97 are overlaid. The ACT/TRC magnitude limit ($V = 11$ mag) is shown for a distance of 150 pc ($A_V = 0.3$ assumed). The star in the bottom right corner (TYC 8648-446-1) is one of the faintest stars in our sample ($V = 11.2$ mag) with larger than average errors in log $(L/L_\odot)$—hence its unusual position. The average 1 σ error bars in log $T_{\rm eff}$ and log $(L/L_\odot)$ are shown.

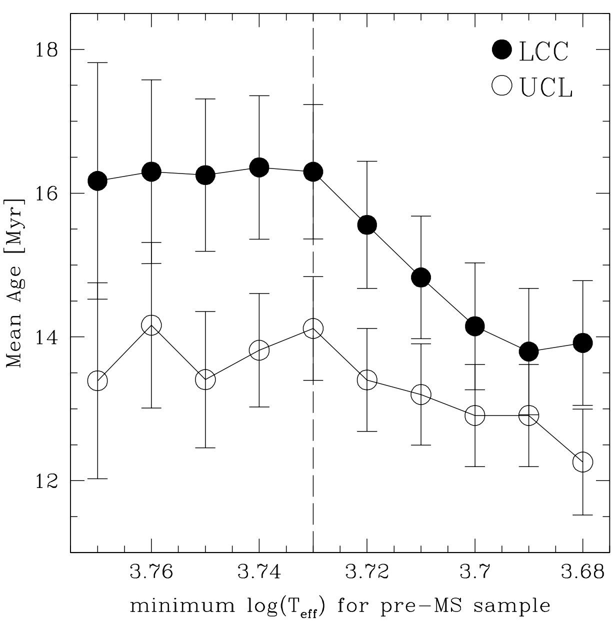

FIG. 7.—Illustration of the effects of magnitude bias on our mean age estimates for the PMS populations. The abscissa is the minimum log $T_{\rm eff}$ threshold for evaluating the mean sample ages (using DM97 tracks). The ordinate is calculated mean age with standard errors of the mean (shown; typically ≈1 Myr). At cooler temperatures (later than K0), the magnitude limit of our survey biases the sample toward more luminous stars, thereby decreasing the mean age estimate. From this diagram, we choose log $T_{\rm eff} = 3.73$ (*vertical dashed line*) as the lower $T_{\rm eff}$ cutoff for evaluating the mean PMS ages. Known spectroscopic binaries are included here but excluded in the final age estimates presented in Table 8. The *observed* isochronal ages and spread are 16 ± 5 Myr for LCC and 14 ± 5 Myr for UCL.

calculation. In calculating the PMS ages of the OB subgroups, we explicitly omit the PMS stars with log $T_{\rm eff}$ < (30% of our sample). This temperature threshold intersects our magnitude limits at ages of ∼25 Myr for stars of 1 $M_\odot$ on the DM97 tracks. That the lines in Figure 7 are nearly flat for log $T_{\rm eff} > 3.73$ suggests that (detectable) stars with ages of greater than 25 Myr are not a significant component of either subgroup (also see discussion in § 8.1).

Figure 8 displays histograms of the isochronal ages for the PMS stars in the LCC and UCL subgroups derived using DM97 and SDF00 evolutionary tracks. These tracks represent the extrema in age estimates for our sample (DM97 is youngest, and SDF00 is oldest). The 1 σ age dispersion among the unbiased samples (log $T_{\rm eff} > 3.73$) is 5–9 Myr for both groups. If we remove the known spectroscopic binaries (see notes in Tables 4 and 5), the age dispersions are 4–8 Myr. Because there may be additional unresolved binaries, this *observed* age spread places an upper limit on the *intrinsic* age spread. As illustrated in Figure 5, the individual H-R diagram positions of the PMS samples have log $T_{\rm eff}$ and log $(L/L_\odot)$ errors that fold onto the evolutionary tracks with age uncertainties of 4–7 Myr. From this analysis, we conclude that the *intrinsic* 1 σ age dispersions in each subgroup must be less than 2–8 Myr (i.e., roughly two-thirds of the star formation took place in less than 4–16 Myr). Using the DM97 PMS ages, which agree best with the turnoff age estimates (§ 7.2), we find intrinsic 1 σ age dispersions of 2 Myr (LCC) and 3 Myr (UCL). *This implies that 68% of the low-mass star formation took place within less than* 4–6 Myr*, and 95% within less than* 8–12 Myr *in the OB subgroups*. Our observational uncertainties and lack of knowledge about the unseen binarity of the PMS sample stars do not allow us to constrain the age spread more precisely than this. The mean age estimates for our unbiased PMS samples (log $T_{\rm eff} > 3.73$, SBs removed) are shown in Table 8. Counter to previous studies, we find that LCC is slightly older than UCL by 1–2 Myr (at 1–3 σ significance), independent of which evolutionary tracks we use. From Figure 8, we also conclude that star formation ceased approximately ∼5–10 Myr ago in the subgroups.

7.2. *Turnoff Ages*

De Geus et al. (1989) published the most recent age estimates for the LCC and UCL groups; however, in light of

TABLE 8
AGE ESTIMATES OF LCC AND UCL

Reference	Tracks	Method	Age (LCC) (Myr)	Age (UCL) (Myr)
1........................	4	PMS	17 ± 1	15 ± 1
1........................	5	PMS	21 ± 2	19 ± 1
1........................	6	PMS	23 ± 2	22 ± 1
1........................	7	Turnoff	16 ± 1	17 ± 1
2........................	8	Turnoff	11–12	14–15
3........................	8, 9	Turnoff	10–11	12–13

NOTES.—Uncertainties are standard errors of the mean. PMS age estimates exclude known SBs and stars with log $T_{\rm eff} < 3.73$, which bias the calculated ages. The turnoff ages from this work are determined using only early B stars classified as members by de Zeeuw et al. (1999).

REFERENCES.—(1) This work; (2) de Geus et al. 1989; (3) de Zeeuw & Brand 1985; (4) D'Antona & Mazzitelli 1997; (5) Palla & Stahler 2001; (6) Siess et al. 2000; (7) Bertelli et al. 1994; (8) Maeder 1981; (9) B. Cogan (private communication cited in de Zeeuw & Brand 1985).

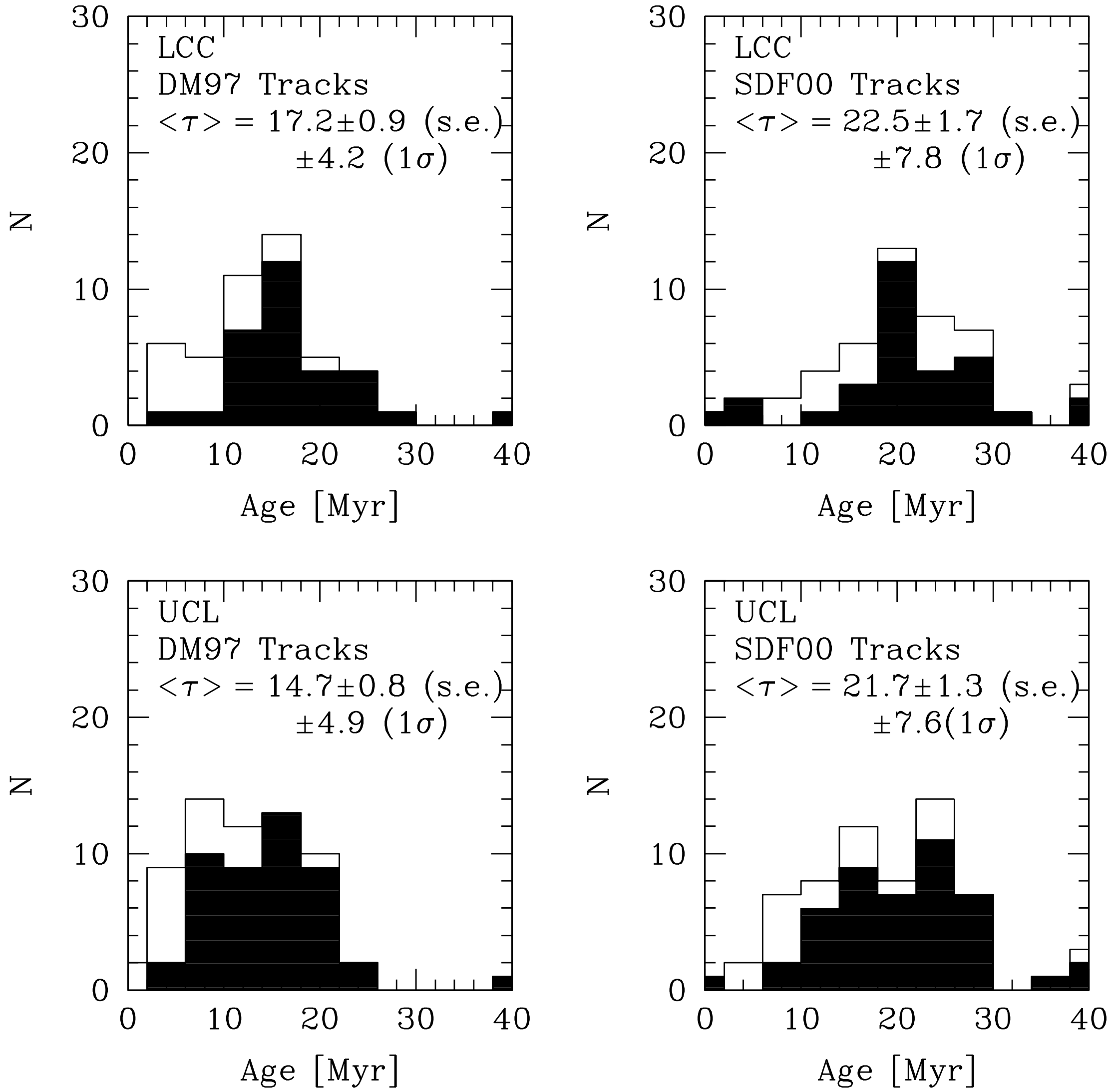

FIG. 8.—Histograms of the isochronal ages for PMS and PMS? candidates in Tables 4 and 5 from the models of DM97 and SDF00. The filled bins are for stars with log $T_{\rm eff} > 3.73$, and the unfilled bins are for the entire (magnitude-biased) sample. Mean isochronal ages (with standard errors of the means and 1 σ uncertainties) are given for the unbiased sample (log $T_{\rm eff} > 3.73$). Outliers with isochronal ages of greater than 40 Myr are counted within the 40 Myr bin.

the new *Hipparcos* distances and subgroup membership lists, we feel it is worthwhile to reevaluate the subgroups' turnoff ages. We construct a theoretical H-R diagram for the B-type subgroup members of UCL and LCC listed both in Table C1 of dZ99 and Tables A2 and A3 of de Bruijne (1999b). Several of the "classical"[6] stars rejected as members by *Hipparcos* from dZ99 are included as well. For input data, we use the following databases in order of availability: (1) *ubvy*β photometry from the database of Hauck & Mermilliod (1998), (2) *UBV* photometry from Slawson, Hill, & Landstreet (1992), and (3) *UBV* photometry from SIMBAD. For distances, we use the secular parallaxes ($\pi_{\rm sec}$) given in column (4) of Tables A2 and A3 of de Bruijne (1999b) when available, or the *Hipparcos* parallaxes ($\pi_{\rm HIP}$). We deredden the stars with *ubvy*β photometry to the B-star sequence of Crawford (1978) using the prescription of Shobbrook (1983). For stars with Stromgren photometry, we calculate $T_{\rm eff}$ using the temperature relation of Napiwotzki, Schönberner, & Wenske (1993). If no *ubvy*β photometry is available, we use *UBV* photometry to calculate the reddening-free index Q (Crawford & Mandwewala 1976) to infer the star's unreddened color. A polynomial fit to Table 15.7 from Drilling & Landolt (2000) is used to calculate $T_{\rm eff}$ as a function of $(B-V)_0$. The BC versus $T_{\rm eff}$ relation of Balona (1994) is used for all stars. We linearly interpolate between the isochrones from Bertelli et al. (1994; $Y = 0.28$, $Z = 0.02$, convective overshoot) to infer ages for the subgroup B stars. The theoretical H-R diagram is shown in Figure 9.

UCL has a well-defined MS turnoff composed of the *Hipparcos* members HIP 67464 (ν Cen; B2 IV), HIP 68245 (ϕ Cen; B2 IV), HIP 68282 (ν^1 Cen; B2 IV–V), HIP 71860 (α Lup; B1.5 III), HIP 75141 (δ Lup; B1.5 IV), HIP 78384 (η Lup; B2.5 IV), and HIP 82545 (μ^2 Sco; B2 IV), as well as

[6] "Classical" members are early-type stars which were included in Sco-Cen membership lists before the *Hipparcos* studies of dZ99.

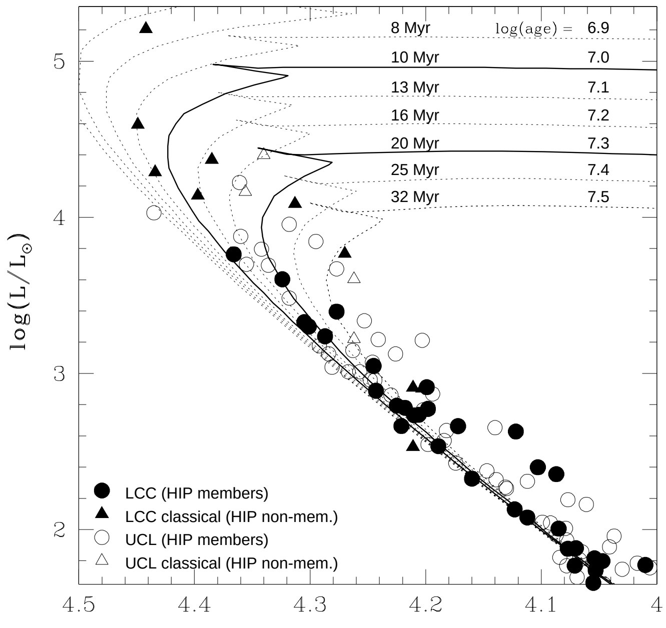

FIG. 9.—Theoretical H-R diagram for the B-star candidate members of the LCC and UCL memberships using the evolutionary tracks of Bertelli et al. (1994). Only the most massive *Hipparcos* members were included in the age estimates. The unusual variable HIP 67472 [μ Cen; B2 Vnpe; log $(L/L_\odot)$, log $T_{\rm eff} = 4.0$, 4.43] was excluded from the UCL turnoff age estimate.

classical members (but *Hipparcos* nonmembers) HIP 82514 (μ_1 Sco; B1.5 Vp) and 73273 (β Lup; B2 III)[7]. The variable star HIP 67472 (μ Cen; B2 Vnpe) was excluded. Using the Bertelli et al. (1994) tracks, the mean age of the seven turnoff *Hipparcos* members is 17 ± 1 Myr. Including the two classical members has a negligible effect on the mean age estimate. Our MS turnoff age estimate for UCL is slightly older than de Geus et al.'s (14–15 Myr) and is close to the mean PMS ages that we found in § 7.1 (15–22 Myr).

LCC lacks a well-defined turnoff; however, we have enough early B stars in the middle of their MS phase with which to make an age estimate. We estimate the age for LCC from the following main-sequence B stars: HIP 59747 (δ Cru; B2 IV), HIP 60823 (σ Cen; B2 V), HIP 61585 (α Mus; B2 IV-V), HIP 63003 (μ^1 Cru; B2 IV-V), and HIP 64004 (ξ^2 Cen; B1.5 V). The mean age for these five stars is 16 ± 1 Myr, similar to what we found for UCL, and it agrees well with the younger end of our PMS age estimates (17–23 Myr). This age estimate is significantly older than previous estimates (10–12 Myr) and warrants more critical examination (§ 8.3).

The new results yielded by our age analysis of the OB subgroups are (1) two-thirds of the low-mass star formation in each subgroup took place in less than a $\sim$5 Myr span (and 95% took place within $\sim$10 Myr), (2) the PMS and B-star ages for LCC and UCL are in approximate agreement, (3) the B-star subgroup memberships defined by *Hipparcos* have ages of 16 ± 1 Myr and 17 ± 1 Myr for LCC and UCL, respectively. We discuss the implications of these results in § 8.

7.3. *The Census of Accretion Disks*

An important question both for star and planet formation is the lifetime of accretion disks around young stars. Statistics for the frequency of active accretion disks around low-mass stars come predominantly from near-IR surveys of young associations and clusters (Hillenbrand & Meyer 1999; Haisch et al. 2001). The samples of low-mass stars surveyed are dominated by embedded associations with ages of less than 3 Myr (e.g., Tau-Aur, Cha I, etc.) and older open clusters with ages of 30–100 Myr (e.g., Pleiades, IC 2602, α Per, etc.). Few well-studied PMS stars of 3–30 Myr old ages have been surveyed. The situation has recently been slightly ameliorated by the discoveries of the TW Hya association and η Cha cluster (Kastner et al. 1997; Webb et al. 1999; Mamajek, Lawson, & Feigelson 1999). Yet these samples are small ($\sim$10–20 stars) and dominated by K- and M-type stars with masses of 0.1–0.8 $M_\odot$. Our PMS star sample is unique in its mass ($\sim$1–1.5 $M_\odot$) and age range ($\sim$10–20 Myr), so measuring its disk frequency provides a valuable datum.

Stars with EW(Hα) > 10 Å in emission are usually called CTTSs, which show spectroscopic signatures of accretion, as well as near-IR excesses (e.g., Hartigan, Edwards, & Ghandour 1995). Stars lacking the strong Hα emission and near-IR excesses are called WTTSs. This can be explained as a correlation between the presence of magnetospheric accretion columns and an inner accretion disk (e.g., Meyer, Calvet, & Hillenbrand 1997; Muzerolle, Hartmann, & Calvet 1998). Our Hα EW measurements are discussed in § 4.2.1, and here we quantify the K-band excess of our targets. We calculate the intrinsic $J-K$ color excess $E(J-K)_0$ as defined by Meyer et al. (1997):

$$E(J-K)_\circ = (J-K)_{\rm obs} - (J-K)_\circ - A_V(A_J - A_K) , \quad (1)$$

where $(J-K)_{\rm obs}$ is the observed color and $(J-K)_0$ is the intrinsic color of an unreddened dwarf star of appropriate spectral type (Kenyon & Hartmann 1995). Uncertainties in each quantity were propagated in order to estimate the signal-to-noise ratio (S/N) of the intrinsic color excess. The distribution of measured $E(J-K)_0$ values indicate a systematic offset of a few hundredths of a magnitude. Our near-IR data set is from the 2MASS working database, so we suspect that the absolute calibration or uncertainties in color correction could be responsible and apply a small color correction to account for it. After the correction, the distribution of $E(J-K)_0$ values is symmetric about zero, with a few positive and negative $\sim$2 σ points. There is only one star with a $E(J-K)_0$ color excess with S/N > 2.5: star 34 (=TYC 9246-971-1) has an intrinsic color excess of $E(J-K)_0 = 0.26 \pm 0.06$, implying a K-band excess. This star also happens to be the only CTT identified in our optical spectra [EW(Hα) = -39 Å]. TYC 9246-971-1 (=PDS 66, Hen 3-892) was originally identified as an emission-line star by Henize (1976) and classified as a CTT in the Pico dos Dias Survey of stars in the *IRAS* PSC catalog (Gregorio-Hetem et al. 1992). By virtue of its position, proper motion, and spectral characteristics, we find that TYC 9246-971-1 is a $\approx$8 Myr old, $\approx$1.2 $M_\odot$ (DM97 tracks) member of the LCC subgroup. Our secular parallax for TYC 9246-971-1 yields a distance of 86^{+8}_{-7} pc; the third nearest of the LCC PMS stars

[7] Note that the two *Hipparcos* nonmembers were found to be probable members by Hoogerwerf (2000) if the long-baseline ACT (HIP 73273) and TRC (HIP 82514) proper motions were used instead of the *Hipparcos* values.

in our sample and among the nearest CTTSs known. Only one out of 58 ($1.7^{+4.0}_{-1.4}$%; 1 σ Poisson) of PMS stars in LCC are classified as bona fide CTTSs, along with none (0/42) of the PMS members of UCL. For our accretion disk frequency statistics, we use the isochronal ages derived from the DM97 evolutionary tracks (which agree well with the turnoff ages) and include the entire sample of 110 PMS stars (including the cooler stars that bias the mean to younger ages). Only one out of 110 ($0.9^{+2.1}_{-0.8}$%; 1 σ) of 1.3 $\pm$ 0.2 (1 σ) $M_\odot$ stars with ages of 13 $\pm$ 1 (s.e.) $\pm$ 6 (1 σ) Myr are CTTSs. This implies that accretion terminates in solar-type stars within the first 15 Myr of their evolution.

8. DISCUSSION

We can address several interesting questions regarding the star formation history of Sco-Cen with data from our survey. Could the Sco-Cen progenitor giant molecular cloud (GMC) have produced a substantial population of low-mass stars for an extended period (greater than 5–10 Myr) *before* conditions were right to form an OB population? Conversely, is there evidence for any low-mass star formation *after* the bulk of the high-mass OB stars formed? The OB star formation in LCC and UCL has apparently destroyed the progenitor GMC through supernovae and stellar winds (e.g., de Geus 1992; Preibisch & Zinnecker 2000). However, the region is not totally devoid of molecular gas (e.g., the Lupus complex). We will first examine whether there is any evidence of star formation prior to the formation of the OB subgroups (§ 8.1) and then assess the evidence for more recent star formation in the UCL region (§ 8.2). We will address the age of LCC in § 8.3 and discuss the formation of the subgroups in § 8.4. Throughout the discussion, we adopt the DM97 ages, since they agree more closely with the turnoff ages than do the SDF00 and PS01 ages.

8.1. *Is There Evidence for Star Formation before the Primary Bursts?*

Is our survey sensitive to older stars that may have preceded the primary star formation episode? Three PMS stars in our sample have isochronal ages of greater than 25 Myr (or undefined as lying below the ZAMS); however, given the uncertainties in $T_{\rm eff}$ and log $(L/L_\odot)$ (Fig. 5), even a coeval $\approx$15 Myr old population would be expected to have *statistical* outliers. Here we explore three possible ways in which older ZAMS stars could have escaped our attention.

One could argue that our surface gravity indicator is biasing our sample against identifying ZAMS stars members (if they exist). If we disregard surface gravity as a criterion, we gain only four more RASS-ACT/TRC stars (all between F8.5 and G1), and only *one* of those would have an isochronal age greater than 25 Myr (TYC 8222-105-1; $\sim$30 Myr). If they were legitimate, older members with real ages of greater than 25 Myr, they should also be among the stars with the oldest *isochronal ages* in our sample, which they are not. This suggests that their secular parallaxes, hence their luminosities, are unjustified, and that they are not members of the OB subgroups. Coincidently, TYC 8222-105-1 is one of the earliest type stars in our sample (F8.5), where our surface gravity indicator has the least fidelity (Fig. 1). We can state that only *one* of the Li-rich stars showing dwarf gravity signatures that is comoving with LCC and UCL has an H-R diagram position and gravity suggestive of ZAMS status.

If a significant ZAMS population existed in LCC and UCL, would our magnitude and X-ray flux limits allow their detection? X-ray surveys of the ZAMS-age clusters IC 2602 and IC 2391 ($\sim$30–50 Myr) by Randich et al. (1995) and Patten & Simon (1996) found that late F and early G ZAMS stars have X-ray luminosities of $L_{\rm X} \simeq 10^{29.0}$ to $10^{30.5}$ ergs s^{-1}, with $L_{\rm X}/L_{\rm bol}$ ranging from $10^{-3.0}$ to $10^{-4.8}$. The X-ray and optical flux limits imposed by the *ROSAT* All-Sky Survey and the Tycho catalog allow us to detect ZAMS sources with $L_{\rm X}/L_{\rm bol} > 10^{-3.2}$ within 140 pc if they exist. If we adopt the X-ray luminosities of the G stars in IC 2602 and IC 2391 as representative for a $\sim$30 Myr old population, we should have detected roughly one-third of a putative Sco-Cen ZAMS population between masses of 1 and 1.2 $M_\odot$. We can put a rough upper limit on the number of greater than 25 Myr old stars in our mass range. Assuming that TYC 8222-105-1 *is* a ZAMS member and that its H-R diagram position is not a statistical fluctuation from the locus of $\sim$15 Myr old stars, we detect one ZAMS star with an age greater than 25 Myr in the mass range (1–1.2 $M_\odot$). Accounting for the two-thirds of the ZAMS stars that would have undetectable X-ray emission and extrapolating over a Kroupa (2001) IMF, this implies a population of $\sim$100 stars with masses greater than 0.1 $M_\odot$. This is $\leq$10% of the stellar population predicted to exist in each OB subgroup ($\sim$1000–2000; § 5.3).

Could such ZAMS stars have left the region we probed? If we postulate that the population was very centrally concentrated and gravitationally bound until the OB stars destroyed the GMC some $\sim$10 Myr ago (de Geus 1992), then a 2 km s^{-1} motion radially away from the subgroup center would have moved the star 20 pc in the past 10 Myr. This distance is the approximate radius of both of the subgroups today (see Fig. 9 of dZ99). Hence, if an older population was concentrated at center of the gravitationally bound GMC until the high-mass stars destroyed the cloud, we would find them within the projected boundaries of the subgroups so long as they inherited velocities of less than 2 km s^{-1}. The kinematic selection procedure of Hoogerwerf (2000) would have selected such stars, since a large velocity dispersion (3 km s^{-1}) was initially assumed.

We conclude that there is no evidence for significant star formation in the LCC and UCL progenitor GMCs before the primary star formation episodes. Our findings are consistent with the idea that molecular clouds form stars over a range of masses and dissipate within timescales of $\sim$10 Myr.

8.2. *Ongoing Star Formation?*

Two obvious sources of young stars may be contaminating the UCL PMS sample. The youngest, unembedded OB subgroup of Sco-Cen is US, with a nuclear age of 5–6 Myr (de Geus et al. 1989). US borders UCL near Galactic longitude 343°, and its space motion and distance are very similar to that of UCL (dZ99). The Lupus molecular clouds are also in the western region of UCL (roughly in the range $335° < l < 345°$ and $+5° < b < 25°$). The T Tauri star population within the major Lupus clouds was surveyed by Hughes et al. (1994), and the region was recently mapped in ^{12}CO by Tachihara et al. (2002). Dozens of pre–main-sequence stars were identified outside of the main cores by a pointed *ROSAT* survey (Krautter et al. 1997) and the All-

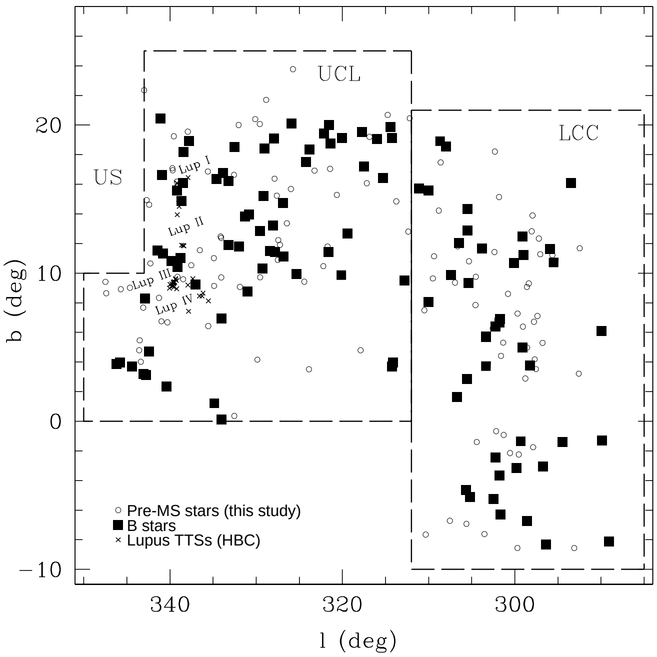

FIG. 10.—Map of the UCL and LCC subgroups of the Sco-Cen OB association (Sco OB2). The B-star population from de Zeeuw et al. (1999) is shown by filled squares. The PMS (and PMS?) sample from this survey is shown as open circles. Pre-*ROSAT* T Tauri stars in the HBC catalog associated with the Lupus cloud are shown as crosses (Herbig & Bell 1988).

Sky Survey (Wichmann et al. 1997b). The clouds lie at $d = 140$ pc (Hughes, Hartigan, & Clampitt 1993), situated spatially between the US and UCL subgroups of Sco-Cen (both $d \simeq 145$ pc). Figure 10 illustrates the positions of the primary Lupus clouds, the pre-*ROSAT* Lupus T Tauri star population, the PMS stars from our survey, and the B-star population of the OB subgroups.

How does the presence of US and the Lupus molecular clouds (and their associated T Tauri stars) affect our findings regarding the mean age of the UCL subgroup? We split our unbiased (log $T_{\rm eff} > 3.73$) PMS and PMS? members of UCL into two groups using the Galactic longitude line 335° as a division. Most of the molecular cloud mass in the Lupus region lies in the range $335° < l < 345°$ (see Fig. 2 of Tachihara et al. 2002). Using the DM97 tracks, we find that the "eastern" UCL PMS sample surrounding the Lupus clouds has a mean age of 13 ± 1 Myr, while the "western" UCL sample is somewhat older (16 ± 1 Myr). The UCL stars with ages of less than 10 Myr are found in greater numbers near the Lupus clouds and US border, supporting the idea that our UCL sample is probably contaminated by more recent star formation. The age estimate of UCL for the stars west of $l = 335°$ is probably more representative of the underlying UCL population.

Three of the youngest stars (HIP 81380, TYC 7858-830-1, and TYC 7871-1282-1; 5–9 Myr; DM97 tracks) in our entire survey are positioned near a clump of eight B stars at (l, b) = (343°, +4°). These three PMS stars also have secular parallax distances of ~200 pc, similar to what de Bruijne (1999b) found for the group of B stars. The secular parallaxes may be biased, however, if this clump has slightly different kinematics than the average UCL motion. This clump may represent substructure within UCL. However, de Bruijne (1999b) was unable to demonstrate that the clump had distinct kinematics or age. The mean *Hipparcos* distance of the clump B stars is 175 pc, with HIP 82514 (μ^1 Sco; B1.5 Vp) and HIP 82545 (μ^2 Sco; B2 IV) as the most massive members. Our identification of three new PMS stars in the same region with similar secular parallaxes supports the notion that this may be a separate subgroup.

Some of our PMS stars were also identified in the *ROSAT* surveys of the Lupus region by Krautter et al. (1997) and Wichmann et al. (1997b; see notes in Table 5). The presence of a significant population of PMS stars outside of star-forming molecular clouds has been attributed by various authors to be because of one or more of the following: (1) slow diffusion (1–2 km s^{-1}) from existing molecular clouds (e.g., Wichmann et al. 1997a), (2) ejection from small *N*-body interactions (Sterzik & Durisen 1995), (3) formation in situ from short-lived cloudlets (Feigelson 1996), or (4) fossil star formation associated with the Gould Belt (e.g., Guillout et al. 1998). Wichmann convincingly showed that most of the young RASS stars in the Lupus region are at a distance of around ~150 pc (similar to previously published distances for the Lupus clouds and UCL), and that the stars are roughly 10 Myr old. Wichmann concludes that the dispersed PMS population is most likely a manifestation of the Gould Belt. The OB subgroups of Sco-Cen are major substructures of the Gould Belt (as defined by age and kinematics; Frogel & Stothers 1977), i.e., UCL is the dominant Gould Belt substructure in the Lupus region. We interpret the presence of dozens of PMS stars near the Lupus clouds to be primarily the low-mass membership of the UCL OB subgroup. Our analysis suggests that younger US or Lupus stars are a minor contaminant to our UCL sample.

8.3. *Is LCC Older than UCL?*

Although our PMS and turnoff age estimates for LCC agree rather well, they are substantially older (by ~50%) than previous values. The de Geus et al. (1989) age estimate (11–12 Myr) appears to hinge primarily on the H-R diagram position of ϵ Cen, with δ Cru, α Mus, and ξ^2 Cen defining the rest of the turnoff isochrone. The latter three stars were confirmed as members by dZ99, but ϵ Cen (the most massive) was rejected. Although our age for ϵ Cen is consistent with de Geus's, we omitted it from our LCC age estimate. If one uses the long-baseline proper motion for ϵ Cen from the new Proper Motions of Fundamental Stars catalog (Gontcharov et al. 2001) and adopts the LCC space motion, convergent point, and formulae of dZ99 (with $v_{\rm int} = 3$ km s^{-1}), ϵ Cen has a 100% membership probability. The resulting secular parallax ($\pi_{\rm sec} = 9.6 \pm 2.0$ mas) agrees well with the *Hipparcos* astrometric parallax ($\pi_{\rm HIP} = 8.7 \pm 0.8$ mas), further strengthening the interpretation that ϵ Cen is a bona fide LCC member. Including ϵ Cen with the other five turnoff stars discussed in § 7.2 does not change our turnoff age estimate, however (16 ± 1 Myr). If one ignores the stars with masses less than that of ϵ Cen, then the 12 Myr Bertelli isochrone would appear to be an acceptable fit for LCC. Because the turnoff is poorly defined, we give equal weight to the next five *Hipparcos* members down the mass spectrum (δ Cru, σ Cen, α Mus, μ^1 Cru, and ξ^2 Cen), which yields an age older than de Geus's.

The star ϵ Cen is one of several classical LCC early B-type member candidates rejected as members of Sco-Cen using the *Hipparcos* astrometry. These stars have been included in Sco-Cen candidate membership lists on and off over the past half-century: HIP 59196 (δ Cen; B2 IVne), HIP 60718A (α^1 Cru A; B0.5 IV), HIP 62434 (β Cru; B0.5 IV), and HIP 68702 (β Cen; B1 III). These stars are $\sim$10–20 $M_\odot$ stars, with inferred ages of $\sim$5–15 Myr and distances of $\sim$100–150 pc. Such stars are extremely rare, and their presence in the LCC region appears to be more than coincidental. Are they all LCC members whose *Hipparcos* proper motions are perturbed because of binarity? *All* five systems are flagged (field No. 59) in the *Hipparcos* catalog as stars with unusual motions due to either unseen companions or variability. A kinematic investigation of these stars and their potential membership in LCC is beyond the scope of this study but is necessary for understanding the global star formation history of the Sco-Cen region. Are these stars bona fide members? If so, why are they so much younger than the other members (both PMS and mid B stars)? If they are not bona fide members, where did they come from? Although our age estimates for the PMS sample and *Hipparcos* early B members appear to be consistent, the presence of these young, B0–B2 classical members (*Hipparcos* nonmembers) hints that the story of star formation in Sco-Cen is more complex than our results reveal.

8.4. *A Star Formation History of Sco-Cen?*

Preibisch & Zinnecker (2000) reviewed the recent star formation history of Sco-Cen (less than 5–10 Myr) in the region of US, UCL, and ρ Oph. They present evidence for external supernovae triggering in the formation of the subgroups. They claim that supernovae shock waves from UCL passed through the US progenitor GMC approximately 5 Myr ago and caused the cloud to collapse. The US group appears to have had at least one supernova in the past $\sim$1 Myr, possibly a deceased massive companion to the runaway O9.5 V star ζ Oph. This supernova contributed to destroying the GMC and producing the US superbubble (de Geus 1992; Hoogerwerf, de Bruijne, & de Zeeuw 2001). The US subgroup appears to be currently triggering star formation in the ρ Oph cloud core. Here we speculate on the global star formation history of the Sco-Cen complex.

The formation of LCC and/or UCL may have been similarly triggered. However, it is unclear if one triggered the formation of the other or vice versa. Our PMS age estimates are consistent with LCC being slightly older than UCL by a few Myr, although they could be coeval. What was the origin of these large OB subgroups? The gas associated with the Sco-Cen complex appears to be part of the Lindblad Ring, a torus of H I and molecular clouds hundreds of parsecs in radius. It is centered roughly near the α Persei cluster and Cas-Tau OB association (Blaauw 1991; Pöppel 1997). The young stars that have formed from this gas complex (i.e., the Gould Belt) share a systematic expansion consistent with a localized origin for the whole complex—probably an expanding gas shell from a large star formation event (e.g., Moreno, Alfaro, & Franco 1999). The gas associated with Sco-Cen appears to be part of a "spur" of neutral hydrogen and molecular clouds that runs from near LCC (including Coalsack, Musca, and Chamaeleon clouds), through Lupus and Ophiuchus, and into the Aquila and Vulpecula Rift regions (see Fig. 3-18 of Pöppel 1997). It is likely that LCC and UCL were among the first clumps in the Lindblad Ring to collapse and form stars (see § 4 of Blaauw 1991), either from self-gravity or triggered from external supernovae events. The LCC and UCL regions formed a large population of OB stars, and their stellar winds and supernovae may indeed have triggered the collapse of the US group. The process might continue over the next 10 Myr as the supernovae from the US and ρ Oph subgroups send shock waves into the vast reservoir of atomic and molecular gas associated with the Aquila Rift (see § 3.4 of Pöppel 1997, and references therein). On the other side of Sco-Cen, there appears to be little gas westward of LCC until one reaches the Vela complex some 400 pc away. The lack of a sufficient gas reservoir probably explains why triggering did not proceed to form OB subgroups west of LCC.

The Sco-Cen subgroups have formed their own network of superbubbles with radii of $\sim$100 pc (de Geus 1992). The superbubbles appear to be largely H I, presumably gas from the progenitor Sco-Cen GMC, as well as the swept-up interstellar medium. In some region, they are associated with well-known nearby molecular cloud complexes: Coalsack, Musca, Chamaeleon, Corona Australis, Lupus, and numerous small high Galactic latitude clouds (e.g., Bhatt 2000). The Lupus clouds are spatially coincident with the western side of the US superbubble; however, no kinematic analysis has been yet undertaken to determine whether the Lupus clouds share in the bubble expansion. The CrA molecular clouds are embedded within the UCL superbubble shell, and the space motion of the T Tauri star population is moving radially away from UCL (Mamajek & Feigelson 2001). Other young stars in the field toward the fourth Galactic quadrant, including the η Cha cluster, TW Hya association, and β Pic group, all have ages of $\sim$10 Myr and are moving radially away from LCC and UCL. Perhaps these stars formed in small molecular clouds that accumulated within the expanding LCC/UCL superbubble shells.

9. CONCLUSIONS

From our spectroscopic survey of an X-ray–selected and kinematically selected sample of late-type stars in the Sco-Cen OB association, we summarize our main findings as follows:

1. We have identified a population of low-mass stars in the Lower Centaurus–Crux (LCC) and Upper Centaurus–Lupus (UCL) OB subgroups with the following properties: (1) G–K spectral types, (2) subgiant surface gravities, (3) lithium-rich, (4) strong X-ray emission ($L_X \simeq 10^{30}$ to 10^{31} ergs s^{-1}), and (5) proper motions consistent with the high-mass members. We classify stars that show these characteristics as bona fide PMS stars or PTTSs. X-ray and kinematic selection (the RASS-ACT/TRC sample) yielded a hit rate of 93% for selecting probable PMS stars, while kinematic selection alone (dZ99 *Hipparcos* sample G–K dwarfs and subgiants) yielded 73%.

2. We estimate the mean age of the PMS population in the LCC subgroup to be 17 $\pm$ 1 Myr (DM97 tracks), 21 $\pm$ 2 Myr (PS01), and 23 $\pm$ 2 Myr (SDF00). For UCL, the PMS population's mean age is 15 $\pm$ 1 Myr (DM97), 19 $\pm$ 1 Myr (PS01), and 22 $\pm$ 1 Myr (SDF00). The UCL PMS estimate appears to be slightly biased toward younger ages (by $\sim$1 Myr) through contamination by Lupus or US members. We also calculate new MS turnoff ages of 16 $\pm$ 1 Myr for LCC and 17 $\pm$ 1 Myr for UCL using the dZ99 *Hipparcos* membership and Bertelli et al. (1994) evolutionary tracks. The UCL PMS and turnoff age estimates are roughly self-consistent and similar to previously published estimates. Our age

estimates for LCC (PMS and turnoff) are older than previous estimates and are equal to or slightly older than UCL.

3. We find that 68% of the low-mass star formation in each subgroup took place within a less than 4–6 Myr span, and 95% took place within less than 8–12 Myr (using DM97 tracks). The conditions were right for producing low-mass stars in the LCC and UCL progenitor molecular clouds for less than 10 Myr.

4. We find the frequency of CTTSs among a PMS population in an OB association with masses of 1.3 ± 0.2 ($1\ \sigma$) $M_\odot$ and ages of 13 ± 1 (s.e.) ± 6 ($1\ \sigma$) Myr (DM97 tracks) to be only $0.9^{+2.1}_{-0.8}$% (1/110). The younger age results from using our entire (i.e., magnitude-biased) sample of PMS stars. Only one star in our sample showed both strong Hα emission and a K-band excess: the previously known CTTS TYC 9246-971-1 (star 34 = PDS 66 = Hen 3-892). This suggests that the disk accretion phase lasts $\lesssim$10–20 Myr in the evolution of solar-type stars in OB associations.

5. We demonstrate that a surface gravity indicator for classifying field G and K stars (Sr II λ4077 to Fe I λ4071) can be used to distinguish whether Li-rich stars are PMS or ZAMS in nature. When this indicator is used in tandem with other youth diagnostics (Li abundance, X-ray emission, Hα emission, and kinematics), one can confidently classify a star as PMS in nature.

E. M. and M. M. acknowledge support through NASA contract 1224768 administered by JPL. E. M. and J. L. were also supported through a NASA/JPL grant. E. M. also thanks the Sigma Xi Research Honor Society for a Grant-in-Aid, which financed part of our observing run. We thank the telescope allocation committee of the Mount Stromlo and Siding Spring Observatories' 2.3 m telescope for their generous allocation of telescope time. This project benefited from discussions and help from J. Beiging, A. Blaauw, J. Carpenter, C. Corbally, J. de Bruijne, T. de Zeeuw, M. Hamuy, L. Hillenbrand, W. Lawson, D. Soderblom, J. Stauffer, and S. Strom. We offer special thanks to Ronnie Hoogerwerf for assistance in the target selection effort and discussions. This publication makes use of data products from the Two Micron All Sky Survey (2MASS), which is a joint project of the University of Massachusetts and the Infrared Processing and Analysis Center (IPAC), funded by NASA and the NSF.

APPENDIX A

THE PRE–MAIN-SEQUENCE $T_{\rm eff}$ SCALE

Pre–main-sequence stars lie between dwarfs (V) and subgiants (IV) on color–absolute magnitude or temperature-luminosity H-R diagrams. A given visual spectral type will correspond to cooler temperatures as surface gravity decreases (e.g., Gray 1991; de Jager & Nieuwenhuijzen 1987). Dwarf temperature scales are often adopted for PMS populations, but it is prudent to account for the effects of surface gravity.

We quantify the effects of log g on the Sp. versus $T_{\rm eff}$ relation using two data sets. First, we fitted a polynomial surface to $T_{\rm eff}$(Sp., log g) using the data from Gray (1991, Table 2). As with most compilations of $T_{\rm eff}$(Sp.) in the FGK star regime, we find that a trinomial is the best low-order fit, and that a linear dependence on log g adequately accounts for the effects of surface gravity on temperature. Our second method finds a similar surface fit to $T_{\rm eff}$(Sp., log g) using published $T_{\rm eff}$ and log g values (Cayrel de Strobel et al. 2001) for the GK standards of Keenan & McNeil (1989) and F standards of Garcia (1989; those within 0.3 dex of solar [Fe/H], and luminosity class IV and V only). We adopt the isochrones from D'Antona & Mazzitelli (1997) for a fiducial log g value as a function of $T_{\rm eff}$ for a coeval 15 Myr old population.

Both assessments yield essentially the same result: dwarf temperature scales for G–K stars should be lowered by 35 K for a 15 Myr old population. The temperature decrement increases for younger ages: 70–40 K for G0–K2 10 Myr old stars, 235–105 K for G0–K2 5 Myr old stars, and 260–180 K for G3–K2 1 Myr old stars. Both techniques yielded a linear dependence of log g on $T_{\rm eff}$(Sp., log g), and the slopes were similar: $\partial T_{\rm eff}/\partial \log g \simeq 220$ K [log (cm s^{-1})]$^{-1}$ for the Keenan standards with Cayrel de Strobel stellar atmosphere data, and $\partial T_{\rm eff}/\partial \log g \simeq 190$ K [log (cm s^{-1})]$^{-1}$ for the interpolation of Gray's (1991, Table 2). Since the evolutionary model isochrones are parallel to the main sequence when the stars are on the radiative tracks (i.e., $\sim$10–30 Myr for $\sim$1 $M_\odot$ stars), the Δlog g between a 15 Myr isochrone and the main sequence is fairly constant over the G–K spectral types. Hence, one naively expects a linear offset in $T_{\rm eff}$(Sp., log g) between the 15 Myr isochrone and the main sequence.

With the 1 σ scatter between published $T_{\rm eff}$(Sp.) relations being $\sim$60 K among G stars, the systematic shift is nearly negligible. Upon comparing several temperature scales from the literature, we adopt the dwarf $T_{\rm eff}$ scale from Schmidt-Kaler (1982) and apply a -35 K offset to correct for the effects of lower surface gravity for a putative 15 Myr old population. We conclude that adopting dwarf $T_{\rm eff}$ versus Sp. scales for PMS stars younger than $\sim$10 Myr will systematically overestimate their $T_{\rm eff}$ values and, in turn, their masses inferred from evolutionary tracks. This could have deleterious systematic effects on derived IMFs for young associations.

APPENDIX B

STANDARDS WITH QUESTIONABLE LUMINOSITY CLASS

Several of the standard stars we observed had H-R diagram positions, published log g values, and Sr II λ4077/Fe I λ4071 ratios (Sr/Fe) that differed from what is expected for their luminosity classes given in Keenan & McNeil (1989). The differences are only at the half of a luminosity-class level. We adopted the Keenan temperature types for all of his standard stars, but we revised the luminosity classes of these stars to bring their H-R diagram positions, Sr/Fe index, and published log g estimates into harmony (Table 9). The Sr/Fe indices for the vast majority of the standards formed loci according to luminosity class (Fig. 1), so we are comfortable using the index as an additional discriminant. The dwarf regression line in the gravity indicator versus temperature indicator plot (Fig. 1) was constructed using only Keenan standards for which his luminosity classification agreed with published log g values and the H-R diagram position.

TABLE 9

Revised Luminosity Classes of Standard Stars

Star	Published Lum. Class	log g Estimates	Sr/Fe Class	H-R Diagram Position	Adopted Luminosity Class
HR 5072	V	3.8–3.9 (IV–V)	IV–V	IV–V	IV–V
HR 4995	IV–V	3.0–3.7 (III/IV)	IV	IV	IV
HR 5409	IV	3.3–3.9 (III/IV)	III–IV	III–IV	III–IV
HR 6608	IIIb	. . .	IV	IV	IV

Notes.—Published luminosity classes from Keenan & McNeil 1989. The range of published log g estimates come from the compilation of Cayrel de Strobel et al. 2001. "Sr/Fe class" is from measuring the Fe i λ4071/Sr ii λ4071 ratio in our spectra and intercomparison to the spectral standards in Table 3 (see Fig. 1). The luminosity class from the H-R diagram position uses the V and $B-V$ data from *Hipparcos* and the standard relations from Appendix B of Gray 1991.

APPENDIX C

POLYNOMIAL FITS

MI6 versus Spectral type.—This flux ratio is Index 6 of Malyuto & Schmidt-Kaler (1997). We measure the index in magnitudes (MI6 $= -2.5 \log [f(\lambda\lambda5125\text{–}5245)/f(\lambda\lambda5245\text{–}5290)]$) and find the following relation for Keenan and Garcia F0–K6 III–IV standards (Table 3) within 0.3 dex of solar metallicity:

$$\mathrm{Sp.} = \begin{cases} 33.26 \pm 0.07 + (22.75 \pm 0.48)\mathrm{MI6} & \text{if } 0.06 < \mathrm{MI6} < 0.26\ , \\ 30.82 \pm 0.16 + (105.38 \pm 8.28)\mathrm{MI6} - (711.74 \pm 173.81)\mathrm{MI6}^2 & \text{if } -0.04 < \mathrm{MI6} < 0.06\ , \end{cases} \tag{C1}$$

where Sp. is the spectral type on Keenan's (1984) scale, i.e., F5 = 28, F8 = 29, G0 = 30, G2 = 31, G5 = 32, G8 = 33, K0 = 34, K1 = 35, and K2 = 36. Intermediate types can be assigned e.g., G9 = 33.5, G9.5 = 33.75, K0+ = 34.25, K0.5 = 34.5, etc. The first equation applies to K0–K6 stars, and the second equation applies to F0–K0 stars. The 1 σ dispersion in these fits is 0.6 subtypes.

λ4374/λ4383 versus spectral type.—This band ratio consists of two 3 Å bands centered on 4374.5 and 4383.6 Å. We measure the index in magnitudes as Y/Fe $= -2.5 \log [f(\lambda4374.5)/f(\lambda4383.6)]$. We find the following relation between the band ratio and Sp. for F0–K6 III–V stars:

$$\mathrm{Sp.} = 25.97 \pm 0.30 + (20.47 \pm 0.90)\mathrm{Y/Fe}\ . \tag{C2}$$

The residual standard deviation to the fit (using 20 Keenan F0–K5 III–V standards within 0.3 dex of solar metallicity) is 0.6 subtypes.

Surface Gravity Index Fe i λ4071/Sr ii λ4077 *versus spectral type*.—We measure a surface gravity index using the flux ratio of two 3 Å bands centered on Fe i λ4071.4 and Sr ii λ4076.9. We measure the flux ratio in magnitudes: Sr/Fe $= -2.5 \log [f(\lambda4071)/f(\lambda4077)]$, and plot against our MI6 spectral type index. The Keenan standard dwarfs confirmed as being main-sequence stars define a narrow locus:

$$\mathrm{Sr/Fe} = -0.078 \pm 0.005 + (2.123 \pm 0.261)\mathrm{MI6} - (8.393 \pm 2.945)\mathrm{MI6}^2 + (15.487 \pm 8.672)\mathrm{MI6}^3\ . \tag{C3}$$

The 1 σ sample standard deviation of this fit is 0.0094 mag in Sr/Fe. The boundary between dwarfs and subgiants in Figure 1 is $-2\,\sigma$ of the dwarf locus. This relation is valid for F9–K6 stars.

Hα *versus spectral type*.—In Figure 2, we fitted the equivalent widths of the Hα feature (at low resolution, the photospheric absorption plus the chromospheric emission) as a function of spectral type for F0–K6 dwarf and subgiant standard stars (Table 3) with the following polynomial:

$$\mathrm{EW(H\alpha)} = 2.983 \pm 0.066 - (0.456 \pm 0.027)(\mathrm{Sp.} - 30) + (2.574 \pm 0.378) \times 10^{-2}(\mathrm{Sp.} - 30)^2\ . \tag{C4}$$

EW(Hα) is measured in angstroms. Sp. is spectral type on Keenan's scale (as before). The sample standard deviation of the polynomial fit to 11 standards was 0.20 Å.

Converting Tycho B– V to Johnson/Cousins System.—The *Hipparcos* catalog gives linear relations between $B_T - V_T$, $B-V$, V, and V_T for stars of a wide range in spectral types. Bessell (2000) compared the *Hipparcos*/Tycho photometry and that of the E region photometric standards and refined the relations between the two systems. Table 2 of Bessell (2000) gives a standard relation between $B_T - V_T$, Johnson/Cousins $B-V$, and $(V-V_T)$ for B–G dwarfs and K–M giants. We fitted the following relations to Bessell's tables:

$$V = V_T + 9.7 \times 10^{-4} - 1.334 \times 10^{-1}(B_T - V_T) + 5.486 \times 10^{-2}(B_T - V_T)^2 - 1.998 \times 10^{-2}(B_T - V_T)^3\ , \tag{C5}$$

$$B-V = (B_T - V_T) + 7.813 \times 10^{-3}(B_T - V_T) - 1.489 \times 10^{-1}(B_T - V_T)^2 + 3.384 \times 10^{-2}(B_T - V_T)^3\ , \tag{C6}$$

$$B-V = (B_T - V_T) - 0.006 - 1.069 \times 10^{-1}(B_T - V_T) + 1.459 \times 10^{-1}(B_T - V_T)^2\ . \tag{C7}$$

The $V(V_T, B_T - V_T)$ polynomial equation (C5) applies to stars from $-0.25 < (B_T - V_T) < 2.0$ (B–M types). Equation (C6) is for stars with $0.5 < (B_T - V_T) < 2.0$, and equation (C7) is for stars with $-0.25 < (B_T - V_T) < 0.5$. We do not quote uncertainties in the polynomial coefficients, since the Bessell relations are already smoothed. These equations fit Bessell's standard relations to 1–2 mmag.

REFERENCES

Balona, L. A. 1994, MNRAS, 268, 119
Basri, G., Marcy, G. W., & Graham, J. R. 1996, ApJ, 458, 600
Bertelli, G., Bressan, A., Chiosi, C., Fagotto, F., & Nasi, E. 1994, A&AS, 106, 275
Bessell, M. S. 2000, PASP, 112, 961
Bessell, M. S., & Brett, J. M. 1988, PASP, 100, 1134
Bessell, M. S., Castelli, F., & Plez, B. 1998, A&A, 333, 231
Bhatt, H. C. 2000, A&A, 362, 715
Blaauw, A. 1946, Ph.D. thesis, Groningen Univ.
———. 1991, in The Physics of Star Formation and Early Stellar Evolution, ed. C. J. Lada & N. D. Kylafis (NATO ASI Series C, 342) (Dordrecht: Kluwer), 125
Bouvier, J., et al. 1997, A&A, 318, 495
Carpenter, J. M. 2001, AJ, 121, 2851
Cayrel de Strobel, G., Soubiran, C., & Ralite, N. 2001, A&A, 373, 159
Covino, E., Alcala, J. M., Allain, S., Bouvier, J., Terranegra, L., & Krautter, J. 1997, A&A, 328, 187
Crawford, D. L. 1978, AJ, 83, 48
Crawford, D. L., & Mandwewala, N. 1976, PASP, 88, 917
Cutispoto, G., Pastori, L., Pasquini, L., de Medeiros, J. R., Tagliaferri, G., & Andersen, J. 2002, A&A, 384, 491
D'Antona, F., & Mazzitelli, I. 1997, Mem. Soc. Astron. Italiana, 68, 807 (DM97)
de Bruijne, J. H. J. 1999a, MNRAS, 306, 381
———. 1999b, MNRAS, 310, 585
de Geus, E. 1992, A&A, 262, 258
de Geus, E., de Zeeuw, P., & Lub, J. 1989, A&A, 216, 44
de Jager, C., & Nieuwenhuijzen, H. 1987, A&A, 177, 217
de Zeeuw, P. T., & Brand, J. 1985, in Birth and Evolution of Massive Stars and Stellar Groups (Dordrecht: Reidel), 102
de Zeeuw, P. T., Hoogerwerf, R., de Bruijne, J. H. J., Brown, A. G. A., & Blaauw, A. 1999, AJ, 117, 354 (dZ99)
Drilling, J. S., & Landolt, A. U. 2000, in Allen's Astrophysical Quantities, ed. A. C. Cox (4th. ed.; New York: AIP Press, Springer)
Duquennoy, A., & Mayor, M. 1991, A&A, 248, 485
ESA. 1997, The Hipparcos and Tycho Catalogues (ESA SP-1200) (Noordwijk: ESA)
Feigelson, E. D. 1996, ApJ, 468, 306
Fleming, T. A., Molendi, S., Maccacaro, T., & Wolter, A. 1995, ApJS, 99, 701
Frogel, J. A., & Stothers, R. 1977, AJ, 82, 890
Garcia, B. 1989, Bull. Inf. CDS, 36, 27
Gehrels, N. 1986, ApJ, 303, 336
Gontcharov, G. A., Andronova, A. A., Titov, O. A., & Kornilov, E. V. 2001, A&A, 365, 222
Gray, D. F. 1991, The Observation and Analysis of Stellar Photospheres (2d ed.; New York: Cambridge)
Gray, R. O. 2000, A Digital Spectral Classification Atlas (Pasadena: IPAC)
Gray, R. O., Graham, P. W., & Hoyt, S. R. 2001, AJ, 121, 2159
Gregorio-Hetem, J., Lépine, J. R. D., Quast, G. R., Torres, C. A. O., & de la Reza, R. 1992, AJ, 103, 549
Guillout, P., Sterzik, M. F., Schmitt, J. H. M. M., Motch, C., & Neuhäuser, R. 1998, A&A, 337, 113
Haisch, K. E., Jr., Lada, E. A., & Lada, C. J. 2001, ApJ, 553, L153
Hamuy, M., Suntzeff, N. B., Heathcote, S. R., Walker, A. R., Gigoux, P., & Phillips, M. M. 1994, PASP, 106, 566
Hartigan, P., Edwards, S., & Ghandour, L. 1995, ApJ, 452, 736
Hauck, B., & Mermilliod, M. 1998, A&AS, 129, 431
Henize, K. G. 1976, ApJS, 30, 491
Herbig, G. H. 1978, in Problems of Physics and Evolution of the Universe, ed. L. V. Mirzoyan (Yervan: Acad. Sci. Armenian SSR), 171
Herbig, G. H., & Bell, K. R. 1988, Lick Obs. Bull., No. 1111
Hillenbrand, L. A., & Meyer, M. R. 1999, BAAS, 31, 1368
Høg, E., et al. 2000a, A&A, 357, 367
———. 2000b, A&A, 355, L27
Høg, E., Kuzmin, A., Bastian, U., Fabricius, C., Kuimov, K., Lindegren, L., Makarov, V. V., & Roeser, S. 1998, A&A, 335, L65
Hoogerwerf, R. 2000, MNRAS, 313, 43
Hoogerwerf, R., & Aguilar, L. A. 1999, MNRAS, 306, 394
Hoogerwerf, R., de Bruijne, J. H. J., & de Zeeuw, P. T. 2001, A&A, 365, 49
Houk, N. 1978, Michigan Catalogue of Two-Dimensional Spectral Types for HD Stars, Vol. 2 (Ann Arbor: Univ. Michigan Dept. Astron.)
———. 1982, Michigan Catalogue of Two-Dimensional Spectral Types for HD Stars, Vol. 3 (Ann Arbor: Univ. Michigan Dept. Astron.)
Houk, N., & Cowley, A. P. 1975, Michigan Catalogue of Two-Dimensional Spectral Types for HD Stars, Vol. 1 (Ann Arbor: Univ. Michigan Dept. Astron.)
Houk, N., & Smith-Moore, M. 1988, Michigan Catalogue of Two-Dimensional Spectral Types for HD Stars, Vol. 4 (Ann Arbor: Univ. Michigan Dept. Astron.)
Houk, N., & Swift, C. 1999, Michigan Catalog of Two-Dimensional Spectral Types for the HD Stars, Vol. 5. (Ann Arbor: Univ. Michigan Dept. Astron.)
Hughes, J., Hartigan, P., & Clampitt, L. 1993, AJ, 105, 571
Hughes, J., Hartigan, P., Krautter, J., & Kelemen, J. 1994, AJ, 108, 1071
Jensen, E. 2001, in ASP Conf. Ser. 244, Young Stars Near Earth: Progress and Prospects, ed. R. Jayawardhana & T. Greene (San Francisco: ASP), 3
Johnson, H. L., & Morgan, W. W. 1953, ApJ, 117, 313
Jones, B. F., Fischer, D., Shetrone, M., & Soderblom, D. R. 1997, AJ, 114, 352
Kastner, J. H., Zuckerman, B., Weintraub, D. A., & Forveille, T. 1997, Science, 277, 67
Keenan, P. C. 1984, in The MK Process and Stellar Classification, ed. R. F. Garrison (Toronto: David Dunlap Obs.), 29
Keenan, P. C., & Barnbaum, C. 1999, ApJ, 518, 859
Keenan, P. C., & McNeil, R. C. 1976, An Atlas of Spectra of the Cooler Stars: Types G, K, M, S, and C (Columbus: Ohio State Univ. Press)
———. 1989, ApJS, 71, 245
Keenan, P. C., & Yorka, S. B. 1988, Bull. Inf. CDS, 35, 37
Kenyon, S. J., & Hartmann, L. 1995, ApJS, 101, 117
Köhler, R., Kunkel, M., Leinert, C., & Zinnecker, H. 2000, A&A, 356, 541
Krautter, J., Wichmann, R., Schmitt, J. H. M. M., Alcala, J. M., Neuhauser, R., & Terranegra, L. 1997, A&AS, 123, 329
Kroupa, P. 2001, MNRAS, 322, 231
Lowrance, P. J., et al. 2000, ApJ, 541, 390
Maeder, A. 1981, A&A, 101, 385
Malyuto, V., & Schmidt-Kaler, Th. 1997, A&A, 325, 693
Mamajek, E. E., & Feigelson, E. D. 2001, in ASP Conf. Ser. 244, Young Stars Near Earth: Progress and Prospects, ed. R. Jayawardhana & T. Greene (San Francisco: ASP), 104
Mamajek, E. E., Lawson, W. A., & Feigelson, E. D. 1999, ApJ, 516, L77
Mashonkina, L., & Gehren, T. 2001, A&A, 376, 232
Mathis, J. S. 1990, ARA&A, 28, 37
Meyer, M. R., Calvet, N., & Hillenbrand, L. A. 1997, AJ, 114, 288
Moreno, E., Alfaro, E. J., & Franco, J. 1999, ApJ, 522, 276
Muzerolle, J., Hartmann, L., & Calvet, N. 1998, AJ, 116, 455
Napiwotzki, R., Schönberner, D., & Wenske, V. 1993, A&A, 268, 653
Palla, F., & Stahler, S. W. 2001, ApJ, 553, 299 (PS01)
Pallavicini, R., Cerruti-Sola, M., & Duncan, D. K. 1987, A&A, 174, 116
Patten, B. H., & Simon, T. 1996, ApJS, 106, 489
Pojmanski, G. 1998, Acta Astron., 48, 35
Pöppel, W. 1997, Fundam. Cosmic Phys., 18, 1
Popper, D. M. 1966, AJ, 71, 175
Preibisch, T., & Zinnecker, H. 1999, AJ, 117, 2381
———. 2000, in ASP Conf. Ser. 198, Stellar Clusters and Associations: Convection, Rotation, and Dynamos, ed. R. Pallavicini, G. Micela, & S. Sciortino (San Francisco: ASP), 219
Randich, S., Aharpour, N., Pallavicini, R., Prosser, C. F., & Stauffer, J. R. 1997, A&A, 323, 86
Randich, S., Gratton, R., Pallavicini, R., Pasquini, L., & Carretta, E. 1999, A&A, 348, 487
Randich, S., Schmitt, J. H. M. M., Prosser, C. F., & Stauffer, J. R. 1995, A&A, 300, 134
Rebull, L. M., Wolff, S. C., Strom, S. E., & Makidon, R. B. 2002, AJ, 124, 546
Rodgers, A. W., Conroy, P., & Bloxham, G. 1988, PASP, 100, 626
Rose, J. A. 1984, AJ, 89, 1238
Schmidt-Kaler, Th. 1982, in Landolt-Börnstein New Series, Group 6, Vol. 2b, Stars and Star Clusters, ed. K. Schaifers & H. H. Voigt (Berlin: Springer-Verlag), 453
Shobbrook, R. R. 1983, MNRAS, 205, 1215
Siess, L., Dufour, E., & Forestini, M. 2000, A&A, 358, 593 (SDF00)
Slawson, R. W., Hill, R. J., & Landstreet, J. D. 1992, ApJS, 82, 117
Smart, W. M. 1968, Stellar Kinematics (London: Longmans)
Soderblom, D. R., Jones, B. F., Balachandran, S., Stauffer, J. R., Duncan, D. K., Fedele, S. B., & Hudon, J. D. 1993, AJ, 106, 1059
Soderblom, D. R., King, J. R., & Henry, T. J. 1998, AJ, 116, 396
Spangler, C., Sargent, A. I., Silverstone, M. D., Becklin, E. E., & Zuckerman, B. 2001, ApJ, 555, 932
Stauffer, J. R., Caillault, J.-P., Gagné, M., Prosser, C. F., & Hartmann, L. W. 1994, ApJS, 91, 625
Sterzik, M. F., & Durisen, R. H. 1995, A&A, 304, L9
Tachihara, K., Toyoda, S., Onishi, T., Mizuno, A., Fukui, Y., & Neuhäuser, R. 2002, PASJ, 53, 1081

Urban, S. E., Corbin, T. E., & Wycoff, G. L. 1998, AJ, 115, 2161
Voges, W., et al. 1999, A&A, 349, 389
Wallace, L., Hinkle, K., & Livingston, W. 1998, An Atlas of the Spectrum of the Solar Photosphere from 13,500 to 28,000 cm^{-1} (3570 to 7405 Å) (Tucson: NOAO)
Webb, R. A., Zuckerman, B., Platais, I., Patience, J., White, R. J., Schwartz, M. J., & McCarthy, C. 1999, ApJ, 512, L63
Wichmann, R., Krautter, J., Covino, E., Alcalá, J. M., Neuhäuser, R., & Schmitt, J. H. M. M. 1997a, A&A, 320, 185
Wichmann, R., Sterzik, M., Krautter, J., Metanomski, A., & Voges, W. 1997b, A&A, 326, 211
Wilking, B. A., Lada, C. J., & Young, E. T. 1989, ApJ, 340, 823

THE ASTRONOMICAL JOURNAL, 131:2360, 2006 April

ERRATUM: "POST–T TAURI STARS IN THE NEAREST OB ASSOCIATION" (AJ, 124, 1670 [2002])

ERIC E. MAMAJEK
Harvard-Smithsonian Center for Astrophysics

AND

MICHAEL R. MEYER AND JAMES LIEBERT
Steward Observatory

In Table 3 the F6 V–type spectral standard star HR 7061 is mistakenly aliased as HD 173677 but should be HD 173667. In §7.2 HIP 68282 is mistakenly aliased as ν^1 Cen ("nu 1") but should be υ^1 Cen ("upsilon 1") according to the Bright Star Catalog (D. Hoffleit & W. H. Warren, Jr. [New Haven: Yale Univ. Obs.; 1991]). The same error in SIMBAD has since been corrected. In Appendix A, third paragraph, the units of slope should be K $[\log(\mathrm{cm\ s^{-2}})]^{-1}$, not K $[\log(\mathrm{cm\ s^{-1}})]^{-1}$. In Appendix C there is an incorrect sign in the second term in equation (C6), and incorrect color ranges were published for equations (C6) and (C7). Equations (C6) and (C7) provide polynomial transformations between the Tycho $(B_T - V_T)$ and Cousins-Johnson $(B - V)$ colors. The correct equation (C6), applicable over the color range $(B_T - V_T) \in [0.40,\ 2.00]$, is

$$\begin{aligned} B - V = {} & (B_T - V_T) - 7.813 \times 10^{-3}(B_T - V_T) \\ & - 1.489 \times 10^{-1}(B_T - V_T)^2 + 3.384 \times 10^{-2}(B_T - V_T)^3. \end{aligned} \tag{C6}$$

The correct formula (C6) was applied in the paper but transcribed incorrectly to the manuscript. Equation (C7) was published correctly, but the published color range is incorrect. For the color range $(B_T - V_T) \in [-0.25,\ 0.40]$, equation (C7) should be used (same as published):

$$\begin{aligned} B - V = {} & (B_T - V_T) - 0.006 - 1.069 \times 10^{-1}(B_T - V_T) \\ & + 1.459 \times 10^{-1}(B_T - V_T)^2. \end{aligned} \tag{C7}$$

We thank John Carpenter for bringing the error in equation (C6) to our attention and François Bonnarel and Christian Nitschelm for pointing out the stellar misidentifications.